

The Institute of Paper Science and Technology

Atlanta, Georgia

Doctoral Dissertation
Reprint

A MATHEMATICAL MODEL OF HIGH INTENSITY PAPER DRYING

A thesis submitted by

Joseph R. Pounder

B.S. 1979, Philadelphia College of Textiles and Science

M.S. 1982, Lawrence University

**in partial fulfillment of the requirements
of The Institute of Paper Chemistry
for the degree of Doctor of Philosophy
from Lawrence University,
Appleton, Wisconsin**

**Publication Rights Reserved by
The Institute of Paper Chemistry**

January, 1986

TABLE OF CONTENTS

	Page
ABSTRACT	1
INTRODUCTION	3
OBJECTIVE	6
EXPERIMENTAL BACKGROUND	7
Introduction	7
Experimental Results	8
Bulk Vapor Flow	11
Liquid Displacement	12
Mechanical Dewatering	13
Zone Development	14
Summary	14
MOVING BOUNDARY MODELS	15
Introduction	15
Temperature-Based Models	15
Enthalpy-Based Models	16
Position-Based Models	17
Drying Models	17
Summary	19
THE MATHEMATICAL MODEL	20
Introduction	20
Elementary Models	21
Description of the Advanced Model	26
Assumptions	26
Advanced Model Equations	31

Zone Continuity and Momentum Equations	32
Zone Thermal Energy Equation	36
Convective-Diffusion Equations	38
Interface Equations	44
Heatup and Transition Regimes	45
Linear Regime	50
Supplementary Relationships	55
Applied Mechanical Pressure	55
Physical Properties	56
Latent Heat Correction Factor	56
Thermal Conductivity	57
Contact Coefficient	57
Compressibility	58
Permeability	61
Model Validation	63
Summary	64
PARAMETRIC STUDY	65
Input Parameters	65
Output Variables	65
Design of Parametric Study	66
Results and Discussion	66
Base Case	67
Comparisons of Drying Behavior	76
Sensitivity Analysis	83
Summary	85
EXPERIMENTAL COMPARISONS	86
Purpose	86

Experimental Conditions	86
Ramp-And-Hold Pressure Pulse	87
Short Duration (Impulse) Pressure Pulse	103
Summary	109
SUMMARY	110
RECOMMENDATIONS	111
ACKNOWLEDGMENTS	112
NOMENCLATURE	113
LITERATURE CITED	118
APPENDIX 1: HIDRYER1 Program and Documentation	125

ABSTRACT

High intensity paper drying is defined as any drying process in which the web is at or above the thermodynamic saturation temperature corresponding to the ambient pressure. Rapid generation of vapor under these circumstances causes the drying process to be driven by a gradient of total pressure and not by a gradient of partial vapor pressure. Therefore, the generated vapor leaves the web by a bulk (convective) flow mechanism rather than a slower diffusion mechanism. The vapor pressure build-up in the web also offers the opportunity for removal of moisture in liquid form, since the fast flowing vapor can displace and/or entrain liquid as it moves through the web. This can result in significantly lower energy usage relative to conventional drying, since only a fraction of the moisture has to be evaporated.

The thesis objective is a mathematical model simple enough to be easily modified or expanded but comprehensive enough to be applicable to a wide variety of process conditions and sheet variables.

Early experiments suggested that the high intensity drying process could be described effectively by a discrete "zone" model. The process is idealized by picturing the sheet as composed of different zones which contain various amounts of fiber, liquid water, and water vapor. The model is based on sets of equations which account for the heat and moisture transfer within and among the zones during three regimes: heatup, transition, and quasi-static. Once the hot surface temperature, boiling point temperature, basis weight, Canadian Standard Freeness, initial moisture ratio, and mechanical pressure pulse are specified, the equations may be solved to predict the moisture content as a function of time.

Comparisons between experimental data and the model's predictions demonstrate that the model qualitatively and quantitatively describes high intensity drying

behavior and provide indirect evidence that the mechanisms on which the model is based actually are in effect under high intensity conditions. An exploratory parametric study shows that the predicted drying behavior is most sensitive to changes in hot surface temperature and sheet basis weight. Peak pressure and freeness have a more moderate effect, and initial moisture ratio has almost no effect. Comparisons to laboratory data show that the model tends to overpredict the extent of liquid moisture removal and underpredict the heat flux. Changing the values of constants in the model modifies the predictions and suggests that a mathematical optimization of all constants, constrained by experimental data, would improve the predictive capability of the model.

INTRODUCTION

Low heat transfer rates, low drying rates, and low mechanical pressures characterize conventional can drying of paper. Moisture removal is dominated by a vapor diffusion mechanism, and average sheet temperatures are well below the boiling point.

In contrast, high intensity drying occurs at high surface temperatures and high mechanical pressures. Heat transfer rates and drying rates are orders of magnitude above those in the conventional process (see Fig. 1 and 2). Moisture removal is dominated by bulk (convective) vapor flow and liquid displacement or entrainment, and sheet temperatures frequently exceed the boiling point.

Mathematical modeling provides a convenient and comprehensive means for exploring the effects of temperature, pressure, freeness, and other factors on high intensity drying behavior. Mathematical modeling complements experimental study by identifying incomplete areas in knowledge of the physical system and suggesting areas for further research. Finally, mathematical modeling offers the opportunity for blending and balancing theoretical and empirical relationships to provide a fast, low-cost investigative tool.

Early experiments indicated that high intensity drying could be described effectively by a discrete "zone" model, since the drying behavior is consistent with other examples of phase change problems involving the development of zones. Initially, two zones of different moisture content were assumed to be present. As more information became available, additional zones were added to the model. Fundamental mass and energy balances for the zones are linked by the boundary conditions and the conditions at the interfaces between the zones. Solving the system of equations allows a prediction of the temperature distribution within

the sheet, the positions and rates of advance of the interfaces, and the moisture content of the sheet as functions of time.

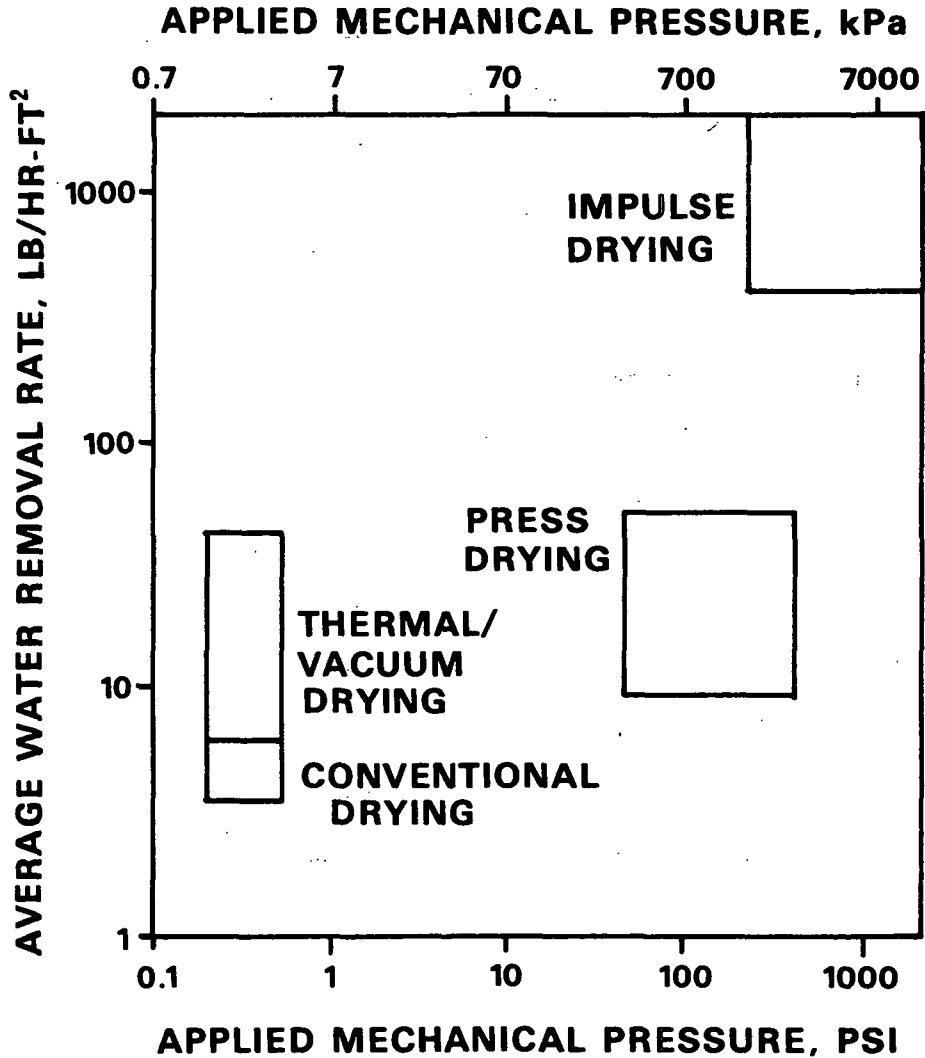


Figure 1. Water removal rates at different applied mechanical pressures for various drying methods.

This thesis presents the objective, experimental background, theoretical background, assumptions, and equations of the model. A parametric study details changes in the model's predictions resulting from changes in process variables. A sensitivity analysis shows the effects of varying certain model constants, and direct comparisons to experimental data demonstrate that the model qualitatively and quantitatively describes high intensity drying behavior.

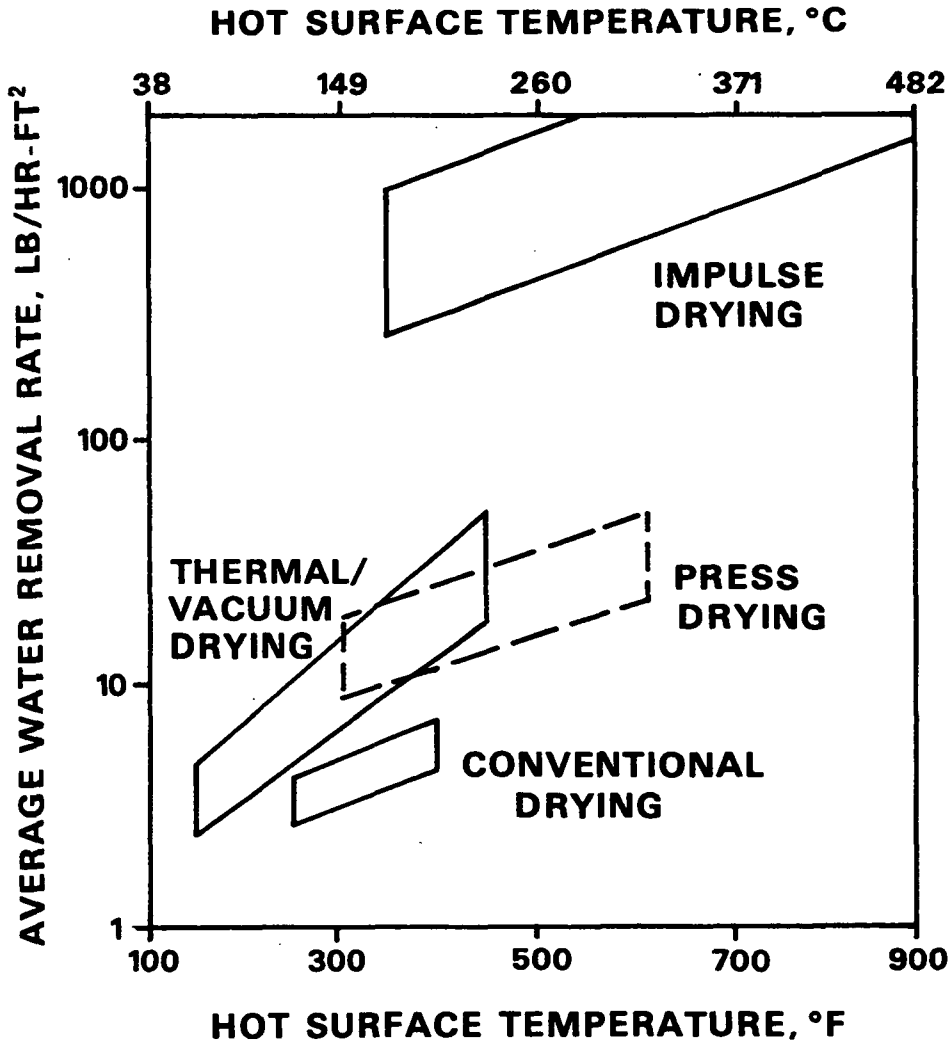


Figure 2. Water removal rates at different hot surface temperatures for various drying methods.

OBJECTIVE

The objective of this thesis is the creation of a mathematical model of high intensity drying simple enough to be easily modified or expanded but comprehensive enough to be applicable to a wide variety of process conditions and sheet variables. The mechanisms of bulk vapor flow and liquid displacement are analyzed within the framework of a moving boundary model, and comparisons to experimental data are used to verify that the model describes high intensity drying behavior.

EXPERIMENTAL BACKGROUND

INTRODUCTION

High intensity paper drying occurs when the web is at or above the thermodynamic saturation temperature corresponding to the ambient pressure. This definition encompasses press drying,¹ where the web is heated from both sides symmetrically, and the "one-sided" drying methods: thermal/vacuum drying,² where the web is dried in a reduced pressure environment; impulse drying,³ where the web is dried in a heated press nip; and one-sided drying where temperatures and mechanical pressures are elevated above conventional conditions.⁴ The conventional conditions are a reference state of surface temperatures from about 127 to 171°C (260 to 340°F) and mechanical pressures from 1.2 to 7 kPa (0.17 to 1 psi). High intensity conditions are on the order of 177 to 399°C (350 to 750°F) and 7 to 4826 kPa (1 to 700 psi).

Experimental investigations into high intensity drying are extensions of the mechanistic studies of conventional paper drying. Within the range of conventional operating conditions, increases in surface temperature and/or mechanical pressure lead to increases in drying rate. Recent publications^{4,5} cite several references in this area, provide data at higher temperatures and pressures, and cite an example of press drying work at very high temperatures and pressures that shows the trend of increasing drying rate continues well beyond conventional conditions. It is clear that a dramatic increase in the drying rate is observed whenever the sheet temperature can be brought to or above the boiling point.

EXPERIMENTAL RESULTS

Figure 3 shows the configuration for the high intensity drying process modeled in this thesis. The paper contacts an impermeable heated surface directly. A felt, wire, or other highly porous material provides an escape path for the vapor and liquid to be removed from the paper, and another impermeable surface is used to exert mechanical pressure on the system. This arrangement causes one-sided heating of the paper. The overall heat and mass transfer are one-dimensional in the direction away from the hot surface. For experimental purposes, thermocouples are placed at various locations in the sheet so that the temperature distribution can be monitored throughout the course of drying.

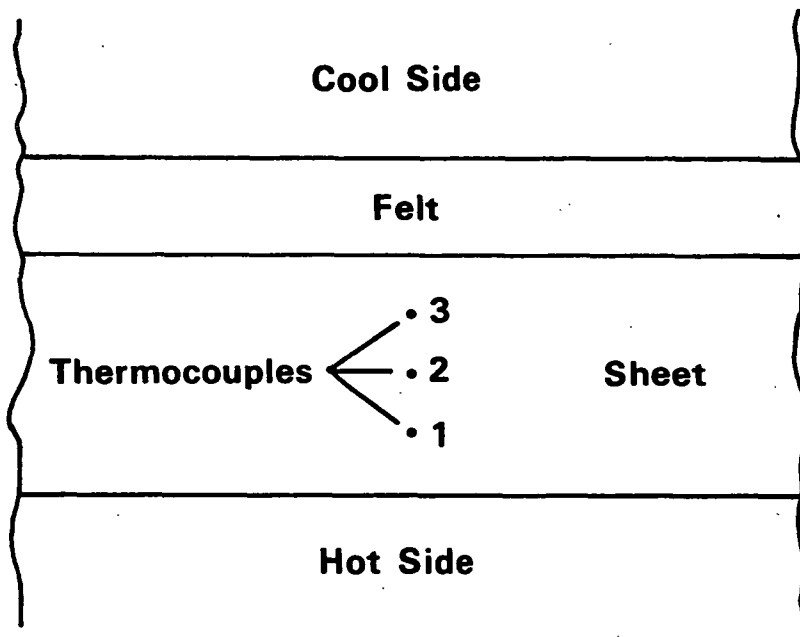


Figure 3. Configuration for one-sided high intensity drying.

Figure 4 depicts a typical sheet temperature history from several types of high intensity drying experiments.⁶⁻⁸ It is important to note that all thermocouples reach a plateau value equal to or above the boiling point at approximately the same time and that this time is much shorter than the time needed to

simply conduct heat to the far thermocouples. The square roots of the times when the temperatures begin to rise above their plateaus are proportional to the distances of the thermocouples from the hot surface. When the temperature exceeds the boiling point, the vapor pressure exceeds the ambient pressure. The extent of the rise is related to the flow resistance of the sheet. The peak pressure is much higher in the high flow resistance cases than in the low flow resistance cases.⁹

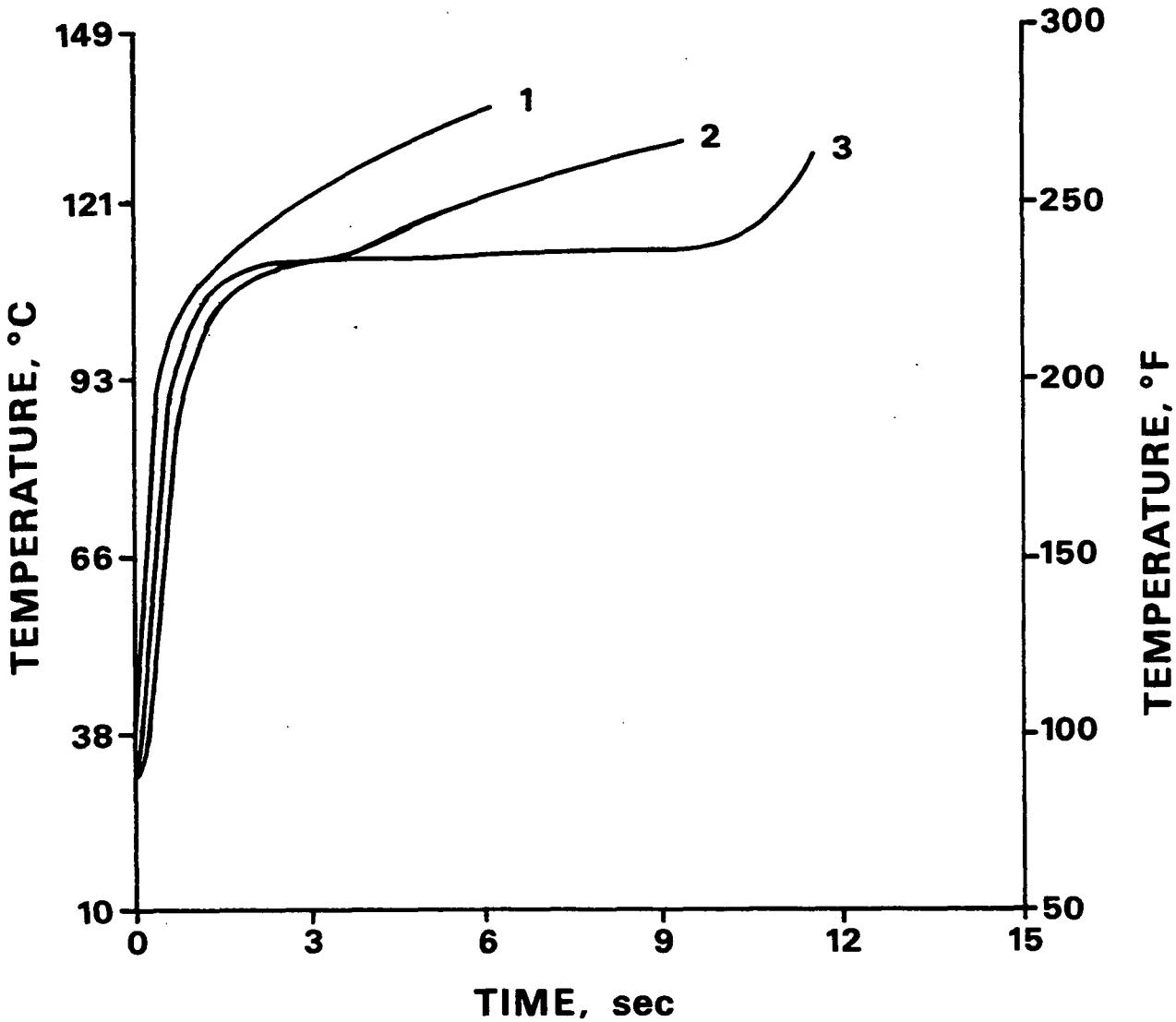


Figure 4. Internal sheet temperatures during high intensity drying.

Figure 5 shows a qualitative comparison between drying rates for conventional and high intensity drying. Four outstanding features differentiate the processes. In high intensity drying the peak drying rate is much greater than in conventional drying. In high intensity drying the peak rate is achieved (almost) instantaneously, but there is a significant heatup time required in conventional drying. The high intensity drying time is much shorter than the conventional drying time, and most importantly from a mechanistic point of view, high intensity drying does not exhibit a "constant rate" period as conventional drying does.

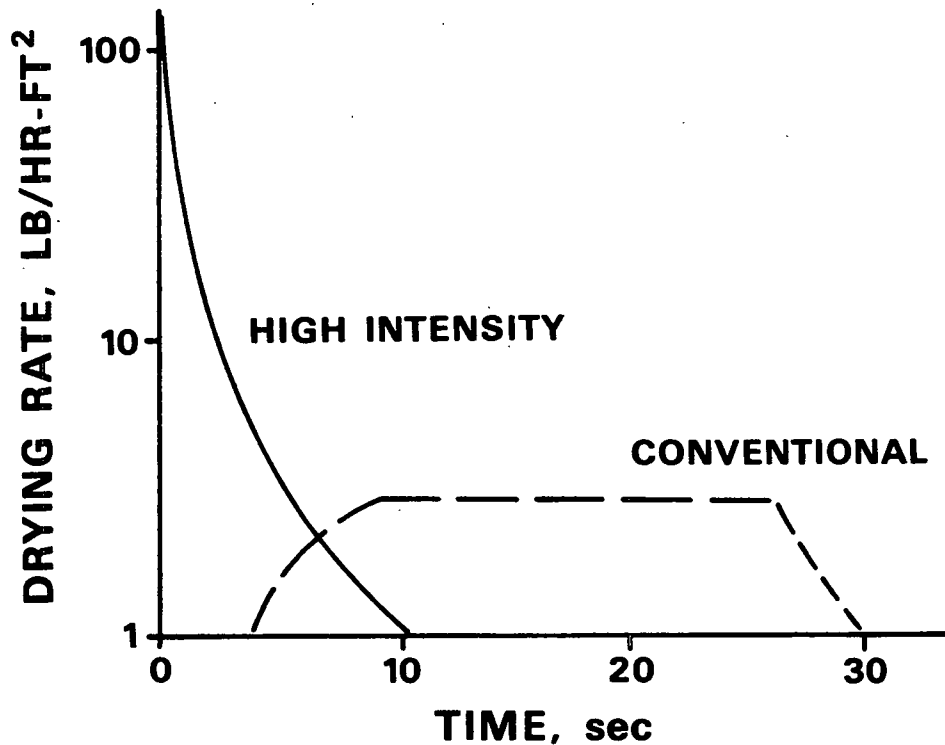


Figure 5. Comparison of high intensity and conventional drying rates.

Figure 6 depicts the results of a study designed to track the liquid distribution in the sheet.⁸ A nonvolatile LiCl tracer is incorporated into the sheet during formation. This tracer moves with liquid water movement. After drying,

a cross section of the sheet is analyzed with the EDAX electron microscope technique to determine the location of the tracer. For conventional drying, most of the tracer is found near the side of the sheet which was adjacent to the hot surface. High intensity drying shows an opposite tracer distribution.

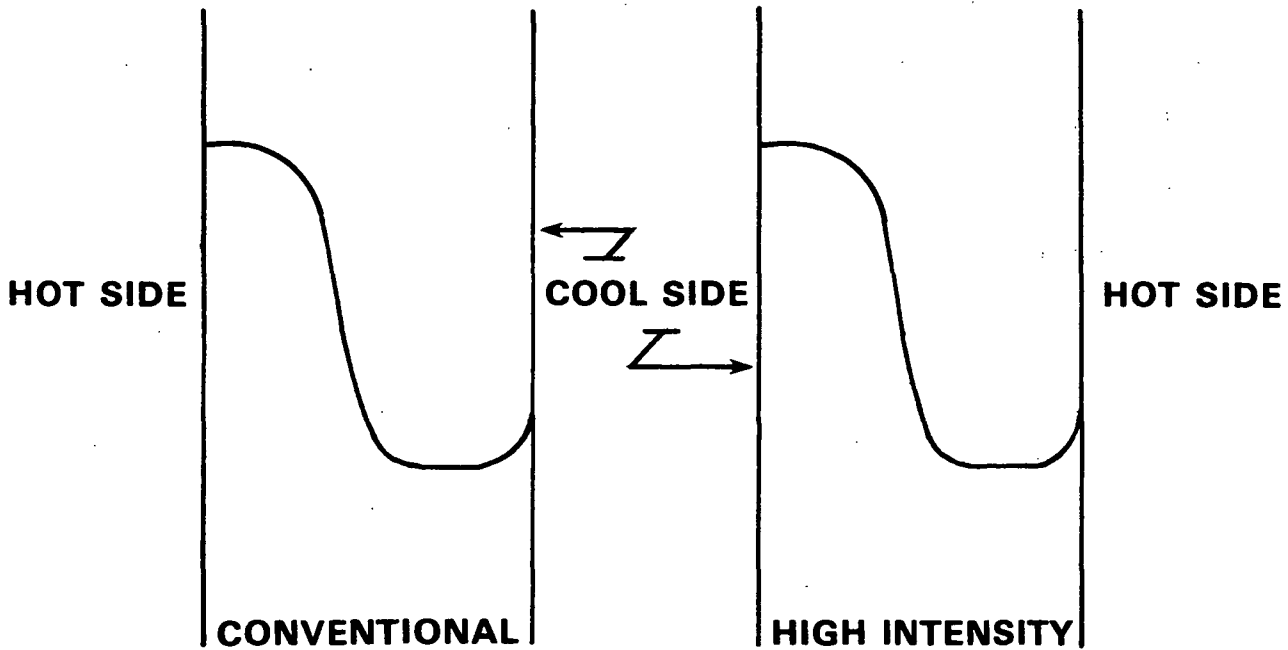


Figure 6. Comparison of tracer distributions for high intensity and conventional drying.

The experimental results lead to the postulation of three dominant mechanisms operative during high intensity drying: bulk vapor flow, liquid displacement and/or entrainment, and the development of zones within the sheet.

BULK VAPOR FLOW

Simple visual observation of a high intensity drying experiment is enough to suggest convective vapor flow. Vapor is forcibly ejected from the sheet. Even under impulse conditions where the nip residence time is as short as 0.005 second, a vapor pulse exiting the sheet is clearly visible. The rapid temperature rise

of thermocouples far from the hot surface supports this mechanism (see Fig. 4). The drying rate is insensitive to ambient air flow rate,⁴ and this would not be true if diffusion were dominant since a diffusion mechanism would depend on convective transport external to the sheet. Finally, direct experimental evidence of vapor flow under a vapor-pressure-gradient driving force comes from a study of steady state heat transfer in a granular porous medium¹⁰ and work involving heat pipes.¹¹ Darcy's law can be used to model the vapor flow in these cases, and while they are not examples of "drying," the fundamental transport mechanisms are identical.

LIQUID DISPLACEMENT

Liquid in the larger pores of a fibrous material can be displaced by a flowing gas. Devices for dewatering paper by passing air through the wet web were described in a patent filed for in March, 1963 and granted November 8, 1966.¹² Extensions of this concept¹³⁻²⁰ have shown that pressure differentials across the sheet on the order of 7 to 210 kPa (1 to 30 psi) can raise solids content from the 10 to 30% range up to the 40 to 45% range. For textile materials, steam pressurized at up to 700 kPa (100 psi) can be used to preheat the web, displace liquid, and raise solids content from around 20% to nearly 80%.²¹

High intensity drying achieves its pressure driving force by vaporizing some liquid in the vicinity of the hot surface. As the vapor tries to escape, it pushes or entrains interfiber liquid out of the sheet. Figure 6 indicates the flow of liquid away from the hot surface. Heat flux determinations reveal that the actual thermal energy input can be on the order of 50% or less than the energy which would be required to raise the sheet to the boiling point and then evaporate all the liquid at that temperature.⁸

Therefore, water has to be removed in liquid form. High intensity, vapor-induced expulsion of liquid droplets has been observed for other porous materials as well.²² Note that since the necessary condition for liquid displacement is a vapor pressure differential across the web, the symmetrical heating of the press drying process precludes this mechanism.

Mechanical Dewatering

High-pressure, short-duration mechanical pressing of paper is a fundamental water removal method used prior to conventional drying. The extent of the dewatering is controlled by the relationship between the applied pressure and time and by either the flow resistance or compressibility of the sheet (or both). In addition to bulk vapor flow and vapor-induced liquid displacement, the temperature and pressure levels in impulse drying encourage effects similar to those found from pressing at higher than normal temperatures.

Pressing at up to 90°C (194°F) can take a sheet at ingoing solids content of 38% and raise it to nearly 50%, depending on temperature, basis weight, and freeness.^{23,24} Additionally, hot pressing offers the possibility for moisture profile control.²⁵ Hot pressing and impulse drying use temperature to decrease the viscosity and surface tension of the water and to decrease the sheet compression resistance. Lower viscosity allows the liquid to flow more easily; this factor should be of key importance in a flow controlled situation. Lower compression resistance allows the sheet to be deformed more easily and should therefore be of key importance in a compression controlled case, particularly when a high percentage of lignin is present. Lower surface tension should benefit both cases by reducing capillary pressure and the possibility of rewetting.

ZONE DEVELOPMENT

Figure 6 indicates the presence of two main zones within the sheet at the end of drying: a zone of lower moisture content close to the hot surface and a zone of higher moisture content, created by liquid flow, far from the hot surface. This in itself is no guarantee of a uniform moving front that progresses through the sheet, but when there is no constant rate drying period (see Fig. 5) and the external boundary layer does not affect the drying,⁴ then a simple approach to modeling the phenomenon is with a moving boundary or zone model.²⁶ The proportionality of the square roots of plateau rise times to thermocouple distances in Fig. 4 is compatible with the classical moving boundary problem called the Neumann problem²⁷ and suggests that an elementary model of high intensity drying might be based on a Neumann-like analysis.

SUMMARY

There is experimental evidence to indicate that high intensity drying might be conveniently described by a moving boundary or zone model based on the bulk vapor flow and liquid displacement mechanisms. In the case of impulse drying, the additional effects of high temperature pressing may contribute to the overall moisture loss by changing the physical properties of the liquid water and/or the sheet compressibility. The similarities between high intensity drying behavior and a classical moving boundary problem suggest a logical starting point for the mathematical modeling.

MOVING BOUNDARY MODELS

INTRODUCTION

Muehlbauer and Sunderland²⁸ present a brief summary of the Neumann problem and an excellent review of the mathematical investigations of moving boundary problems up until 1965. Substantial work in this area since then has centered on obtaining solutions to moving boundary problems with boundary and/or initial conditions or assumptions about key thermal properties which are different than those in the original and early analyses. Generally, the problems deal with one-dimensional heat transfer through one phase of a material to the interface with a different phase of the same material. The models usually treat melting or solidification problems, and mass transfer is not considered except in rare cases of convection in the liquid phase. The models either calculate the temperature or enthalpy distribution and position of the interface within the material or track the positions of isotherms that progress through the material.

TEMPERATURE-BASED MODELS

The original temperature-based model was formulated by Neumann. Details of the model are in.²⁷ Heat conduction equations for each phase or "zone" coupled with appropriate initial, boundary, and interface conditions allow a prediction of the temperature distribution and interface position within a semi-infinite medium. Extensions of this model allow for phase transitions over a range of temperatures^{29,30} and a modified rate of interface advance due to the different densities of the two phases.³¹ Simple dependence of thermal conductivity on temperature is treated analytically,³² and clever numerical schemes handle more complicated dependencies of conductivity and density.^{33,34}

The primary problems with these methods, with reference to drying, are that they deal only with semi-infinite media and that they deal only with the presence of a one-component (multiphase) system. Paper behaves as a finite medium with regard to heat transfer during drying and contains two or more components (fiber, water, air, etc.). Integral transform methods have been applied to solve the problem in finite media of various geometries and with boundary conditions of the first, second, and third kinds,³⁵ but the problem of multiple components remains.

ENTHALPY-BASED MODELS

When knowledge of the exact position of a phase change interface is not required, modeling the system in terms of an enthalpy equation often leads to greatly simplified (numerical) solution methods.³⁶ In elementary cases, the solution of the enthalpy-based analysis is identical to that of the analytical temperature-based problem. In this method, the temperature-based model is formulated and then converted to an enthalpy-based model by using a relationship between temperature and enthalpy.^{37,38} This relationship describes the latent heat effect as a large jump in heat capacity over a very narrow temperature range. The advantages of this approach are: there are no conditions to be satisfied at the phase change boundary; there is no need to track the position of the phase change boundary accurately; there is no need to consider the regions on either side of the boundary separately; and it is possible to vary the range of temperatures over which the transition takes place.³⁸ It is also relatively easy to extend this technique to more than one dimension.³⁹

The disadvantage of this method is that it can lead to problems when convective effects need to be considered. In a model of high intensity drying,

convection of vapor and liquid is a key mechanism, and so an enthalpy-based method is not directly applicable.

POSITION-BASED MODELS

The Isotherm Migration Method (IMM) and its modifications are alternatives to the temperature- and enthalpy-based approaches. IMM tracks the position of a given isotherm within the medium, and distance replaces temperature as the dependent variable.^{40,41} It is another attempt to avoid calculating the exact position of the phase change front.

While IMM is flexible and capable of handling more than one moving front, it is limited because it requires some analytical solution to "start" the process. This analytical solution is an exact solution for very short times, places all isotherms in the slab, and sets an initial temperature profile to start the finite difference numerical scheme. Thus, IMM is somewhat limited in that an analytical solution may not exist to start the process. The lack of an analytical starting solution, however, is a relatively minor shortcoming compared to its inability to handle convective aspects of problem.

DRYING MODELS

Drying differs significantly from simple moving boundary problems, since drying involves simultaneous heat and mass transfer. Furthermore, drying takes place within a matrix of solid material from which a volatile component is evaporated. The strong coupling of heat and mass transfer in drying thus requires a careful extension of the general concepts of moving boundary problems.

An exact solution of an evaporation problem in porous media has been known since 1975.⁴² This is the most elementary case involving constant surface

temperature, constant evaporation temperature, and a semi-infinite medium. Penetrating front models for finite media have evolved, generally for freeze drying applications.⁴³⁻⁴⁷ The geometry of the models is such that the medium is heated either symmetrically or with one face perfectly insulated and impermeable. The heat and mass transfer occur in opposite directions, and therefore these models are directly applicable only to press drying or to drying in which the heated surface is permeable.

Most models do not account for the hygroscopic nature of the matrix, but models for drying of wood⁴⁸⁻⁵⁰ and other materials⁵¹ do include this factor. However, these also involve opposite heat and mass transfer.

Models which calculate the pressure rise inside the porous medium are not applicable because they either use a diffusion mechanism for vapor transport⁵² or they assume a constant evaporation temperature but calculate the vapor flux based on a total pressure gradient.^{53,54} These are also opposite heat and mass transfer cases.

Strek and Nastaj have used the moving boundary concept to model the falling rate period in vacuum drying of a bed of granular material.⁵⁵ Heat and mass transfer are in the same direction, but the experimental conditions are drastically different than those in high intensity paper drying. Mild temperature gradients and large bed thicknesses lead to very long drying times. The nature of the granular material is unlike that of cellulose papermaking fibers; the bed is not compressible and thickness is not sensitive to changes in moisture content.

Baines used a moving boundary concept to model a conventional drying process,⁵⁶ and Ahrens used the concept in modeling high intensity drying.^{9,57} The Ahrens model is highly simplified and based on descriptions of the physical

processes dominant in high intensity conditions. The model is mathematically identical to an elementary analysis of the one-dimensional freezing of water.⁵⁸ The Ahrens model gives reasonable agreement with experimental data and serves as the starting point from which this thesis has been developed.

SUMMARY

Moving boundary models in general prove unsatisfactory for the description of high intensity drying because: they deal with only one component; they assume a constant phase transition temperature equal to the normal phase transition temperature of the one component; they model processes with heat and mass transfer in opposite directions; they usually deal only with boundary conditions of the first kind; they do not account for vapor-pressure-induced liquid convection; and/or they present analytical solutions only for semi-infinite media.

Of the drying models, an elementary one possesses the required characteristics to be used as a starting point for further development. The Ahrens model, which is mathematically identical to a simplified analysis of a freezing water problem, is the starting point of this thesis.

THE MATHEMATICAL MODEL

INTRODUCTION

For modeling purposes, the high intensity process is pictured as a series of linked mechanisms. As the sheet is brought into contact with the hot surface, heat flow into the sheet through a finite contact resistance raises its temperature in a "heatup" regime. The contact resistance depends on the mechanical pressure and on the degree of saturation of the sheet next to the hot surface. Because of the high thermal diffusivity of the (metal) hot surface, its temperature does not change much in reality and remains constant in the mathematical model.

If the sheet surface temperature adjacent to the hot surface becomes incrementally greater than the thermodynamic saturation temperature corresponding to the ambient pressure, then the vapor pressure difference across the sheet is assumed to cause slug flow of the interfiber liquid and air. The position of this slug flow interface defines the limit of linear temperature gradients and thermodynamic saturation so that no vapor flows into the outer zone until the temperature gradient there becomes linear due to heat transfer by conduction and liquid convection within the sheet.

If the sheet becomes saturated before the inner surface temperature exceeds the boiling point, liquid water starts to be mechanically expressed from the sheet and vapor induced liquid flow does not begin until the inner surface temperature exceeds the thermodynamic saturation temperature corresponding to the hydraulic pressure at the inner surface.

Once vapor induced liquid flow starts, the sheet is in the "transition" regime where zones of different moisture content develop inside the sheet. A dry zone is created by evaporation. A zone with water trapped inside the fibers is created

when interfiber water is pushed ahead and the evaporative front has not yet reached the trapped water. If the heat transfer is such that the sheet's outer surface temperature exceeds the boiling point, then a second evaporative front can move into the sheet if the rate of liquid flow toward the cool side is less than the rate of evaporation there.

The "linear" or quasi-static regime begins when all temperature gradients become linear due to heat transfer or when they become linear because all interfiber water has been removed (and the interface defining the limit of linear gradients no longer exists).

ELEMENTARY MODELS

The Ahrens model is formulated to describe macroscopic trends and is based on a few of the physical processes judged to be controlling under high intensity conditions. Figure 7 diagrams the configuration considered.

The paper is divided into a dry zone (devoid of liquid water) adjacent to the hot surface and a wet zone with stagnant liquid adjacent to the dry zone. δ is the time-varying dry zone thickness and δ_T is the total thickness of the fully dry sheet. The wet zone is assumed to be at the boiling point temperature (TB) that corresponds to the ambient pressure. Thus, there is no heatup or transition regime.

The process is considered to be controlled by the rate of heat transfer from the hot surface (at constant temperature T_H) to the paper. The vapor generated at the dry-wet interface flows through the partially saturated wet zone and out of the sheet. The flow resistance of the wet zone is considered to be negligible so that the vapor is generated essentially at TB. (In any case, the difference between the interface temperature and TB would be much less than the

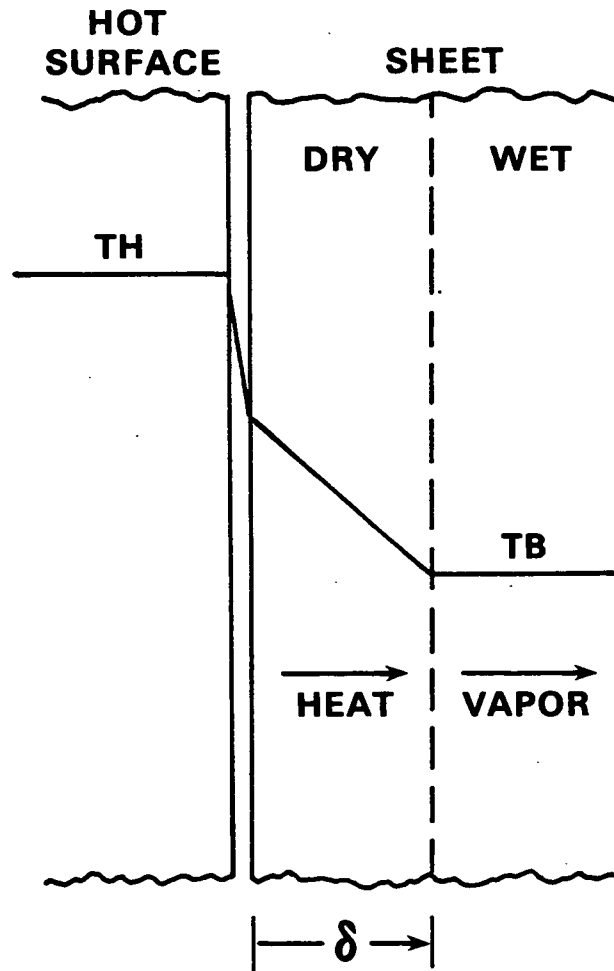


Figure 7. Configuration for Ahrens two zone model.

difference between T_H and T_B). The state of the system is described by an equation for heat flux

$$Q = U*(T_H - T_B) \quad (1)$$

where Q is the heat flux and U is the overall heat transfer coefficient. As a consequence of assuming a linear temperature gradient in the dry zone, U is defined by

$$\frac{1}{U} = \frac{1}{Hc} + \frac{\delta}{Kd} \quad (2)$$

where H_c is the thermal contact coefficient between the hot surface and the sheet and K_d is the thermal conductivity of the dry zone (both assumed constant). The interface energy balance is

$$Q = \epsilon * S * \rho_w * \Delta h * \frac{d\delta}{dt} \quad (3)$$

where ϵ and S are the porosity and saturation of the wet zone, ρ_w is the density of water, Δh is the latent heat (all assumed constant), and t is time; and the relative mass of water removed is

$$MREL = \frac{\delta}{\delta_T} \quad (4)$$

Equations (1) through (3) can be combined to solve for δ as a function of time by separating the variables and using the initial condition that $\delta = 0$ at time = 0. The moisture removal (drying curve) is then given by:

$$MREL = \sqrt{\frac{1}{BI^2} + \tau} - \frac{1}{BI} \quad (5)$$

where BI is the dimensionless Biot number defined by:

$$BI = \frac{H_c * \delta_T}{K_d} \quad (6)$$

and τ , a dimensionless time variable, is defined by:

$$\tau = \frac{2 * K_d * (T_H - T_B) * t}{\Delta h * M_o * \delta_T} \quad (7)$$

where M_o is the initial mass of water present per unit area.

The limiting case of "perfect" thermal contact between the sheet and hot surface ($BI = \infty$) reduces to a zone model with the interface location being directly proportional to the square root of time. Figure 8 graphs the results and⁹ gives some comparisons to experimental data.

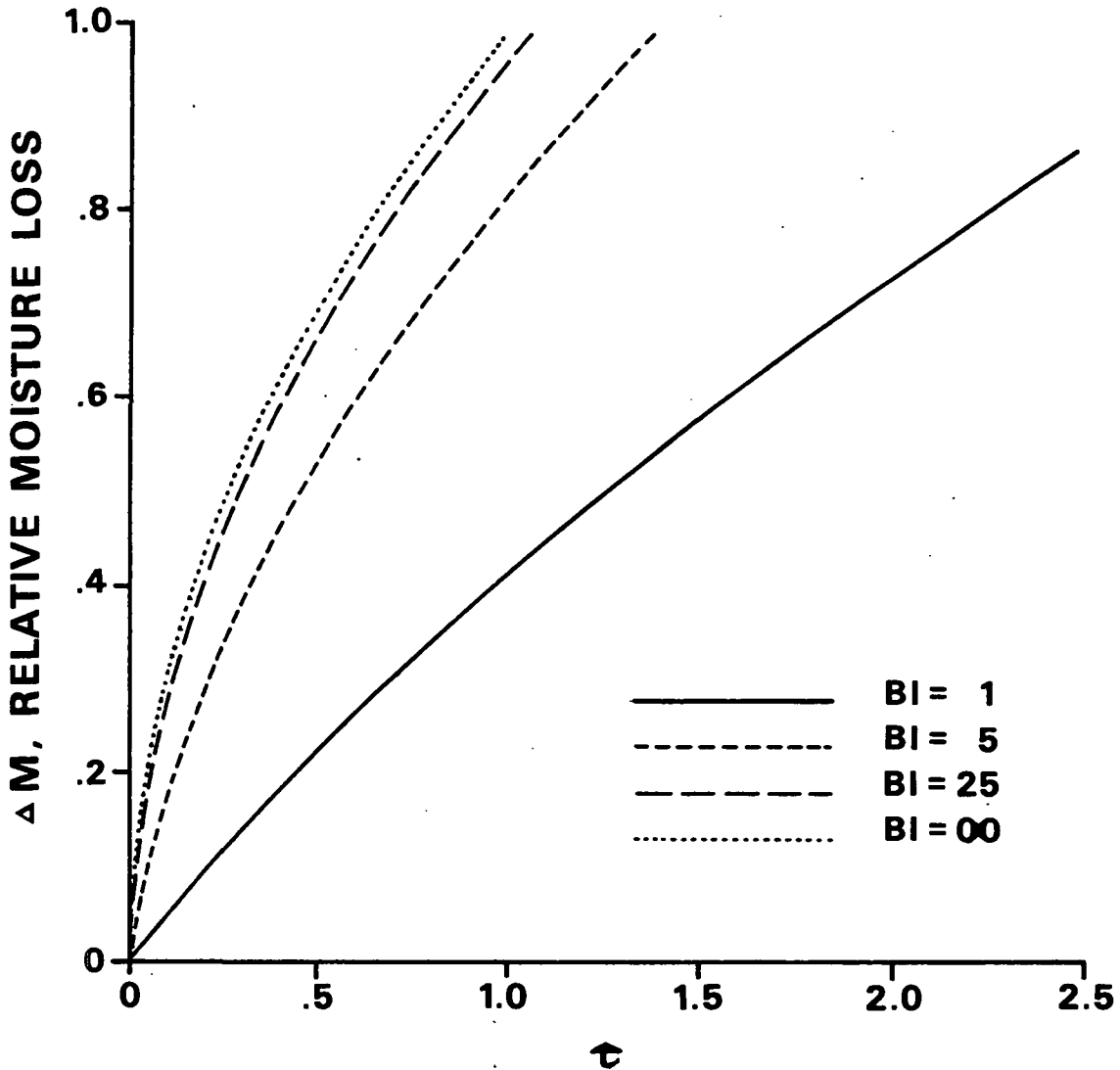


Figure 8. Moisture removal as a function of dimensionless time with Biot number as a parameter for the Ahrens model.

If the permeability of the wet zone were zero, heat transferred by conduction would cause an evaporative front to move into the sheet from the cool side

toward the hot side. Making the same assumptions as in the Ahrens model (stagnant liquid, constant properties, etc.) allows a calculation of moisture loss from:

$$MREL = 1 + \frac{1}{BI} - \sqrt{1 + \frac{2}{BI} + \frac{1}{BI^2} - \tau} \quad (8)$$

where BI and τ are calculated based on the wet zone thermal conductivity and δ_T is the initial sheet thickness. Figure 9 shows the drying curves for this model.

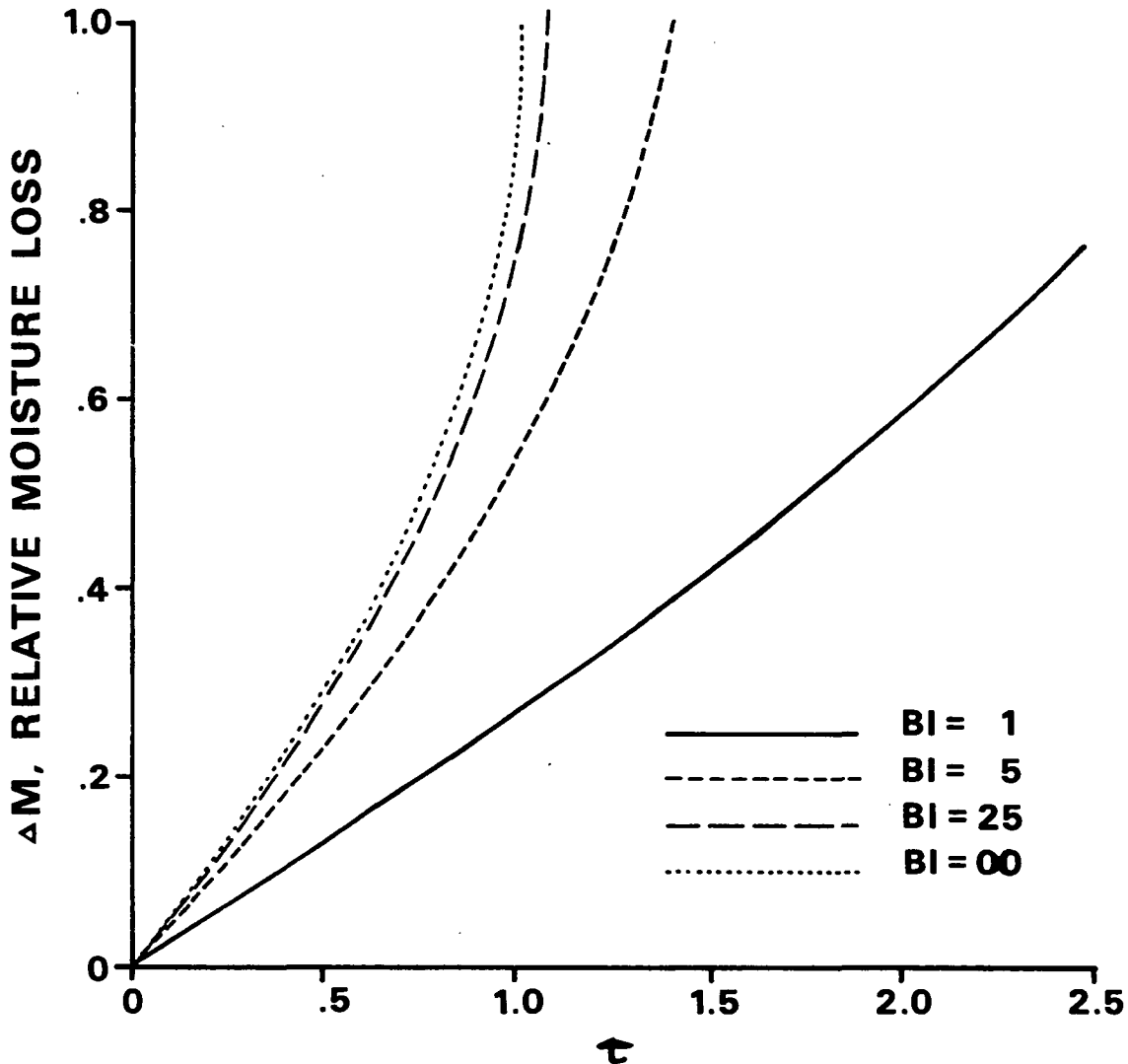


Figure 9. Moisture removal as a function of dimensionless time with Biot number as a parameter for the second limiting case.

DESCRIPTION OF THE ADVANCED MODEL

This thesis is developed from the Ahrens model of high intensity drying. The elementary analysis is extended by accounting for flowing liquid, elevated phase transition temperatures resulting from sheet flow resistance, and hygroscopic effects on latent heat at zone interfaces. The advanced model idealizes the high intensity paper drying process by picturing the sheet as composed of different zones which contain various amounts of fiber, liquid water, and water vapor. The model is based on sets of equations which account for the heat and moisture transfer within and among the zones during three regimes: heatup, transition, and quasi-static. Once the hot surface temperature, boiling point temperature, basis weight, Canadian Standard Freeness (CSF), initial moisture ratio, and mechanical pressure pulse are specified, the equations may be solved to predict the moisture content as a function of time.

The heat and mass balance equations are combined with supplementary equations that describe the nature of the pressure pulse; the liquid and vapor physical properties; and the thermal, compression, and permeability properties of the sheet. The complete model is converted to a FORTRAN program called HIDRYER1.

The program is used to run simulations of various drying conditions by calculating the rates of interface advance, multiplying the rates by a small time increment, and adding to the old values to obtain updated estimates of interface position, zone basis weight, and sheet moisture content.

ASSUMPTIONS

The fundamental assumptions of the model are listed in this section. Other assumptions are listed as they are invoked.

- A1. Heat is transferred to the sheet from the hot surface by conduction only.
- A2. The hot surface is an impermeable boundary.
- A3. There is no conductive heat flux from the sheet to the felt.
- A4. The vapor pressure at the sheet-felt interface is equal to the ambient pressure because of the negligible felt flow resistance.
- A5. Heat and mass transfer occur only in one dimension.
- A6. In the continuity equation, vapor and liquid storage terms within a zone are negligible.
- A7. Change of phase occurs only at the zone interfaces.
- A8. Porosity, saturation, and physical properties are uniform within a zone, but can differ from one zone to another and vary with time.
- A9. Darcy's law is sufficient to describe liquid and vapor flow.
- A10. The fiber flow can be described by a compression equation such that the fiber velocity at any point in a zone is linearly related to the velocities of the interfaces bounding the zone.
- A11. Potential and kinetic energy contributions to the energy equation are negligible compared to thermal energy transfer.
- A12. Conversion of mechanical energy to thermal energy is negligible.
- A13. In energy calculations, the density, thermal conductivity, and specific heat of water vapor are negligible compared to those quantities for liquid water and fiber.
- A14. Local thermal equilibrium exists at all points.
- A15. Gravity effects are negligible.
- A16. A representative value for the vapor and liquid physical properties of a zone may be obtained by calculating the values of

these properties at the temperatures of the interfaces bounding the zone and averaging the results.

- A17. There is no net capillary force on a zone and there is no capillary pressure gradient within a zone.
- A18. Fibers have a zero lumen volume and, in zones where water is present, a constant apparent cell wall density equal to 1.0 g/cc.⁵⁹
- A19. Hygroscopic effects on vapor pressure reduction and moisture distribution in the zones are neglected.
- A20. As the inner zones develop, air is pushed ahead of the progressing interfaces so that the gas in zones with linear temperature gradients is composed of vapor only.

Assumptions A1 through A4 are the overall boundary conditions on the sheet. A1 simply states that radiation heat transfer to the sheet from the hot surface is negligible. Paper emissivity is low and the hot surface-to-sheet temperature difference declines rapidly after contact. A2 means that the hot surface is solid, not porous, and no mass is transferred through it. A3 indicates that the thermal contact from the sheet to the felt is minimal compared to the contact between the hot surface and sheet. A4 means that there is no substantial pressure differential across the felt. Note that this is a condition on the pressure at the outer surface, not a condition on the temperature there.

A5 is an approximation to the overall direction of heat and mass transfer because the thickness of the sheet is much less than the lateral dimensions.

A6 through A8 pertain to the continuity equations for the model. A6 is an assumption of slug flow to simplify the transport calculations. A7 and A8 allow each zone to be characterized by its own unique value of moisture content and

state that this moisture content is not altered by vapor condensing within the zone.

A9 and A10 are for the momentum equations. Darcy's law is the momentum equation for flowing liquid and vapor. Calculations show that the Reynolds number is well within the appropriate regime for suitable application of Darcy's law.⁶⁰ A10 allows the momentum equation for the deforming fiber bed to be replaced by a simple compression equation and states that each zone undergoes its own uniform compression.

Assumptions A11 through A15 pertain to the energy equation. All are standard assumptions used in drying models.^{61,62}

A16 is made so that unique values can characterize a zone's vapor and liquid properties and variations with position in the zone can be neglected.

A17 might appear to be the most questionable approximation. The capillary pressure is typically calculated with the Laplace equation

$$P_{cap} = \frac{2 * \gamma * \cos \theta}{r} \quad (9)$$

where P_{cap} is the capillary pressure, γ is the liquid surface tension, θ is the contact angle, and r is the pore radius. First, this applies to pores of circular cross section and therefore should NOT apply to paper since it has irregularly shaped pores. Second, at high drying temperatures the surface tension of water is drastically reduced and this serves to decrease P_{cap} . Third, even at elevated mechanical pressure there are still many pores in the sheet with large radii.⁶³ Fourth, the equation applies to a SATURATED pore, and it requires very

large mechanical pressures to achieve interfiber saturation. Therefore, at least in the initial stages of drying, the larger pores remain unsaturated.

When the sheet does become saturated, then a significant capillary pressure might be expected. However, it is exactly in this regime (wet pressing) that moisture loss by liquid expression dominates water removal and so the "drying" (evaporative) aspect becomes a secondary process. Thus, A17 may not be as bad an approximation as it would first appear to be. The net result is that the liquid pressure (and its gradient) is identical to the vapor pressure (and its gradient).

A18 is a means of trapping a certain fraction of liquid inside the fibers, thereby making it unavailable for vapor-induced displacement. Since the actual density of cellulose is about 1.55 g/cc, an apparent cell wall density of 1.0 g/cc means that roughly one-third of the fiber volume can contain liquid. Given the density of water and a "typical" fiber cross-sectional area, it is possible to determine the moisture ratio at which the fibers just become saturated.

Furthermore, by holding the apparent cell wall density fixed, a limit is placed on the minimum porosity attainable. Compressing the sheet is equivalent to moving the fibers closer together. The porosity of the zone can be no lower than the fiber wall porosity (about 0.33). In dry zones, A18 allows the porosity to go to zero by removing the apparent cell wall density restriction. Since there is no water there to occupy the space, the fiber wall can collapse.

A19 is made so that the moisture distribution in a zone can be treated as uniform and so that the vapor pressure is simply a function of the temperature. However, the hygroscopic effect on the heat of desorption is accounted for, since it strongly influences heat transfer calculations. This is detailed later in the thesis.

A20 is a convenience to simplify the mass and energy equations in zones of linear temperature gradient (zones where vapor flow is handled by Darcy's law) and to eliminate the need for a detailed gas continuity equation in the outer zone during the transition regime.

ADVANCED MODEL EQUATIONS

Continuity and energy equations determine the temperatures and rates of change of position of the interfaces and describe the heat and mass transfer within each zone. The interfaces separate zones of different moisture content. Figure 10 shows each kind of zone that may be present and the terminology for the zones, interfaces, and temperatures. Interface 1 separates zone 1 (no liquid moisture), which is adjacent to the hot surface, from zone 2 (liquid moisture only inside the fibers). Interface 2 separates zone 2 from zone 3 (liquid moisture inside and outside the fibers), or zone 2 from zone 4 (no liquid moisture), which can develop if heat is transferred to the far side of the sheet faster than interfiber liquid can flow there. Interface 3 separates zone 3 from zone 4. If zone 3 does not exist, either because there is initially not enough moisture present to saturate the fibers or because all the interfiber liquid is pushed out or evaporated, HIDRYER1 places interface 3 at δ_T .

The reasonable assumption of linear temperature gradients in zones 1 and 2 because of the low moisture contents and the porosities, and because of the low specific heat of cellulose, introduces a considerable simplification to the required calculations. For example, the energy equations for these zones are converted from partial differential equations to algebraic ones (which are easily solved provided the interface temperatures can be determined). Thus, the zone concept is a means of simplifying a more "continuous" type of model by limiting the regions over which detailed calculations have to be performed.

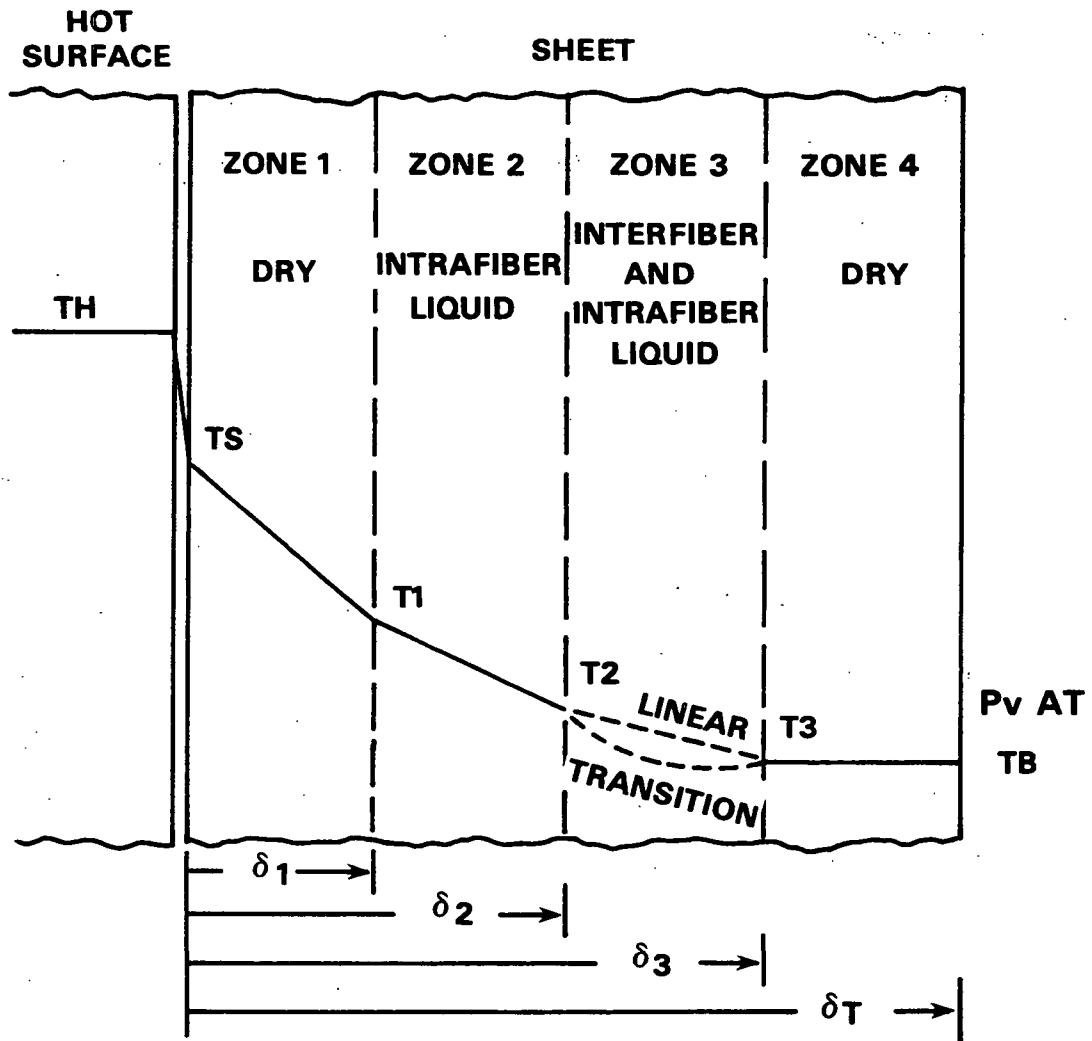


Figure 10. Zone, interface, and temperature designations for advanced model equations.

Zone Continuity and Momentum Equations

Consider the one-dimensional flow of a mixture of fibers, liquid water, and a gas composed of water vapor. Consider further that a certain fraction of the liquid water is trapped within the fibers and moves at the fiber velocity. The continuity equation is:

$$\begin{aligned} \frac{\partial}{\partial t} (\rho_F * (1-\epsilon) + \rho_w * (1-a) * \epsilon * S + \rho_w * a * \epsilon * S + \rho_v * \epsilon * (1-S)) = \\ - \frac{\partial}{\partial z} (\rho_F * (1-\epsilon) * V_f + \rho_w * (1-a) * \epsilon * S * V_f \\ + \rho_w * a * \epsilon * S * V_{water} + \rho_v * \epsilon * (1-S) * V_{gas}) \end{aligned} \quad (10)$$

where ρ_F , ρ_W , and ρ_V are the fiber, water, and vapor densities; a is the fraction of liquid water external to the fibers; V_f , V_{water} , and V_{gas} are the fiber, water, and vapor velocities relative to the fixed origin; z is the position coordinate and t is time.

Darcy's law, the momentum equation for the flowing gas and liquid, is used to describe the velocities of the flowing gas and liquid relative to the moving fibers.⁶⁴

$$V_v = \epsilon * (1-S) * (V_{gas}-V_f) = - \frac{K_a * K_v}{\mu_v} * \frac{\partial P_v}{\partial z} \quad (11)$$

$$V_w = a * \epsilon * S * (V_{water}-V_f) = - \frac{K_a * K_w}{\mu_w} * \frac{\partial P_w}{\partial z} \quad (12)$$

where V_v and V_w are the vapor and liquid superficial velocities relative to the moving fibers; K_a is the absolute permeability; K_v and K_w are the vapor and liquid relative permeabilities; P_v and P_w are the vapor and liquid pressures; and μ_v and μ_w are the vapor and liquid viscosities.

With these definitions, the continuity equation can be written as:

$$\frac{\partial D}{\partial t} = - \frac{\partial}{\partial z} (D * V_f + \rho_w * V_w + \rho_v * V_v) \quad (13)$$

where

$$D = \rho_F * (1-\epsilon) + \rho_w * \epsilon * S + \rho_v * \epsilon * (1-S) \quad (14)$$

However, $\rho_v \ll \rho_w < \rho_F$, and with

$$S = \frac{(1-\epsilon) * M_R * \rho_F}{\rho_w * \epsilon} \quad (15)$$

then

$$D = \rho_F * (1-\epsilon) * (1+MR) \quad (16)$$

where MR is the moisture ratio.

The momentum equation for each zone of the fiber matrix is replaced by a power law compression equation:

$$C = M * p^N \quad (17)$$

where C is the dry fiber concentration (mass/total volume), and where each zone has its own compression constants (M and N) and effective mechanical pressure (P); the assumption of uniform zone compressibility gives

$$V_f = \frac{\bar{L}}{L} * \frac{\partial L}{\partial t} + V_f' \quad (18)$$

where \bar{L} is the distance inside the zone measured from the zone's interface closer to the origin, L is the zone thickness, $\partial L/\partial t$ is the "compression velocity" or change in zone thickness caused by P, and V_f' is the compression velocity of the zone interface closer to the origin with respect to that (fixed) origin.

For an unsaturated medium during the heatup regime, make the approximation that $V_{water} = V_f$ so that $V_w = 0$. (This is a compression model, not a wet pressing model.) For this case, and for an unsaturated or saturated zone in the transition or linear regimes, use assumption A6 so that the continuity equation becomes

$$\frac{\partial D}{\partial t} = - \frac{\partial}{\partial z} (D * V_f) \quad (19)$$

If the sheet becomes saturated during heatup, its compression is significantly affected by the buildup of a substantial internal hydraulic pressure. The overall continuity equation can be separated into its fiber and water components and combined with Darcy's law to produce:

$$\frac{\partial MR}{\partial t} = \frac{\rho_w * Ka * Kw}{(1-\epsilon) * \rho_F * \mu_w} * \frac{\partial^2 P_w}{\partial z^2} \quad (20)$$

Write $\partial MR/\partial t$ as $(\partial MR/\partial L) * (\partial L/\partial t)$ and when $S = 1$, $\partial MR/\partial L = \rho_w/BW$ where BW is the sheet basis weight. With $BW/L = (1-\epsilon) * \rho_F$ and $Kw = 1$ when $S = 1$, Eq. (20) becomes

$$\frac{1}{L} * \frac{\partial L}{\partial t} = \frac{Ka}{\mu_w} * \frac{\partial^2 P_w}{\partial z^2} \quad (21)$$

Let

$$P_w = A_1 + A_2 * z + A_3 * z^2 \quad (22)$$

so that

$$\frac{\partial P_w}{\partial z} = A_2 + 2 * A_3 * z \quad (23)$$

and

$$\frac{\partial^2 P_w}{\partial z^2} = 2 * A_3 \quad (24)$$

At $z = 0$, $\partial P_w/\partial z = 0$ and therefore $A_2 = 0$. Integrating Eq. (22) from $z = 0$ to $z = L$ and noting that at $z = L$ $\partial P_w/\partial z = 2 * A_3 * L$ and $P_w = P_{atm}$ (the ambient pressure) allows a calculation of A_1 and A_3 to yield:

$$P_w = P_{atm} + \frac{\mu_w * (z^2 - L^2)}{2 * Ka * L} * \frac{\partial L}{\partial t} \quad (25)$$

For simplicity, define an integral-average hydraulic pressure such that

$$\overline{P_w} = P_{atm} - \frac{\mu_w * L}{3 * K_a} * \frac{\partial L}{\partial t} \quad (26)$$

and use $P = P_{mech} - \overline{P_w}$ in the compression equation, where P_{mech} is the absolute applied mechanical pressure. The applied mechanical pressure is the sum of P_{mechg} (the gage mechanical pressure) and ambient pressure and therefore

$$P = P_{mechg} + \frac{\mu_w * L}{3 * K_a} * \frac{\partial L}{\partial t} \quad (27)$$

With $C = M * P^N = BW/L$ and $K_a = 1/(R * C)$ then

$$\frac{\partial L}{\partial t} = \frac{3 * ((C/M)^{1/N} - P_{mechg})}{\mu_w * BW * R} \quad (28)$$

R , the specific filtration resistance, is a function of P_{mechg} ; P_{mechg} is a prescribed function of time, so Eq. (28) is an initial value problem solvable by standard numerical techniques once L at $t = 0$ is specified.

Zone Thermal Energy Equation

Consider a one-dimensional energy equation where energy is transferred only by conduction or convection. Using the same kinds of manipulation as in the continuity equation gives:

$$\begin{aligned} \frac{\partial}{\partial t} (D_c * T) = & - \frac{\partial}{\partial z} (-K * \frac{\partial T}{\partial z} \\ & + (D_c * V_f + \rho_w * C_{pw} * V_w + \rho_v * C_{pv} * V_v) * T \end{aligned} \quad (29)$$

where T is temperature, K is thermal conductivity, C_{pw} and C_{pv} are the constant pressure specific heats of water and vapor, and where

$$Dc = \rho_F * (1-\epsilon) * C_{pf} + \rho_w * \epsilon * S * C_{pw} + \rho_v * \epsilon * (1-S) * C_{pv} \quad (30)$$

C_{pf} is the constant pressure specific heat of cellulose and with Eq. (15)

$$Dc = \rho_F * (1-\epsilon) * (C_{pf} + MR * C_{pw}) \quad (31)$$

Observe that $Dc = b * D$ where

$$b = \frac{(C_{pf} + MR * C_{pw})}{(1 + MR)} \quad (32)$$

Expand and rearrange Eq. (29) noting that b is independent of z within a given zone and use continuity Eq. (13) to simplify; divide by $b * D$ to obtain

$$\begin{aligned} \frac{\partial T}{\partial t} + \frac{T}{b} * \frac{\partial b}{\partial t} + \frac{T}{D} * \frac{\partial}{\partial z} \left(\left(\frac{C_{pw}}{b} - 1 \right) * \rho_w * V_w + \left(\frac{C_{pv}}{b} - 1 \right) * \rho_v * V_v \right) = \\ \frac{K}{b * D} * \frac{\partial^2 T}{\partial z^2} - \left(V_f + \frac{\rho_w * C_{pw} * V_w}{b * D} + \frac{\rho_v * C_{pv} * V_v}{b * D} \right) * \frac{\partial T}{\partial z} \end{aligned} \quad (33)$$

For a nonsaturated medium $\partial b / \partial t = 0$ (C_{pf} and C_{pw} held constant). Using the slug flow assumption and the approximation $\rho_v * C_{pv} / (b * D) = 0$ gives

$$\frac{\partial T}{\partial t} = \frac{K}{b * D} * \frac{\partial^2 T}{\partial z^2} - V_f * \frac{\partial T}{\partial z} \quad (34)$$

for the nonsaturated heatup regime (with $V_w = 0$ as before) and

$$\frac{\partial T}{\partial t} = \frac{K}{b * D} * \frac{\partial^2 T}{\partial z^2} - \left(V_f + \frac{\rho_w * C_{pw} * V_w}{b * D} \right) * \frac{\partial T}{\partial z} \quad (35)$$

for the saturated heatup regime and the saturated or nonsaturated outer zone during the transition regime. Equations (34) and (35) must be solved to yield the temperature profiles.

For the inner zone during transition and all zones during the quasi-static regime no energy equation is required, since all temperature gradients are assumed linear.

Convective-Diffusion Equations

Two general methods available for the solution of Eq. (34) and (35) are transformation of variables and numerical solution. Transform Eq. (34) by defining $x = z/L$ and $t' = t$ so that $\partial x/\partial z = 1/L$, $\partial x/\partial t = -(z/L^2) * \partial L/\partial t$, $\partial t'/\partial z = 0$, and $\partial t'/\partial t = 1$. Thus, $\partial T/\partial z = (1/L) * \partial T/\partial x$, $\partial^2 T/\partial z^2 = (1/L^2) * \partial^2 T/\partial x^2$, and $\partial T/\partial t = \partial T/\partial t' - (z/L^2) * \partial L/\partial t * \partial T/\partial x$. Since $V_f = (z/L) * \partial L/\partial t$, substitution converts Eq. (34) to

$$\frac{\partial T}{\partial t'} = \psi * \frac{\partial^2 T}{\partial x^2} \tag{36}$$

where

$$\psi = \frac{K}{b * D * L} \tag{37}$$

The initial condition is $T = T_I$ at $t' = 0$ for all x . The boundary conditions are: $BI * (T_H - T) = -\partial T/\partial x$ at $x = 0$ and $\partial T/\partial x = 0$ at $x = 1$. The first BC is a statement of the imperfect thermal contact between the hot surface and sheet with $BI = H_c * L/K$. The second BC is the assumption of no conductive heat flux from the sheet to the felt.

Equation (35) requires different transformations depending on its application to the saturated heatup or saturated or nonsaturated transition regimes. For the saturated heatup regime continuity demands $V_w = -(z/L) * \partial L/\partial t$. The same transformation of variables as for Eq. (34) gives

$$\frac{\partial T}{\partial t'} = \psi * \frac{\partial^2 T}{\partial x^2} + \phi * \frac{\partial T}{\partial x} \quad (38)$$

with ψ as in Eq. (37) and

$$\phi = - \frac{\rho_w * C_{pw} * x}{b * D * L} * \frac{\partial L}{\partial t'} \quad (39)$$

The initial and boundary conditions are the same as before.

The application of Eq. (35) to the outer zone during transition requires a different transformation. The outer zone is designated as zone 3 and is bounded by interfaces 1 and 3 or 2 and 3. Define $x = (z - L_2 - L_1)/L_3$ and $t' = t$ so that $\partial x/\partial z = 1/L_3$, $\partial x/\partial t = -(\partial L_1/\partial t + \partial L_2/\partial t + x * \partial L_3/\partial t)/L_3$, and again $\partial t'/\partial z = 0$ and $\partial t'/\partial t = 1$. L_1 , L_2 , and L_3 are the thicknesses of zones 1, 2, and 3. Substitution into Eq. (35) yields an equation of the form of Eq. (38) with

$$\psi = \frac{K}{b * D * L_3} \quad (40)$$

and

$$\phi = \frac{\rho_w * C_{pw} * V_w}{b * D * L_3} \quad (41)$$

The value of V_w is uniform in zone 3 by the slug flow assumption and is calculated using Darcy's law (with the pressure gradient given by the vapor pressure drop across zone 3). The initial condition for this case is the temperature distribution just after the heatup regime. The boundary conditions are that the heat conducted to interface 1 or 2 is just balanced by the sum of the heat conducted into zone 3 and a "source" or "sink" term composed of the latent heat and the net condensation or evaporation at interface 1 or 2. The other boundary condition is that there is no net conductive heat flux past interface 3.

A numerical scheme is needed to solve Eq. (38). A stable, high-order accuracy, finite difference method is available which uses weighted finite differences to overcome calculational instabilities.⁶⁵ This method also removes some severe restrictions on the time step-grid spacing combination typical of other convective-diffusion numerical solutions. The second spatial derivative is treated as a central difference:

$$\frac{\partial^2 T}{\partial x^2} = \frac{T(i+1,j) - 2 * T(i,j) + T(i-1,j)}{\Delta x^2} \quad (42)$$

where Δx is the grid spacing, i is the grid number ($i = 1$ to $i = k$), and j is the time increment number. The time derivative is treated as a forward difference:

$$\frac{\partial T}{\partial t'} = \frac{T(i,j+1) - T(i,j)}{\Delta t} \quad (43)$$

where Δt is the time increment. The temperature gradient is treated as an upstream weighted difference. Since $\phi > 0$ for the outer zone cases considered in this thesis,

$$\frac{\partial T}{\partial x} = \frac{2 * T(i+1,j) + 3 * T(i,j) - 6 * T(i-1,j) + T(i-2,j)}{6 * \Delta x} \quad (44)$$

Equations 42 through 44 are combined to give

$$\begin{aligned} T(i,j+1) = & (A - B/3) * T(i+1,j) + (1 - 2 * A - B/2) * T(i,j) \\ & + (A + B) * T(i-1,j) - (B/6) * T(i-2,j) \end{aligned} \quad (45)$$

where

$$A = \frac{\psi * \Delta t}{\Delta x^2} \quad (46)$$

and

$$B = \frac{\phi * \Delta t}{\Delta x} \quad (47)$$

and HIDRYER1 maintains

$$\Delta t < \frac{\Delta x}{2 * \psi / \Delta x + \phi / 2} \quad (48)$$

Equation 45 applies from $i = 3$ to $i = k-1$. At $i = 2$, a central difference operator is used for $\partial T / \partial x$ to give

$$\begin{aligned} T(2,j+1) &= (A - B/2) * T(3,j) + (1 - 2 * A) * T(2,j) \\ &+ (A + B/2) * T(1,j) \end{aligned} \quad (49)$$

At the boundaries $i = 1$ and $i = k$ the operative equation is derived by integrating the energy equation over a half interval.⁶⁶ At $x = 0$, integrate from 0 to $\Delta x/2$ to obtain:

$$\frac{\Delta x}{2} * \frac{\partial T}{\partial t'(avg)} = \psi * \left. \frac{\partial T}{\partial x} \right|_0^{\Delta x/2} - \bar{\phi} * T \Big|_0^{\Delta x/2} \quad (50)$$

$\bar{\phi}$ and $\partial T / \partial t'(avg)$ are averages over the half interval such that

$$\bar{\phi} = \frac{\phi(\Delta x/2) + \phi(0)}{2} \quad (51)$$

and

$$\frac{\partial T}{\partial t'(avg)} = \frac{1}{2} * \left(\frac{\partial T}{\partial t'(\Delta x/2)} + \frac{\partial T}{\partial t'(0)} \right) \quad (52)$$

Let

$$\frac{\partial T}{\partial t'(\Delta x/2)} = \frac{1}{2} * \left(\frac{\partial T}{\partial t'(\Delta x)} + \frac{\partial T}{\partial t'(0)} \right) \quad (53)$$

so that

$$\frac{\partial T}{\partial t'(\text{avg})} = \frac{1}{4} * \left(\frac{\partial T}{\partial t'(\Delta x)} + 3 * \frac{\partial T}{\partial t'(0)} \right) \quad (54)$$

and Eq. (33) can be used to find the time derivatives at $x = \Delta x$ and $x = 0$.

Let

$$\frac{\partial T}{\partial x(\Delta x/2)} = \frac{1}{2} * \left(\frac{\partial T}{\partial x(\Delta x)} + \frac{\partial T}{\partial x(0)} \right) \quad (55)$$

Apply the boundary condition $BI*(TH - T(1,j)) = -\partial T/\partial x(0)$ and

$$\frac{\partial T}{\partial x(0)} = \frac{2}{\Delta x} * T \Big|_0^{\Delta x/2} \quad (56)$$

to get $T(\Delta x/2)$. Let

$$\frac{\partial T}{\partial x(\Delta x)} = \frac{-2 * T(1,j) - 3 * T(2,j) + 6 * T(3,j) - T(4,j)}{6 * \Delta x} \quad (57)$$

to get

$$\begin{aligned} T(1,j+1) = & T(1,j) - (T(2,j+1) - T(2,j))/3 \\ & + 4 * B * BI * \Delta x * (TH - T(1,j))/3 + (2 * A/9) * (6 * BI * \Delta x \\ & * (TH - T(1,j)) - 2 * T(1,j) - 3 * T(2,j) + 6 * T(3,j) - T(4,j)) \end{aligned} \quad (58)$$

At the cold side, integrate from $x = 1 - \Delta x/2$ to $x = 1$. Apply the boundary condition $\partial T/\partial x(1) = 0$ and use similar averaging techniques to get

$$\begin{aligned} T(k,j+1) = & T(k,j) - (T(k-1,j+1) - T(k-1,j))/3 \\ & - (2*A/9) * (2 * T(k,j) + 3 * T(k-1,j) - 6 * T(k-2,j) + T(k-3,j)) \end{aligned} \quad (59)$$

Observe that when $\phi = 0$ Eq. (45), (49), (58), and (59) are solutions of Eq. (36) and so all cases are covered.

As δ_2 and δ_3 move into the sheet, a modification of the numerical method is employed. The first grid point in the transition zone is designated as i' . The last grid point of the transition zone is designated as i'' . δ' and δ'' are the distances of these points from the origin. Because the distance between these special grid points and the interfaces closest to them may not correspond to the usual grid point spacing, temperatures at i' , i'' , and the grid points adjacent to them must be calculated based on uncentered finite differences.

Taylor series expansions for the temperatures at the grid points around the one in question can be added, subtracted, and combined to give

$$\begin{aligned}
 T(i',j+1) = & T(i',j) - \phi * \Delta t * (T(i'+1,j) - T_x)/(\Delta x + \text{DIFF}') \\
 & + 2 * \psi * \Delta t * (T(i'+1,j))/(\Delta x * (\Delta x + \text{DIFF}')) \\
 & - T(i',j)/(\Delta x * \text{DIFF}') + T_x/(\text{DIFF}' * (\Delta x + \text{DIFF}')) \quad (60)
 \end{aligned}$$

where T_x is either T_1 or T_2 depending on which interface is involved. The model treats the transition zone as if it were part of one large zone undergoing heating and compression. Instead of applying boundary conditions and calculating new temperatures for all the grid points, the model simply calculates the bounding interface temperatures from the interface equations and applies these temperatures directly. In terms of the relative (dimensionless) distance Δx

$$\text{DIFF}' = \frac{BW_3 * (1 + BW_4/BW)}{BW} - \Delta x * (1 - i' + i'') \quad (61)$$

At the other end

$$\begin{aligned}
 T(i'',j+1) = & T(i'',j) - \phi * \Delta t * (T_x - T(i''-1,j))/(\Delta x + \text{DIFF}'') \\
 & + 2 * \psi * \Delta t * (T_x/(\text{DIFF}'' * (\Delta x + \text{DIFF}''))) \\
 & - T(i'',j)/(\Delta x * \text{DIFF}'') \\
 & + T(i''-1,j)/(\Delta x * (\Delta x + \text{DIFF}'')) \quad (62)
 \end{aligned}$$

where

$$\text{DIFF}'' = \Delta x - \frac{\text{BW3} * \text{BW4}}{\text{BW}} \quad (63)$$

and T_x is either T_2 or T_3 . The new temperature at $i'+1$ is found from Eq. (49). If DIFF' is equal to Δx or if the interface advances across a grid point, then Eq. (49) is also used at i' and Eq. (60) is bypassed. All other interior points are calculated with Eq. (45), but the temperature at i'' is found with Eq. (62) if DIFF'' is less than Δx and the interface does not cross a grid point.

Interface Equations

During the high intensity drying process zones of different moisture content develop inside the sheet. These zones are bounded by interfaces at various temperatures. The temperatures determine the rates of heat transfer and rates of change of interface position; since the interfaces separate zones of different moisture content, their positions are directly related to the overall sheet moisture content. Refer to Fig. 10 for the zones that may be present and the terminology for the zones, interfaces, and temperatures.

The "dry" zones contain water vapor. Zone 2 contains liquid water only inside the fibers. Zone 3 contains liquid water inside and outside the fibers.

Consider a "general" interface. Heat, liquid, and gas (vapor only) flow toward the interface on the (-) side close to the hot surface and flow away from the interface on the (+) side toward the felt. The net mass flux results in a change in interface position and is calculated from

$$(\rho_w * V_w(+)) - \rho_w * V_w(-)) + (\rho_v * V_v(+)) - \rho_v * V_v(-)) = \epsilon * S * \rho_w * d\delta/dt \quad (64)$$

for interfaces 1 and 2 and

$$\rho_w * V_w(-) - (\rho_v * V_v(+) - \rho_v * V_v(-)) = \epsilon * S * \rho_w * d\delta/dt \quad (65)$$

at interface 3. There is no liquid flow on the (+) side of interface 3 (unless $\delta_3 = \delta_T$) because any flow past δ_3 would be absorbed by the dry fibers in zone 4.

An energy balance gives

$$Q(-) = Q(+) + (\rho_v * V_v(+) - \rho_v * V_v(-)) * (\Delta h + \Delta h^*) \quad (66)$$

at interfaces 1 and 2; at interface 3 the energy balance gives

$$Q(-) = (\rho_v * V_v(+) - \rho_v * V_v(-)) * (\Delta h + \Delta h^*) \quad (67)$$

where Δh^* is the average heat of desorption at the interface.

Heatup and Transition Regimes

During the heatup regime there is only one zone (2 or 3) present, since the sheet starts and stays at uniform saturation. Interface 1 is at $z = 0$. Interface 2 is at δ_T if zone 2 is present and at $z = 0$ if zone 3 is present. Interface 3 is at δ_T . It is assumed that no evaporation takes place during heatup.

When TS is raised incrementally above the saturation temperature corresponding to the hydraulic pressure at $z = 0$, the liquid in the pores of the sheet sees the apparent pressure gradient corresponding to the vapor pressures at TS and TB. The liquid is assumed to flow in slug flow, and δ_2 defines the limit of thermodynamic saturation (and linear temperature gradient) so that no vapor flows past δ_2 in transition. For the first time increment the only nonzero term of Eq. (64) is $\rho_w * V_w(+)$. By assumption, the vapor and liquid pressures are identical and Darcy's law for the flowing liquid is

$$V_w = - \frac{Ka_3 * K_w}{\mu_w} * \frac{\partial P_v}{\partial z} \quad (68)$$

where Ka_3 is the absolute permeability of zone 3. To link the mass and energy balance equations write $\partial Pv/\partial z$ as $(\partial Pv/\partial T) * (\partial T/\partial z)$. The correct expression for $\partial T/\partial z$ is $(TB - TS)/\delta_T$, the virtual gradient that the liquid experiences. Then, from Eq. (64) and (68)

$$\rho_w * KAKW * \frac{\partial Pv}{\partial T} * \frac{(TS - TB)}{(\mu_w * \delta_T)} = \epsilon' * S' * \rho_w * D2 \quad (69)$$

where $KAKW = Ka_3 * K_w$, ϵ' and S' are the interfiber porosity and saturation (since only interfiber water flows), and $D2$ is the rate of change of position of δ_2 due only to vapor-induced liquid flow. This rate multiplied by $BW * \Delta t/\delta_T$ gives an increment in the basis weight of zone 2 and a corresponding decrement in the basis weight of zone 3. The increment or decrement is added to the old value of zone basis weight to get a new value at $TIME(new) = TIME(old) + \Delta t$. The liquid properties are evaluated at TS .

If no interfiber water exists, the transition regime is simply a continuation of the heatup regime calculation until the temperature at δ_T is raised incrementally above TB . Then, a dry zone propagates into the sheet toward the hot surface. This case is treated later.

After the first time increment, two cases can occur: δ_1 and δ_2 are either equal or they are unequal. When $\delta_1 = \delta_2$ the only nonzero term in Eq. (64) is $\rho_w * Vw(+)$. Since no vapor flows $Q(-) = Q(+)$, where $Q(-) = U * (TH - T2)$ and $Q(+) = K3 * (T2 - T')/(\delta' - \delta_2)$. U is defined so that $1/U = 1/Hc + \delta_2/K1$. T' is the temperature at the first finite difference grid point in zone 3, δ' is the distance of this grid point from the origin, and $K1$ and $K3$ are the thermal conductivities of zones 1 and 3. From the heat balance, a new value for $T2$ is isolated as

$$T_2 = \frac{T_H + I * T'}{1 + I} \quad (70)$$

where

$$I = \left(\frac{1}{H_c} + \frac{\delta_2}{K_1} \right) * \left(\frac{K_3}{\delta_1 - \delta_2} \right) \quad (71)$$

Of course, when $\delta_1 = \delta_2$, $T_1 = T_2$. The mass balance gives the rate of advance of interface 2 using Eq. (69) with the (virtual) temperature gradient $(T_2 - T_3)/(\delta_3 - \delta_2)$. If $\delta_3 = \delta_T$ then T_B is used in place of T_3 .

If δ_1 and δ_2 are not equal, then equations are needed at both interfaces. At δ_1 , $\rho_v * V_v(+)$ is the only nonzero mass flow term. Thus,

$$\rho_v * \frac{K_{a2}}{\mu_v} * \frac{\partial P_v}{\partial T} * \frac{(T_1 - T_2)}{(\delta_2 - \delta_1)} = \epsilon_2 * S_2 * \rho_w * D_4 \quad (72)$$

D_4 is the rate of advance of δ_2 due solely to evaporation. ϵ_2 and S_2 are the porosity and saturation of zone 2. Vapor properties are evaluated at T_1 and T_2 and then averaged. In the heat balance, $Q(-) = U * (T_H - T_1)$ and $Q(+) = K_2 * (T_1 - T_2)/(\delta_2 - \delta_1)$. Isolating for T_1 gives

$$T_1 = \frac{T_H + I * T_2}{1 + I} \quad (73)$$

where

$$I = \left(\frac{1}{H_c} + \frac{\delta_1}{K_1} \right) * \frac{1}{(\delta_2 - \delta_1)} * \left(\frac{\rho_v * K_{a2} * (\Delta h + \Delta h^*)}{\mu_v} * \frac{\partial P_v}{\partial T} + K_2 \right) \quad (74)$$

The vapor properties, except Δh , are averaged using T_1 and T_2 . Δh is evaluated at T_1 only and Δh^* is the latent heat correction factor based on the moisture ratios of zones 1 and 2.

At δ_2 , $\rho_w * Vw(+)$ and $\rho_v * Vv(-)$ are the mass flow terms. $\rho_v * Vv(-)$ at δ_2 is just $\rho_v * Vv(+)$ at δ_1 . $\rho_w * Vw(+)$ is derived as for Eq. (68) and (69) so that

$$\frac{\rho_w * KAKW * (T2 - T3)}{\mu_w * (\delta_3 - \delta_2)} * \frac{\partial P_v}{\partial T} - \frac{\rho_v * Ka2 * (T1 - T2)}{\mu_v * (\delta_2 - \delta_1)} * \frac{\partial P_v}{\partial T} = \epsilon' * S' * \rho_w * D5 \quad (75)$$

D5 is the net rate of motion of δ_2 . Vapor and liquid properties are averaged with T2 and T3 or T1 and T2 as appropriate. In the heat balance, Q(-) is the same as Q(+) at δ_1 . $Q(+) = K3 * (T2 - T') / (\delta' - \delta_2)$, so that

$$T2 = \frac{II * T1 + T'}{1 + II} \quad (76)$$

where

$$II = \left(\frac{K2}{K3} + \frac{\rho_v * Ka2 * (\Delta h + \Delta h^*)}{\mu_v * K3} * \frac{\partial P_v}{\partial T} \right) * \frac{(\delta' - \delta_2)}{(\delta_2 - \delta_1)} \quad (77)$$

The vapor properties are evaluated in the usual way. Equations (73) and (76) then yield

$$T1 = \frac{(1 + II) * TH + I * T'}{1 + I + II} \quad (78)$$

$$T2 = \frac{II * TH + (1 + I) * T'}{1 + I + II} \quad (79)$$

HIDRYER1 calculates T' and then finds T1 and T2.

If $\delta_3 = \delta_T$ and T3 is equal to TB then

$$\frac{K3}{\Delta h + \Delta h^*} * \frac{(T3 - T'')}{\Delta x} = \epsilon_3 * S3 * \rho_w * D6 \quad (80)$$

where T'' is the temperature of the first finite difference grid point just toward the origin relative to δ_3 . If T_3 is less than T_B then $D_6 = 0$.

The liquid mass flow to δ_3 is given by the first term of Eq. (75) so that

$$\epsilon' * S' * D_2 = \epsilon_3 * S_3 * D_7 \quad (81)$$

The net change in the position of δ_3 is determined by the sum of D_6 and D_7 . The new value of T_3 comes from the finite difference temperature calculations.

If δ_3 is not equal to δ_T then

$$\frac{\rho_v * Ka_4 * (T_3 - T_B)}{\mu_v * (\delta_T - \delta_3)} * \frac{\partial P_v}{\partial T} = - \epsilon_3 * S_3 * \rho_w * D_6 \quad (82)$$

and Eq. (81) still applies. The heat balance yields

$$T_3 = \frac{T'' + III * T_B}{(1 + III)} \quad (83)$$

where

$$III = \frac{\rho_v * Ka_4 * (\Delta h + \Delta h^*)}{\mu_v * K_3} * \frac{\partial P_v}{\partial T} * \frac{(\delta_3 - \delta'')}{(\delta_T - \delta_3)} \quad (84)$$

δ'' is the distance of the T'' grid point from the origin. HIDRYER1 calculates T'' and then T_3 .

Once the interface temperatures have been calculated, the change in interface position (zone basis weight) is performed. The rate of change of basis weights is found from:

$$DBW1DT = RATE1 * BW1/L1 \quad (85)$$

$$DBW2DT = RATE2 * BW3/L3 - DBW1DT \quad (86)$$

$$DBW3DT = (RATE3 - RATE2) * BW3/L3 \quad (87)$$

$$DBW4DT = -RATE3 * BW3/L3 \quad (88)$$

where RATE1 is either 0 or D4, RATE2 is either D2 or D5, and RATE3 is the sum of D6 and D7. These are multiplied by Δt and added to the old basis weight values to get new values. The temperatures at the new positions are calculated and the cycle continues.

If no interfiber water exists at the end of heatup, the transition regime is a continuation of heatup until the temperature at δ_T is raised incrementally above TB. δ_2 moves into the sheet toward the hot surface. There is no liquid flow term and all evaporation occurs at δ_2 . Equation (82) is applicable with T3 replaced by T2, δ_3 by δ_2 , and ϵ_3 and S3 by ϵ_2 and S2. T2 is calculated by Eq. (83) with appropriate substitutions.

Linear Regime

The linear (quasi-static) regime begins when $\delta_2 = \delta_3$ (if interfiber water is present) or when all the temperature gradients in the outer zone become linear due to heat transfer. Vapor can flow through all zones in this regime. Several possible cases exist. If $\delta_1 = \delta_2$ and δ_3 is not equal to δ_T then the heat balance gives:

$$T_2 = \frac{(1 + I) * T_H + II * T_B}{1 + I + II} \quad (89)$$

$$T_3 = \frac{I * T_H + (1 + II) * T_B}{1 + I + II} \quad (90)$$

where

$$I = \frac{\frac{K_3}{\Delta h + \Delta h^*} + \frac{\rho_v * KAKV}{\mu_v} * \frac{Pv}{\partial T}}{\frac{\rho_v * Ka_4}{\mu_v} * \frac{\partial Pv}{\partial T}} * \frac{(\delta_T - \delta_3)}{(\delta_3 - \delta_2)} \quad (91)$$

$$II = \left(\frac{1}{Hc} + \frac{\delta_2}{K1} \right) * \left(\frac{1}{\delta_3 - \delta_2} \right) * \left(K3 + \frac{\rho_v * KAKV * (\Delta h + \Delta h^*)}{\mu_v} * \frac{\partial P_v}{\partial T} \right) \quad (92)$$

and $KAKV = Ka3 * Kv$. The vapor properties in II and the numerator of I are evaluated using T2 and T3. The latent heat term in I is evaluated at T3 and corrected using the moisture ratios of zones 3 and 4. The latent heat term in II is evaluated at T2 and corrected using the moisture ratios of zones 1 and 3. The vapor properties in the denominator of I are evaluated using T3 and TB.

If δ_1 is not equal to δ_2 and δ_3 is not equal to δ_T then

$$T1 = \frac{(1 + IV) * TH + I * TB}{1 + I + IV} \quad (93)$$

$$T2 = \frac{IV * TH + (1 + I) * TB}{1 + I + IV} \quad (94)$$

$$T3 = \frac{II * III * TH + (1 + I + II) * TB}{1 + I + IV} \quad (95)$$

where I is given by Eq. (74) and

$$II = \frac{\frac{K2}{\Delta h + \Delta h^*} + \frac{\rho_v * Ka2}{\mu_v} * \frac{\partial P_v}{\partial T}}{\frac{K3}{\Delta h + \Delta h^*} + \frac{\rho_v * KAKV}{\mu_v} * \frac{\partial P_v}{\partial T}} * \frac{(\delta_3 - \delta_2)}{(\delta_2 - \delta_1)} \quad (96)$$

$$III = \frac{\frac{K3}{\Delta h + \Delta h^*} + \frac{\rho_v * KAKV}{\mu_v} * \frac{\partial P_v}{\partial T}}{\frac{\rho_v * Ka4}{\mu_v} * \frac{\partial P_v}{\partial T}} * \frac{(\delta_T - \delta_3)}{(\delta_3 - \delta_2)} \quad (97)$$

and $IV = II * (1 + III)$. Vapor properties in the numerator of II are evaluated with T_1 and T_2 . The latent heat in II is at T_2 and the correction is made with the moisture ratios of zones 2 and 3. The vapor properties in the denominator of II and the numerator of III are evaluated with T_2 and T_3 ; the denominator of III is evaluated with T_3 and T_B . The latent heat term is at T_3 and corrected with the moisture ratios of zones 3 and 4.

If δ_1 is not equal to δ_2 and zone 3 does not exist, then

$$T_1 = \frac{(1 + I) * T_H + II * T_B}{1 + I + II} \quad (98)$$

$$T_2 = \frac{I * T_H + (1 + II) * T_B}{1 + I + II} \quad (99)$$

where

$$I = \frac{\frac{K_2}{\Delta h + \Delta h^*} + \frac{\rho_v * Ka_2}{\mu_v} * \frac{\partial P_v}{\partial T}}{\frac{\rho_v * Ka_4}{\mu_v} * \frac{\partial P_v}{\partial T}} * \frac{(\delta_T - \delta_2)}{(\delta_2 - \delta_1)} \quad (100)$$

and II is given by Eq. (74). Vapor properties in the numerator of I are evaluated with T_1 and T_2 . The latent heat is at T_2 and corrected with the moisture ratios of zones 2 and 4. The vapor properties in the denominator of I are evaluated with T_2 and T_B .

The mass transfer terms for the linear regime are similar to those previously outlined for the transition regime with the additional consideration that when $\delta_1 = \delta_2$ there may be evaporation and flow of vapor. The mass transfer equations that apply when $\delta_1 = \delta_2$ are

$$\rho_v * \frac{KAKV}{\mu_v} * \frac{\partial P_v}{\partial T} * \frac{(T_2 - T_3)}{(\delta_3 - \delta_2)} = \epsilon_3 * S_3 * \rho_w * D_1 \quad (101)$$

$$\rho_w * \frac{KAKW}{\mu_w} * \frac{\partial P_v}{\partial T} * \frac{(T_2 - T_3)}{(\delta_3 - \delta_2)} = \epsilon' * S' * \rho_w * D_2 \quad (102)$$

$$\rho_v * \frac{KAKV}{\mu_v} * \frac{\partial P_v}{\partial T} * \frac{(T_2 - T_3)}{(\delta_3 - \delta_2)} = \epsilon_2 * S_2 * \rho_w * D_3 \quad (103)$$

where D1 represents the evaporation of interfiber and intrafiber water, D2 is the slug flow of interfiber water, and D3 is the evaporation of intrafiber water accompanying D2. HIDRYER1 selects the larger of D1 or D2 (or D1 if they are equal) as the rate of advance. If D1 is equal to or larger than D2, δ_1 and δ_2 move according to D1. If D2 is larger, δ_2 moves according to D2 and δ_1 moves according to D3.

When δ_1 is not equal to δ_2 , the mass balance gives

$$\rho_v * \frac{Ka_2}{\mu_v} * \frac{\partial P_v}{\partial T} * \frac{(T_1 - T_2)}{(\delta_2 - \delta_1)} = \epsilon_2 * S_2 * \rho_w * D_4 \quad (104)$$

which is the evaporation of intrafiber water at δ_1 and

$$\rho_v * \frac{KAKV}{\mu_v} * \frac{\partial P_v}{\partial T} * \frac{(T_2 - T_3)}{(\delta_3 - \delta_2)} = \epsilon' * S' * \rho_w * D_5 \quad (105)$$

which is the evaporation of interfiber liquid at δ_2 . The expression for D2 also applies at δ_2 and HIDRYER1 selects the larger of D2 or D5 as the rate of advance of δ_2 .

At δ_3

$$\frac{-K3}{(\Delta h + \Delta h^*)} * \frac{(T2 - T3)}{(\delta_3 - \delta_2)} = \epsilon_3 * S3 * \rho_w * D6 \quad (106)$$

and Eq. (81) also applies. Note that if D1 or D5 is greater than D2 then D2 is set = 0 and so D7 = 0. δ_3 is advanced according to the sum of D6 and D7.

In the special case where zone 3 is not present, the expression for D4 is used to advance δ_1 and

$$\frac{-K2}{(\Delta h + \Delta h^*)} * \frac{(T1 - T2)}{(\delta_2 - \delta_1)} = \epsilon_2 * S2 * \rho_w * D8 \quad (107)$$

is used for δ_2 .

The size of the time increment used depends on the magnitudes of D1, D2, etc. δ_1 can never pass δ_2 , and δ_2 can never pass δ_3 . HIDRYER1 calculates the largest time increment which will not violate the interface position criterion or the finite difference stability criterion and compares it to DT0, the default time increment. The smaller of the two is chosen and used.

Because the interface temperature calculations involve vapor and liquid properties whose values depend on the temperatures, an iterative procedure is used such that a temperature is calculated and averaged with the previous temperature to obtain an updated value. The updated value is used for property calculations, and a new temperature is determined. The new temperature is averaged with the previously updated one and the cycle continues for a fixed number of iterations.

SUPPLEMENTARY RELATIONSHIPS

The following relationships are in the form of correlations which yield the required quantity, given an original input parameter or a value calculated in a previous step of the program.

Applied Mechanical Pressure

The nature of the applied mechanical pressure is specified in the form of input parameters. The peak pressure and time to achieve that pressure are required. HIDRYER1 offers the option of either a ramp-and-hold pressure pulse or a pulse that duplicates a press nip. The ramp-and-hold pulse rises linearly with time to the peak pressure value and maintains pressure at the peak value until drying is complete (at a final moisture content of 6%). An extremely short rise time mimics a step change in pressure.

The press-nip pulse uses a sinusoidal function to create a symmetrical pressure pulse that achieves its peak value at the input rise time. Thus, the "nip residence time" is twice the input rise time. HIDRYER1 terminates when the moisture content reaches its target value or when the nip residence time is exceeded.

The functional forms for the pressure options are:

$$P = A1 + A2 * \frac{TIME}{RISTIM} \quad (108)$$

and

$$P = A1 + \frac{A2}{2} * (1 + \text{sine}(\frac{A3 * TIME}{RISTIM} + A4)) \quad (109)$$

where A1 is some small but finite pressure value (contact pressure at time zero) required for the compressibility equation; A2 is the peak pressure, which is an

input parameter; A3 is the numerical constant π multiplied by 3600; and A4 is the numerical constant π multiplied by 1.5. The factor of 3600 is required since HIDRYER1 calculates TIME in hours and RISTIM, the time required to achieve the peak pressure, is specified in seconds.

Typical RISTIM values are on the order of 0.05 second. A1 is arbitrarily given the value of 0.7 kPa (0.1 psi), and A2 is specified in the input conditions.

Physical Properties

The vapor and liquid physical properties are derived by modeling steam table data with a multiple regression analysis program over the range from 0 to 232°C (32 to 450°F).⁶⁷ The functional form for the properties is:

$$\text{PROP} = B1 + T * (B2 + T * (B3 + T * (B4 + T * B5))) \quad (110)$$

where PROP is the property to be determined (latent heat, specific volume, etc.) and T is the temperature.

Latent Heat Correction Factor

The hygroscopic nature of cellulose requires that an additional quantity of energy above that of the latent heat (at a given temperature) be supplied during drying. This quantity is usually treated as a correction factor to the latent heat. Data on vapor pressure reduction in the presence of cellulose can be used to calculate the incremental heat of desorption at a given moisture ratio and temperature. Available data from⁶⁸ have been used to derive a functional relationship for the incremental heat of desorption over the range of 65 to 80°C (149 to 176°F) from moisture ratios of 0.01 up to 0.24.⁶⁹ Above moisture ratios of 0.24 the heat of desorption becomes infinitesimal relative to the latent heat.

The correlation has the form:

$$\Delta h' = C1 * \exp(C2 * MR) \quad (111)$$

where $\Delta h'$ is the heat of desorption, C1 has a value of 1157.5 kJ/kg (497.63 BTU/lbm), and C2 has a value of -14.9522.

Because HIDRYER1 assumes a step change in moisture ratio from one zone to the next, an integral-average latent heat increment at each interface is used as the correction factor and is defined by integrating Eq. (111) from the moisture ratio of one zone to the moisture ratio of the adjacent zone so that:

$$\Delta h^* = D1 * \frac{\exp(D2 * MR_i) - \exp(D2 * MR_f)}{MR_f - MR_i} \quad (112)$$

where D1 has a value of 77.4 kJ/kg (33.28 BTU/lbm) and D2 has a value of -14.9522.

Thermal Conductivity

The thermal conductivity is evaluated using the parallel conductor model^{61,70} and neglecting the contribution of vapor conductivity. The thermal conductivity is given by:

$$K = E1 * (1-\epsilon) + E2 * \epsilon * S \quad (113)$$

where E1 and E2 are the thermal conductivities of cellulose and water, 0.24 W/m-K (0.14 BTU/ft-hr-°F) and 0.682 W/m-K (0.394 BTU/ft-hr-°F), and are assumed constant.

Contact Coefficient

The relationship for the contact coefficient between the sheet and the hot surface has the form:

$$h_c = F_1 * (1-\epsilon) + F_2 * \epsilon * S \quad (114)$$

where F_1 is the contact coefficient for dry cellulose, obtained from data in,⁷¹ that depends on the mechanical pressure⁷² and F_2 is a value typical of a boiling heat transfer coefficient between water and a flat plate that is on the order of $5678 \text{ W/m}^2\text{-K}$ ($1000 \text{ BTU/ft}^2\text{-hr-}^\circ\text{F}$).

Compressibility

Mathematical descriptions of saturated sheet compression originate in the modeling of wet pressing. The sheet is modeled in one of three ways: a power law model relating the concentration of fibers to the mechanical pressure; a Kelvin body model describing the sheet thickness in terms of the applied pressure and certain viscoelastic constants; and a combination model using a power law to describe fiber bending and a time dependent expression for fiber compression.

Strictly speaking, a power law model applies only to an equilibrium condition and not to a dynamic compression case. However, modification of the basic power law^{73,74} to account for time dependent effects is possible.⁷⁵ A Kelvin body (spring and dashpot in parallel) exhibits a first order response to a step change in pressure and therefore only models flow-controlled pressing phenomena, which also exhibit a first order response.⁷⁶ The combination model treats fiber bending with a power law expression and models fiber compression as a rate process, since it is time dependent.⁷⁷ After short times (milliseconds), the rate of change of the fiber compression contribution is very small in comparison with the value of the bending contribution. Thus, it should be sufficient to describe the thickness in terms of just the bending term (power law) along with some slight correction which may amount to a nearly constant fraction of the bending term.

HIDRYER1 uses the power law compression model because it is the simplest and most easily modified model and because the most data are available for relating

its constants to commonly measured sheet properties such as freeness and basis weight. The form of the power law is:

$$C = M * p^N \quad (115)$$

The coefficients M and N vary with the degree of beating^{78,79} and the moisture ratio of the sheet.⁷⁹ Data from,⁷⁹ although limited to pressures on the order of 7 kPa (1 psi), demonstrated that the power law describes the compression behavior of unsaturated sheets as well as saturated sheets. Using this information, expressions for evaluating M and N at different moisture ratios are obtained by multiple linear regression.⁸⁰ The form is:

$$\text{COEFF} = G1 + G2 * \text{MR} + \frac{G3}{\text{MR} + 1.5} + \frac{G4}{(\text{MR} + 1.5)^2} + \frac{G5}{\text{MR} + 1} + \frac{G6}{(\text{MR} + 1)^2} \quad (116)$$

where COEFF is either M or N and the values of G1 through G6 change depending on whether M or N is to be calculated and on the freeness of the pulp in the sheet.

To account for the dependence on refining, the values for the regression constants in Eq. (116) are determined for the same pulp at two available freeness levels⁷⁹ and fit to a parabola with an assumed minimum at a freeness of 100 CSF. (Below 100 CSF, M and N are held fixed at the 100 CSF values.) Thus, each constant in Eq. (116) is found from an expression of the form:

$$\text{CONST} = H1 + H2 * \frac{(\text{CSF} - H3)^2}{H4} \quad (117)$$

where CONST represents G1 through G6 and H1 through H4 change depending on which value of G is to be calculated.

The compressibility of a sheet is known to be highly temperature dependent. Data describing the overall gain in moisture removal by pressing at elevated

temperatures are available,²³ but no data are available on the specific changes in sheet compressibility constants. To account for this effect, the value of M calculated from Eq. (116) is (arbitrarily) multiplied by a function of the mean temperature of the zone such that:

$$M' = M * \left(\frac{TBAR}{TI}\right)^{I1} \quad (118)$$

where M' is the modified M value, TBAR is the average zone temperature, TI is the initial sheet temperature at which M and M' are identical, and I1 is an exponent less than unity (0.25 in HIDRYER1) so that the temperature effect moderates as TBAR increases.

A moist but unsaturated sheet can be brought to saturation if the mechanical pressure is high enough. To account for this observed behavior, the value of N is modified by making it a function of the effective mechanical pressure on the sheet. The effective mechanical pressure is the applied pressure minus the hydraulic pressure. N_{sat}, the value of N which would give a saturated sheet at a reference pressure equal to or greater than the peak pressure, is calculated and N becomes a function of this saturation value and the original value (N_{ref}) calculated from Eq. (116) so that there is a smooth transition in the N value as effective pressure increases. N can never be greater than N_{sat} since the reference pressure is equal to or greater than the peak pressure. N can never be less than N_{ref} since the pressure is never less than the A1 constant in the pressure function. The form is:

$$N = J1 + J2 * \left(\frac{P-J3}{J4}\right)^{J5} \quad (119)$$

where J1 and J2 depend on N_{ref} and N_{sat}, and J3 and J4 depend on the value of the large reference pressure chosen. J5 is the reciprocal of an odd integer and

provides a smooth transition from N_{ref} to N_{sat} as effective mechanical pressure changes.⁸¹

Permeability

The final supplementary relationship is that of permeability. Methods of characterizing permeability are based on theoretical or empirical relationships modeling permeability as a function of sheet porosity and/or fiber cross-sectional shape.^{63,82-85} The empirical relationships are, of course, limited to the ranges of porosities and fiber types investigated. The theoretical approaches in this class are of limited applicability because the fiber is assumed to be of smooth (but not necessarily circular) cross sectional shape. Consequently, the theoretical relationships tend to predict permeabilities larger (by one or two orders of magnitude) than experimentally determined ones, except at high porosities and/or freenesses.

Paper fibers have many fibrils extending into the interfiber space. While the volume of the fibrils is generally small in comparison to the volume occupied by the bulk of the fiber, the effect of the fibrils on the flow properties is quite dramatic. The amount of fibrils depends on the extent to which the fiber has been physically degraded. Since Canadian Standard Freeness is a commonly performed test and gives a reasonable (but indirect) indication of the trend of the flow properties, it seems likely that a relationship between permeability and CSF would be both convenient and consistent with a model based on macroscopic trends.

An empirical linear relationship exists between $\ln(\text{CSF})$ and the square root of specific filtration resistance^{86,87} over a range of 100 to 700 CSF. The relationship has the form:

$$\ln(\text{CSF}) = K_1 + K_2 * \sqrt{R} \quad (120)$$

The calculated value of R is for a given pressure drop across the mat. Data at a variety of pressure drops on the order of 7 kPa (1 psi) and a broad range of freeness values define a family of curves of R vs. pressure drop whose shape is roughly independent of freeness.⁸⁸ Thus, by selecting some reference pressure (Pref) and the specific filtration resistance (Rref) at this pressure, a generalized relationship can be developed,⁷² such as:

$$R = L_1 + L_2 * P + L_3 * \sqrt{P} \quad (121)$$

where L1 depends on Rref, and L2 and L3 depend on Rref and Pref. The pressure drop in a saturated flow experiment is equivalent to the effective mechanical pressure exerted on the mat, and the permeability is related to R by:

$$K_a = \frac{1}{R * C} \quad (122)$$

Therefore, there is a direct link between mechanical pressure and permeability (for a given CSF).

The permeability determined in saturated flow experiments is the absolute permeability; this is the permeability in the presence of only one flowing species. To adjust for the presence of two or more flowing species, the absolute permeability is generally multiplied by a correction factor called the relative permeability. Relative permeabilities vary between zero and unity and typical relationships are:⁸⁹

$$K_w = S' M_1 \quad (123)$$

and

$$K_v = (1 + N_1 * S') * (1 - S')^{N_2} \quad (124)$$

where M1 is on the order of 4 and N1 and N2 are each on the order of 3. These relationships were developed for granular media. To be consistent with the

saturation concept for which they were developed, they are based here on the interfiber saturation of the paper, since it is the interfiber liquid (or intergranular liquid) that impedes the flow of vapor. This also makes them consistent with measurements of liquid relative permeability for paper at very low moisture ratios because below a critical but finite moisture ratio the liquid relative permeability becomes infinitesimally small.⁹⁰

HIDRYER1 is organized so that the values for constants used in the supplementary relationships are grouped in DATA statements and/or COMMON statements. Therefore, modification of the model by changing the numerical value of a constant is a simple procedure. Most supplementary relationships are implemented in either the form of a SUBROUTINE or a FUNCTION so that changing the functional form also becomes simple. Refer to Appendix 1 for a detailed program listing.

MODEL VALIDATION

HIDRYER1 is the culmination of a series of drying models that began with a numerical implementation of the Ahrens model. First, the analytical solution to the Ahrens model was programmed to provide a reference for future comparisons. Next, the equations of the Ahrens model were programmed and solved numerically to duplicate the analytical result.⁹¹ This numerical model was expanded by accounting for effects such as heat conduction into the outer zone, the influence of permeability on interface temperature, vapor-pressure-induced liquid flow, and an initial heatup period. At each stage of development, the model's predictions were compared to the previous version of the model to demonstrate that the advanced case reduced to the simpler case if conditions consistent with the less stringent assumptions were introduced into the advanced model.

The result was a model called HIDRYER that assumed zones of constant permeability and porosity. It was based primarily on low mechanical pressure cases

where the thickness did not change much as drying progressed, but gave good agreement with experimental data even in higher pressure cases,⁹² since any values for porosity, thickness, heat transfer coefficient, and permeability could be specified as inputs and held fixed through the drying simulation.

The final step was to convert HIDRYER to HIDRYER1 by specifying the required supplementary relationships that determine how porosity, etc., vary with pressure, temperature, moisture ratio, and freeness. Each relationship was tested separately before being incorporated into HIDRYER and then tested again after incorporation to verify that it had been implemented correctly. Thus, the model was validated at each stage of development so that the predictions of HIDRYER1 are a result of the model and its assumptions and not a result of problems in the FORTRAN coding of the equations.

SUMMARY

Fundamental heat and mass transfer relationships, with supplementary property equations, have been assembled into a model of high intensity paper drying. The model has been converted into a FORTRAN program called HIDRYER1.

The following sections describe simulations involving an exploratory or "parametric" study to determine the basic behavior of the model and direct comparisons to laboratory data to check on the values of constants used in the model.

PARAMETRIC STUDY

INPUT PARAMETERS

HIDRYER1 requires the user to provide values for hot surface temperature (TH), boiling point temperature (TB), basis weight (BW), Canadian Standard Freeness (CSF), initial moisture ratio (MRO), default time increment (DTO), peak mechanical pressure (PMAX), and pressure rise time (RISTIM). Additionally, the user must specify choices for the following options: ramp-and-hold or sinusoidal pressure pulse; English or SI units; and two options for a packaged subroutine used to calculate sheet thickness when the sheet becomes saturated during the heatup regime. These last two options select either a variable-order Adams predictor-corrector method or Gear's method for solving a differential equation and specify how the Jacobian matrix is to be calculated (analytically, by finite differences, etc.).

OUTPUT VARIABLES

HIDRYER1 produces two types of output: printed output and output stored on magnetic disk. The printed output consists of the input parameters and the following calculated values: time (SEC), amount of moisture removed relative to the initial amount present (MREL), sheet surface temperature (TS), temperatures at the various interfaces in the sheet (T1, T2, T3), positions of the interfaces relative to total sheet thickness (RATIO1, RATIO2, RATIO3), total sheet thickness (DELTAT), instantaneous heat flux (Q), overall heat transfer coefficient (OHTC), and the gage vapor pressure corresponding to T1 (PGAUGE). The disk output does not include the input parameters, but contains all the calculated values of the printed output plus the temperature at a point midway through the basis weight of the sheet (TMID). Other variables calculated in the program can be obtained by modifying the WRITE statements in the output subroutine.

DESIGN OF PARAMETRIC STUDY

The effect of various input parameters on drying behavior is determined by running the program at different sets of conditions for each of the two pressure pulse options. Table 1 lists the parameters and the values investigated. The center column gives the values for the base case. Results from all other cases are compared against this base case and are generated by varying the value of an individual parameter from its base value while maintaining all other parameters at their base case values. The pressure option is designated as either RAMP or SINE.

Table 1. Input parameter values for parametric study.

<u>Parameter</u>	<u>Minimum</u>	<u>BASE</u>	<u>Maximum</u>
TH, °C(°F)	148.9(300)	204.4(400)	260.0(500)
MRO	1.00	1.25	1.50
BW, g/m ² (lbm/ft ²)	50.25(0.0105)	102.50(0.0210)	205.00(0.0420)
CSF	300	450	600
PMAX, kPa(lbf/in ²)	2068(300)	3447(500)	4826(700)
RISTIM, s	0.005	0.010	0.050

RESULTS AND DISCUSSION

The HIDRYER1 program was allowed to run to completion or for one hour of CPU time, whichever was shorter. In general, the SINE cases took about 20 seconds to run. The exception is the SINE case with 0.050 second RISTIM, which took about 18 minutes of CPU time. The RAMP cases averaged around 30 minutes of CPU time, and no case took longer than 38 minutes.

Base Case

Figures 11 through 18 show the results of the base case with the RAMP pressure option. Figure 11 is the drying curve for this experiment. Two points on the curve are significant. The first point, at about 0.04 second, signals the onset of drying. Examination of the numerical output reveals that the transition regime actually started at about 0.02 second, but it takes several time increments of the transition regime before noticeable (on the graph) drying occurs. The second point, at about 0.13 second, signals the end of the transition regime and the onset of the linear regime. The steep slope of the drying curve in the transition regime indicates that the drying is dominated by liquid dewatering in this period. The abrupt change in slope at the start of the linear regime indicates a shift to an evaporation and bulk vapor flow dewatering mechanism.

Figure 12 traces the sheet thickness history. The rapid pressure rise during the heatup period causes a rapid sheet compression early in the process. As the pressure levels off and as the transition regime begins, the hydraulic pressure in the sheet builds and reduces the rate of compression. As more and more liquid is removed from the sheet, it becomes easier to compress and the rate of compression increases until all the interfiber liquid is removed (which coincides with the onset of the linear regime in this case). Once the interfiber liquid is removed, the permeability of the sheet increases and results in low hydraulic (vapor) pressure. The rate of compression slows as the moisture removal becomes dominated by an evaporation mechanism and the sheet approaches its final (zero moisture content) thickness.

Figure 13 tracks the relative position of the various interfaces in the sheet. Interfaces 1 and 2 move together from the start of the transition regime for a short time. In this period, the heat transfer rate is able to keep up

with the liquid flow rate. At about 0.05 second the liquid dewatering rate becomes greater than the heat transfer (evaporation) rate and interface 2 progresses into the sheet faster than interface 1. When interface 2 reaches the cool side of the sheet, the linear regime begins and heat transferred to the cool side causes evaporation. Interface 2 then recedes back toward the hot side. As interface 2 reaches the far side of the sheet the inflection and change in slope of the curve for ΔM signals the shift from liquid dewatering and internal sheet evaporation to an evaporation-only mechanism. Interface 3 is held at ΔT because evaporation at the outer surface does not occur until all interfiber water is removed.

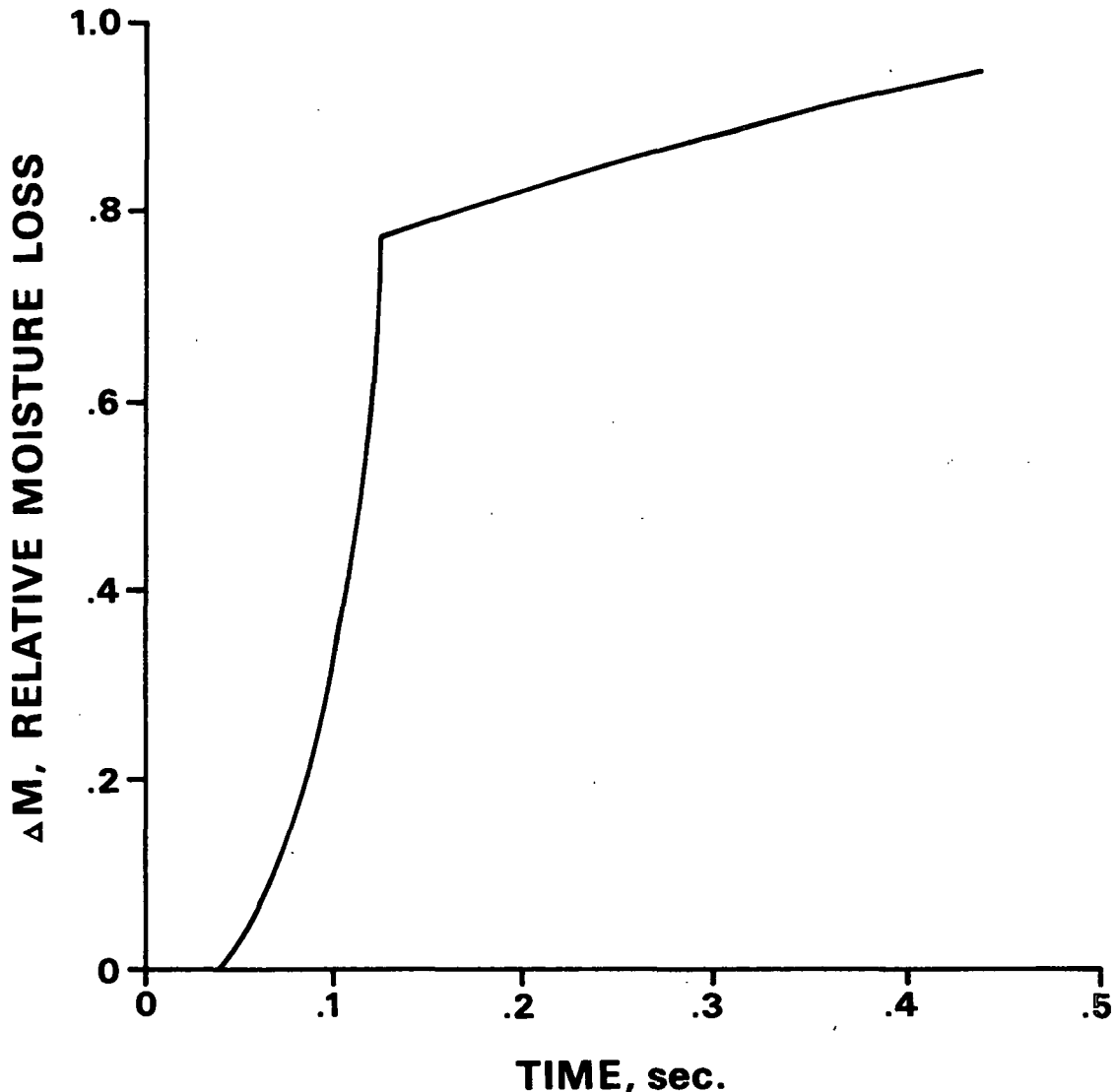


Figure 11. Moisture removal as a function of time for the RAMP base case.

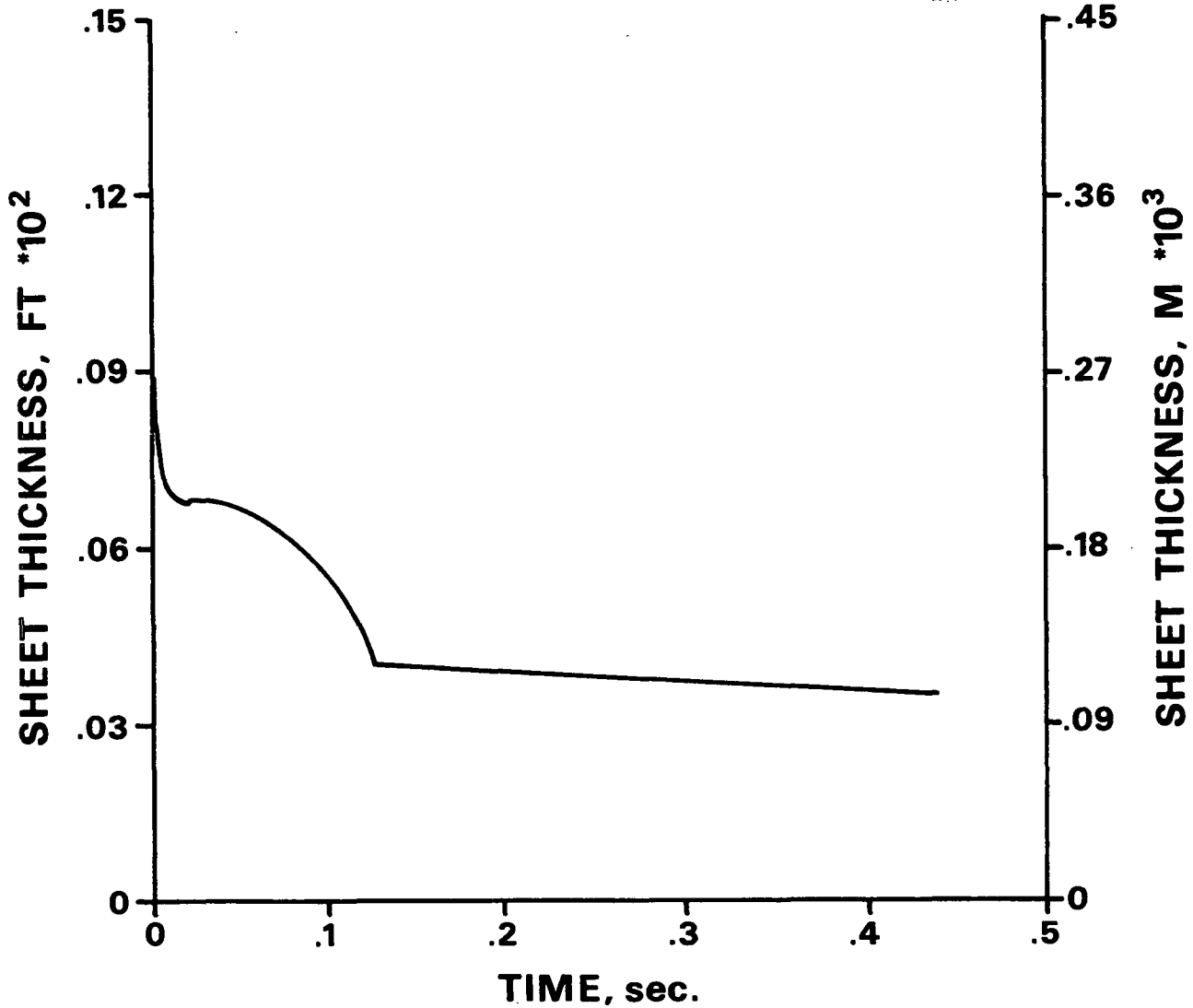


Figure 12. Sheet thickness as a function of time for the RAMP base case.

Figure 14 shows the temperature history of the interfaces. T_S , T_1 , and T_2 move together until the transition regime starts. T_3 begins to rise then because of the quantity of heat transferred by convecting liquid. T_1 and T_2 remain together until interface 2 moves faster than interface 1. T_2 and T_3 become identical when interface 2 reaches ΔT_{AT} and the linear regime starts. T_2 rises as interface 2 moves back into the sheet so that a vapor pressure gradient (determined by sheet permeability) can be maintained. T_3 is fixed at T_B since interface 3 is held at ΔT_{AT} .

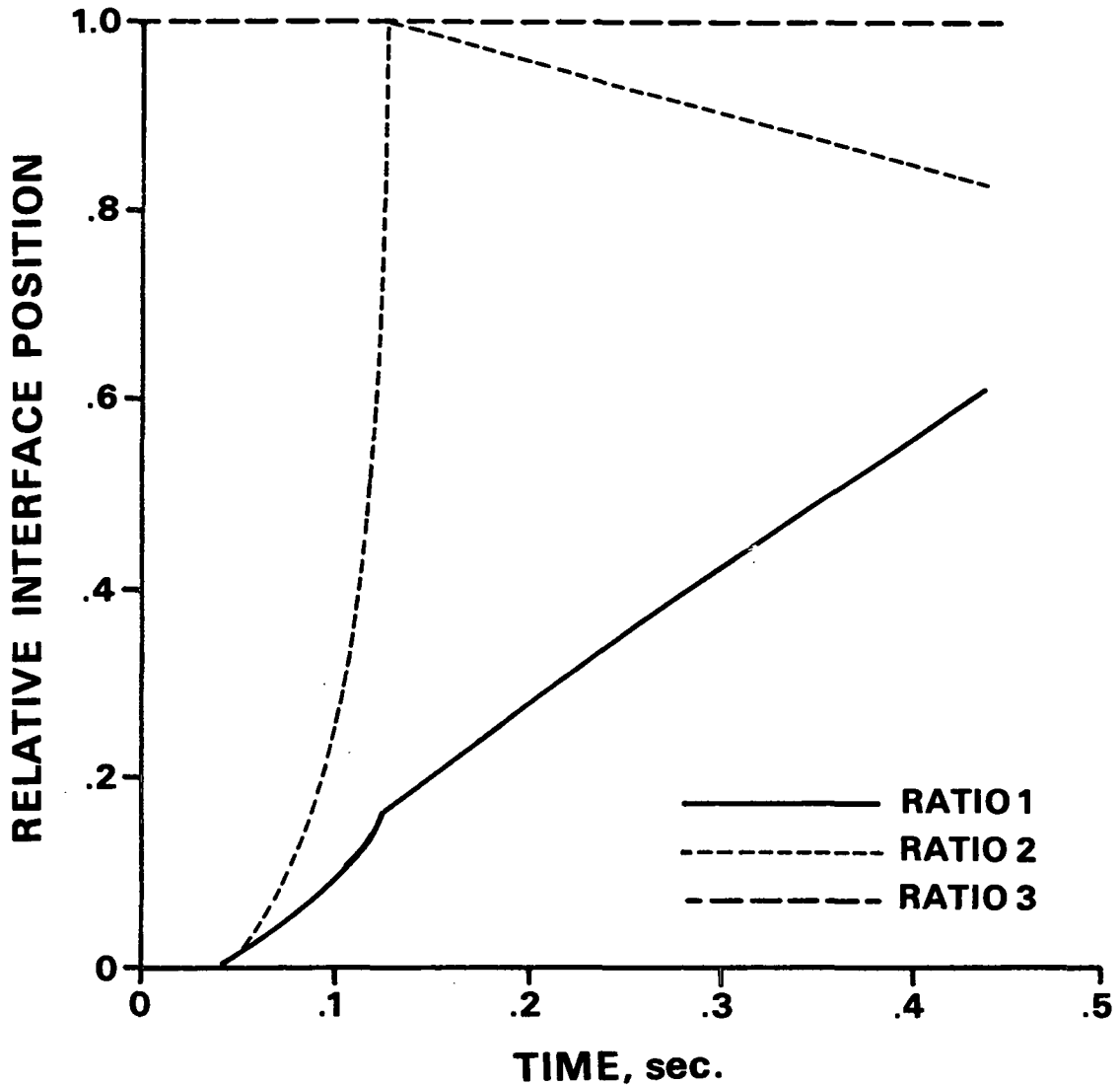


Figure 13. Interface positions relative to total sheet thickness as functions of time for the RAMP base case.

Figure 15 depicts the gage vapor pressure corresponding to the value of T_1 . The two abrupt drops and recoveries of vapor pressure occur at points where a slug of liquid is pushed through the sheet and the heat rate has to "catch up" to sustain continued flow. The first point occurs as interfaces 1 and 2 move into the sheet. The second point occurs as interface 2 moves ahead of interface 1. In both cases a zone of high vapor permeability (relative to zone 3) is suddenly created. This causes T_1 (and the vapor pressure corresponding to T_1) to

drop since the flow resistance is reduced. As the interfaces progress, T_1 must increase to sustain continued vapor and liquid flow at points in the interior of the sheet.

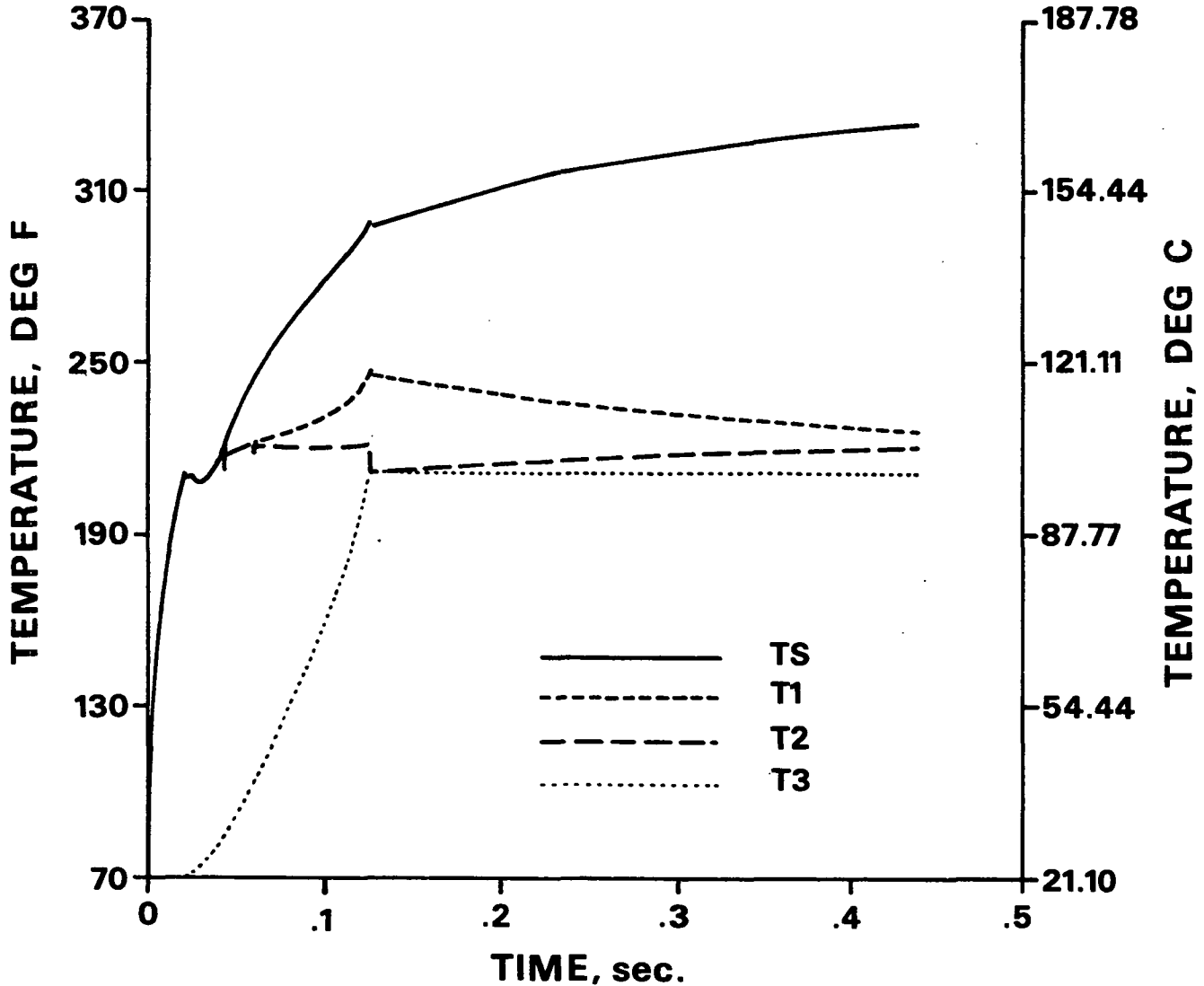


Figure 14. Sheet surface temperature and interface temperatures as functions of time for the RAMP base case.

Figure 16 traces the temperature at a point half way through the basis weight of the sheet. Since this does not always correspond to the instantaneous location of an interface, T_{MID} has to be interpolated based on the positions of the interfaces relative to the total sheet basis weight. Conduction in the

compressing sheet during heatup causes the internal temperature to rise above its initial value earlier than the cool side does. The temperature rises steadily until the linear regime when the rate of compression and the drying rate slow significantly. TMID achieves a nearly constant level until interface 2 moves far enough back into the sheet to affect the thermal behavior of the sheet's interior.

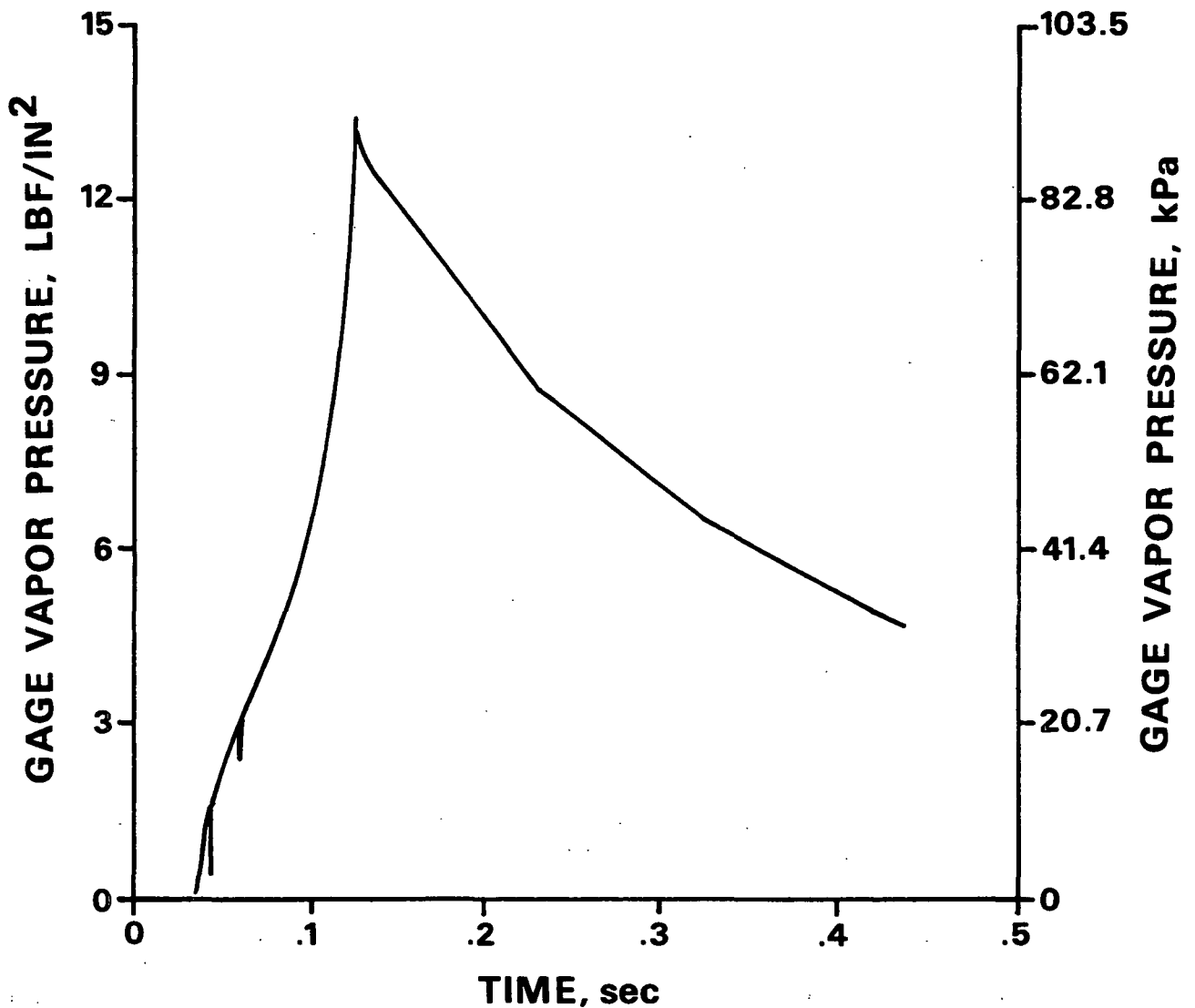


Figure 15. Gage vapor pressure corresponding to T1 as a function of time for the RAMP base case.

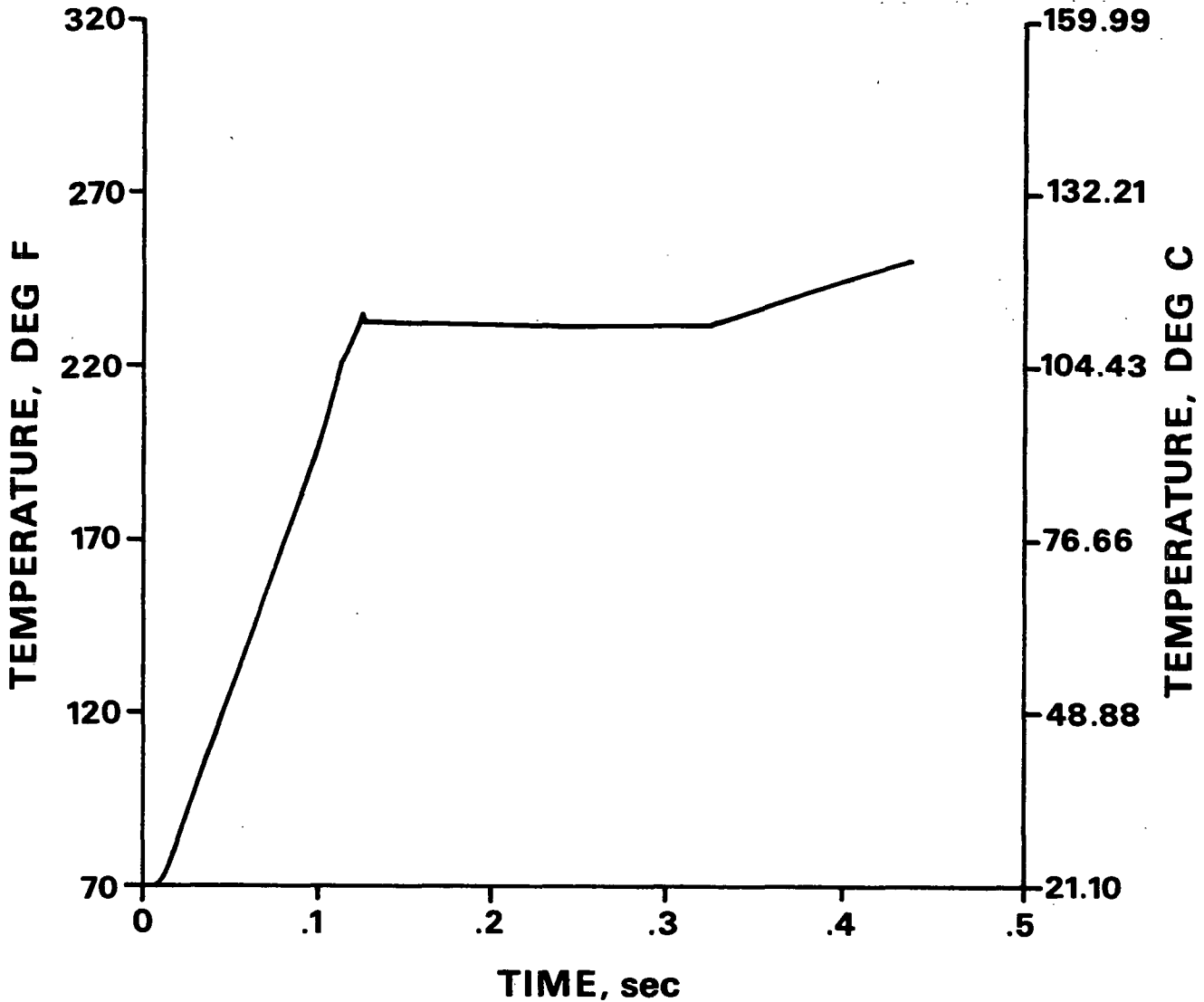


Figure 16. Temperature at one-half the sheet basis weight as a function of time for the RAMP base case.

Figure 17 graphs the heat flux from the hot surface to the sheet. Note that the hot surface temperature is assumed constant. The initial portion of the heat flux is controlled by the shape of the pressure pulse. The heat flux is initially zero and rises to its peak as the pressure peaks. When the pressure stabilizes, the heat penetrates the sheet, causing a temperature rise and a sharp drop in heat flux. Just as the transition regime begins, the drop in the heat flux moderates and when the linear regime begins the heat flux slowly

approaches an equilibrium value (zero) as the sheet approaches an equilibrium condition (dry).

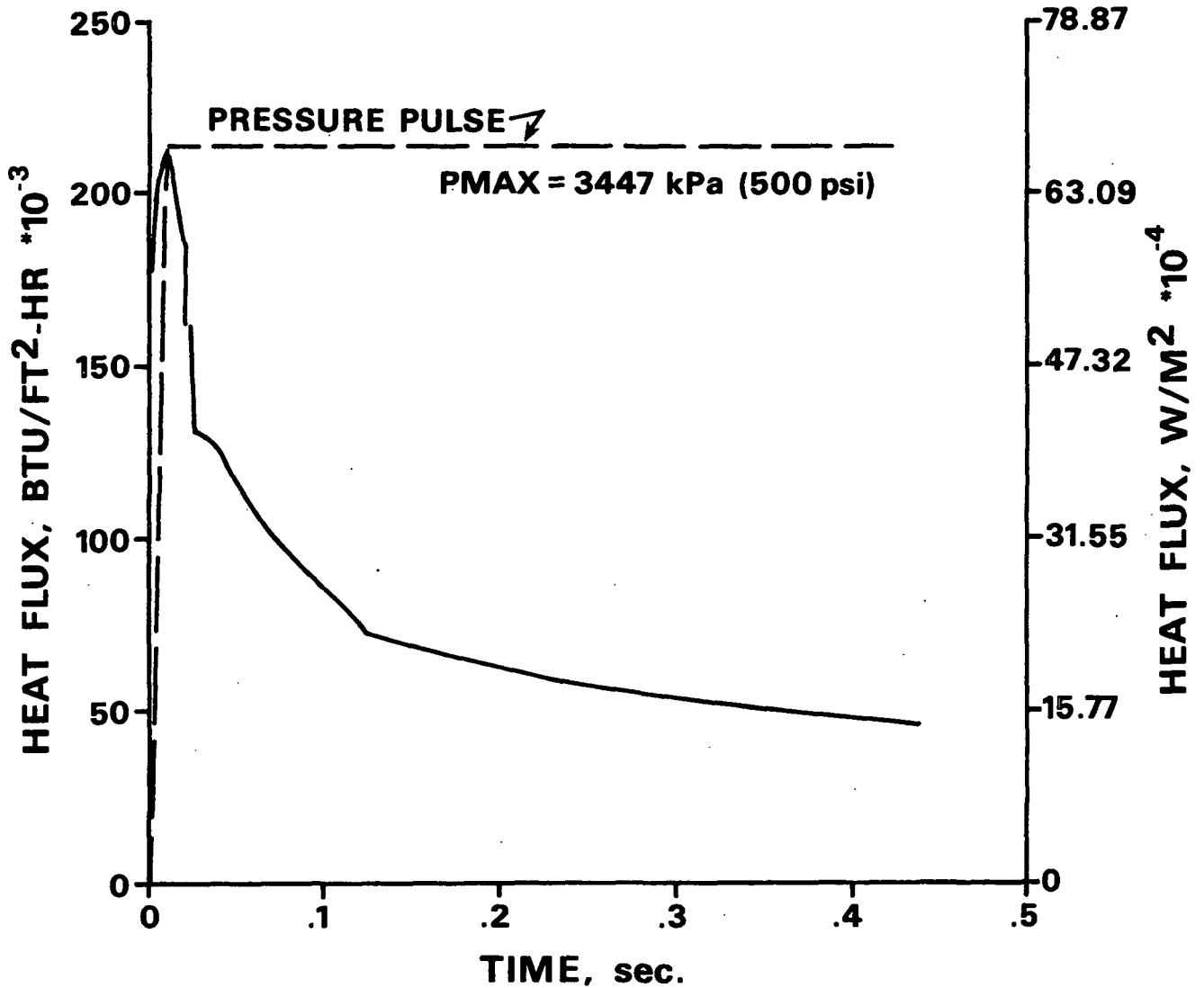


Figure 17. Heat flux as a function of time for the RAMP base case.

Figure 18 presents the history of the overall heat transfer coefficient. This quantity is calculated by dividing the heat flux by the difference between T_H and T_{MID} . OHTC parallels the heat flux curve until transition begins. As Q moderates and T_{MID} continues to rise, OHTC remains somewhat constant. As the

linear regime begins, OHTC again parallels Q since TMID stabilizes. As TMID starts to rise again, its increase is offset by the decrease in Q to yield a constant OHTC value.

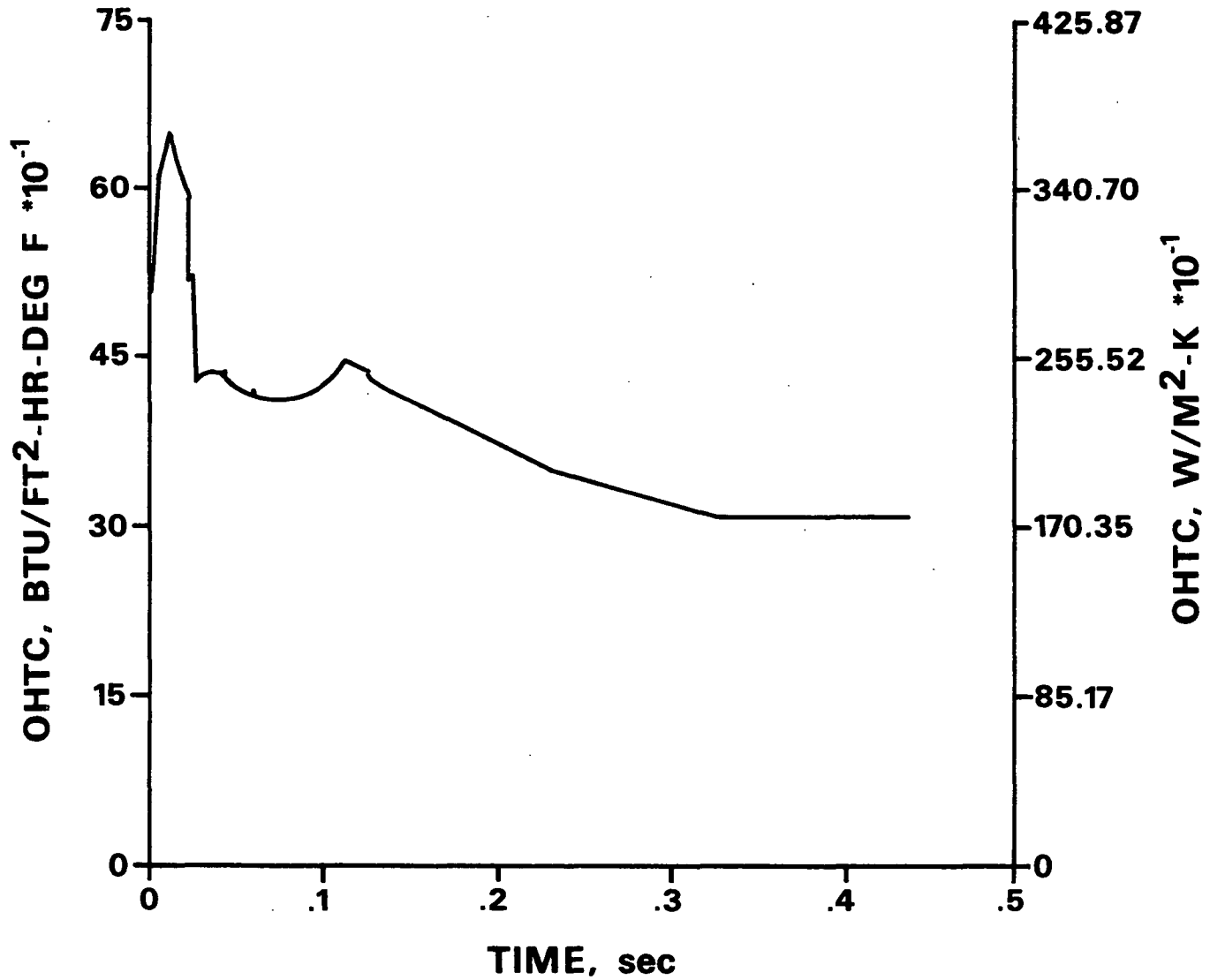


Figure 18. Overall heat transfer coefficient as a function of time for the RAMP base case.

The behavior of the base case for the niplike pressure pulse is not shown. The variables essentially match the RAMP pressure base case up until the peak

pressure is reached. After that, the values plateau and decline slightly as the pressure rapidly declines. The SINE case with 0.05 second RISTIM is the only niplike case that predicts any moisture removal. This is shown in a later figure in comparison with the moisture removal predicted for the various RAMP pressure rise times. (For the conditions selected the sheet is still in the heatup regime for all but this one SINE case.)

Comparisons of Drying Behavior

Figures 19 through 24 show comparisons of the drying behavior for the values of the input parameters given in Table 1. Results from all cases are compared against the base case and are generated by varying the value of an individual parameter from its base value while maintaining all other parameters at their base values. The drying curve stops when the sheet reaches 6% moisture content or, in one case, when the niplike pressure pulse drops to its starting value. The heatup regime accounts for 5 to 10% of the total drying time; the transition regime accounts for 10 to 45% of the total time; and the linear regime accounts for 50 to 80% of the total time. The base case results for drying time to 6% moisture content fall in between the times predicted for the minimum and maximum parameter values.

Figure 19 displays the effect of hot surface temperature on the drying curve. As anticipated, higher hot surface temperature results in shorter drying time and there is nearly a one-to-one correspondence between drying time and the driving force ($T_H - T_B$). The greatest benefits of higher hot surface temperature are reduction of the heatup time and higher driving force (drying rate) in the linear regime.

Figure 20 shows the effect of initial moisture ratio on the drying curve. There is little effect on total drying time because the moisture removal is

dominated by the (rapid) liquid dewatering mechanism. The time required to evaporate the remaining water during the linear regime is comparable for each initial moisture ratio case.

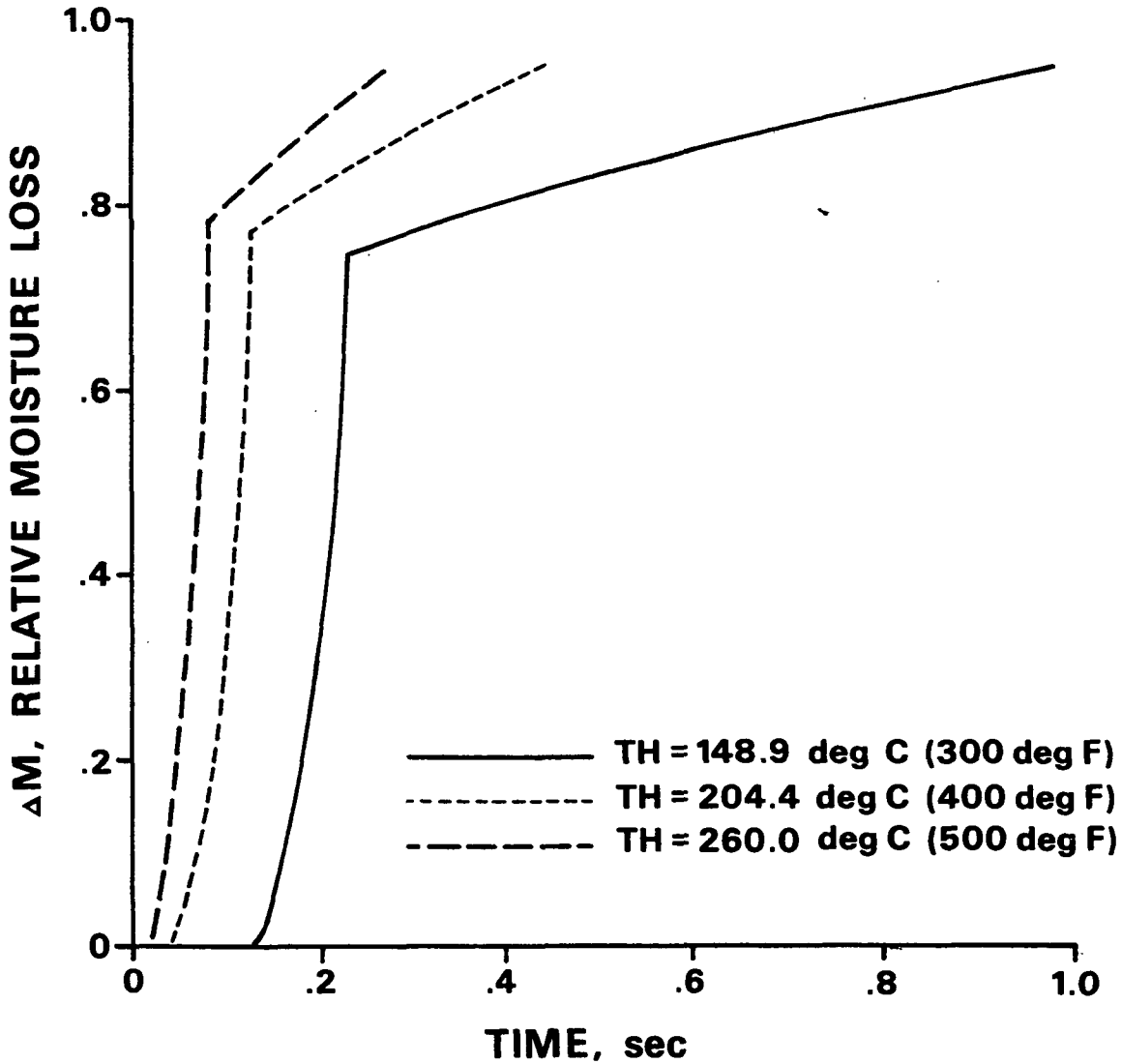


Figure 19. Effect of hot surface temperature on moisture removal for RAMP cases.

Figure 21 presents the effect of basis weight on drying. The heatup time for each basis weight is comparable, but the slopes of the liquid dewatering portion are distinctly different. In the lowest basis weight case, the heat can

penetrate far into the sheet in a short time and liquid motion can be sustained at its initial pace. In the heavier basis weights (thicker sheets), the heat only penetrates into a fraction of the total sheet thickness and after liquid motion starts, it takes some amount of time for a sufficient quantity of heat to penetrate further and sustain the flow. In the linear regime, the heat and mass have a shorter distance to travel in the lower basis weight cases and the drying rate is faster than in the heavier basis weight examples.

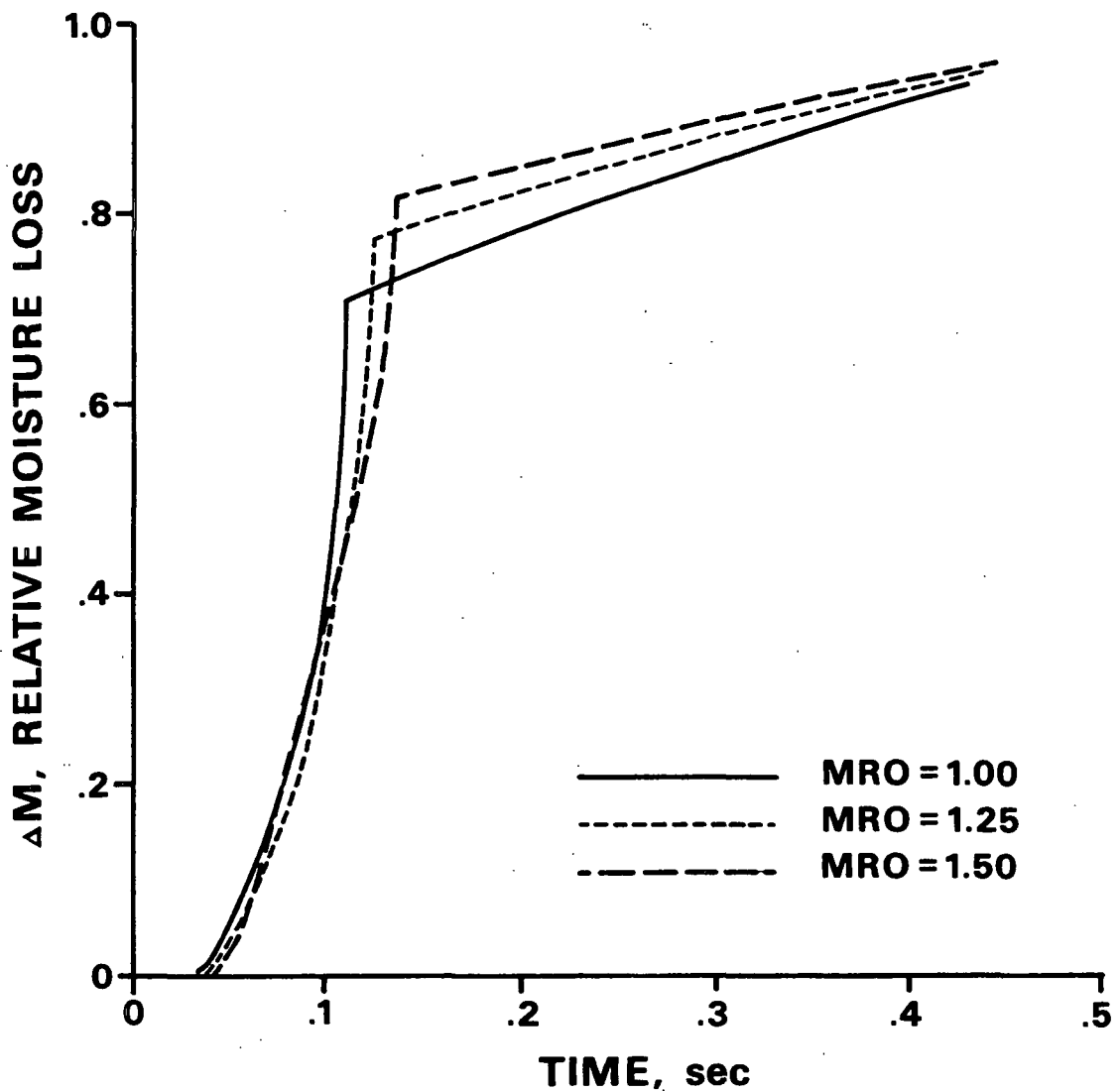


Figure 20. Effect of initial moisture ratio on moisture removal for RAMP cases.

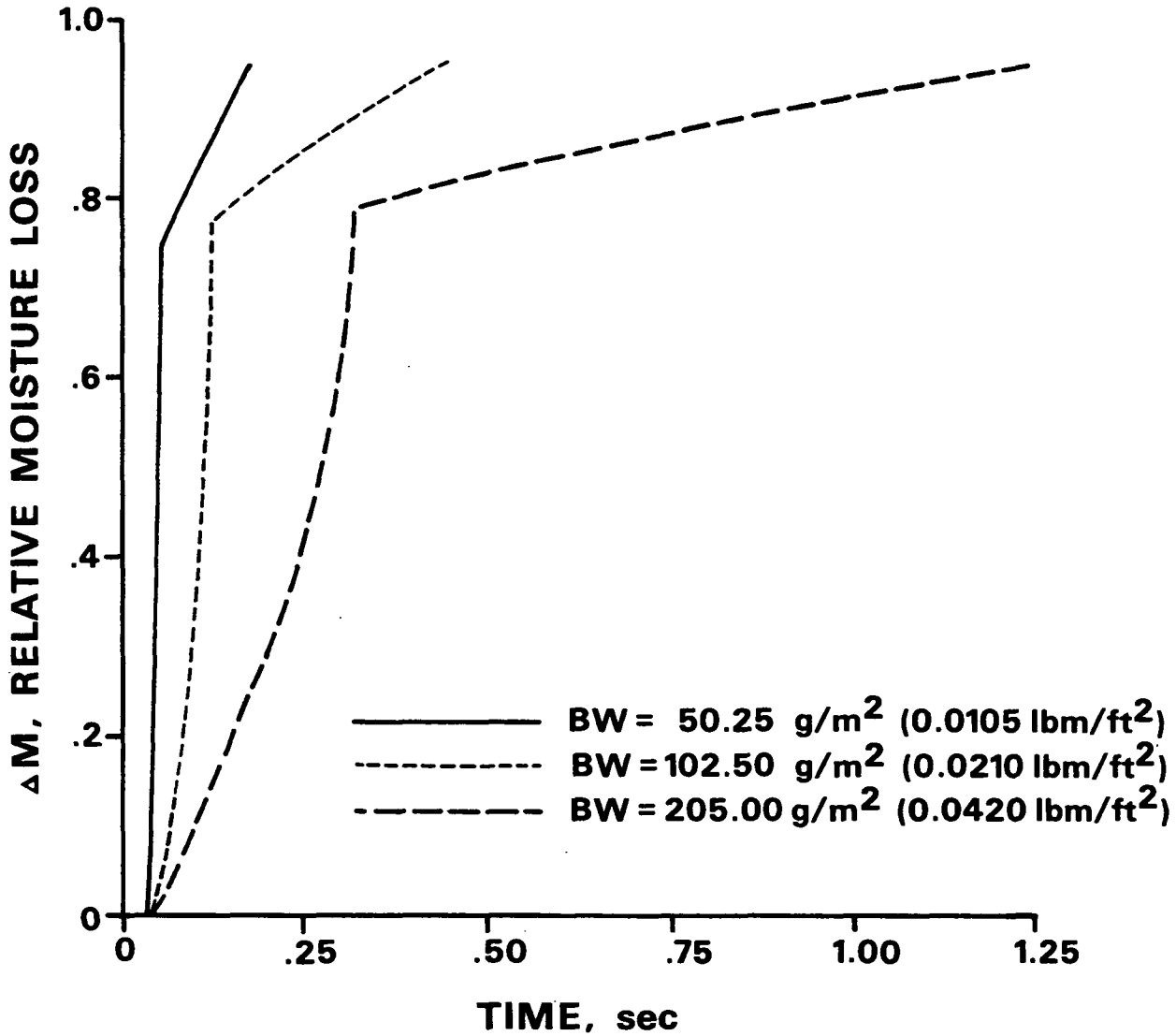


Figure 21. Effect of basis weight on moisture removal for RAMP cases.

Figure 22 shows how Canadian Standard Freeness affects drying. Lower CSF gives a more compressed sheet (at a given mechanical pressure), and in the case of 300 CSF liquid is removed from the sheet by mechanical dewatering in addition to the thermally induced liquid dewatering. The decrease in permeability accompanying lower CSF is not enough to offset the gains in drying resulting from a more compact sheet (which is better able to transfer heat) and the higher internal sheet temperatures going into the linear regime.

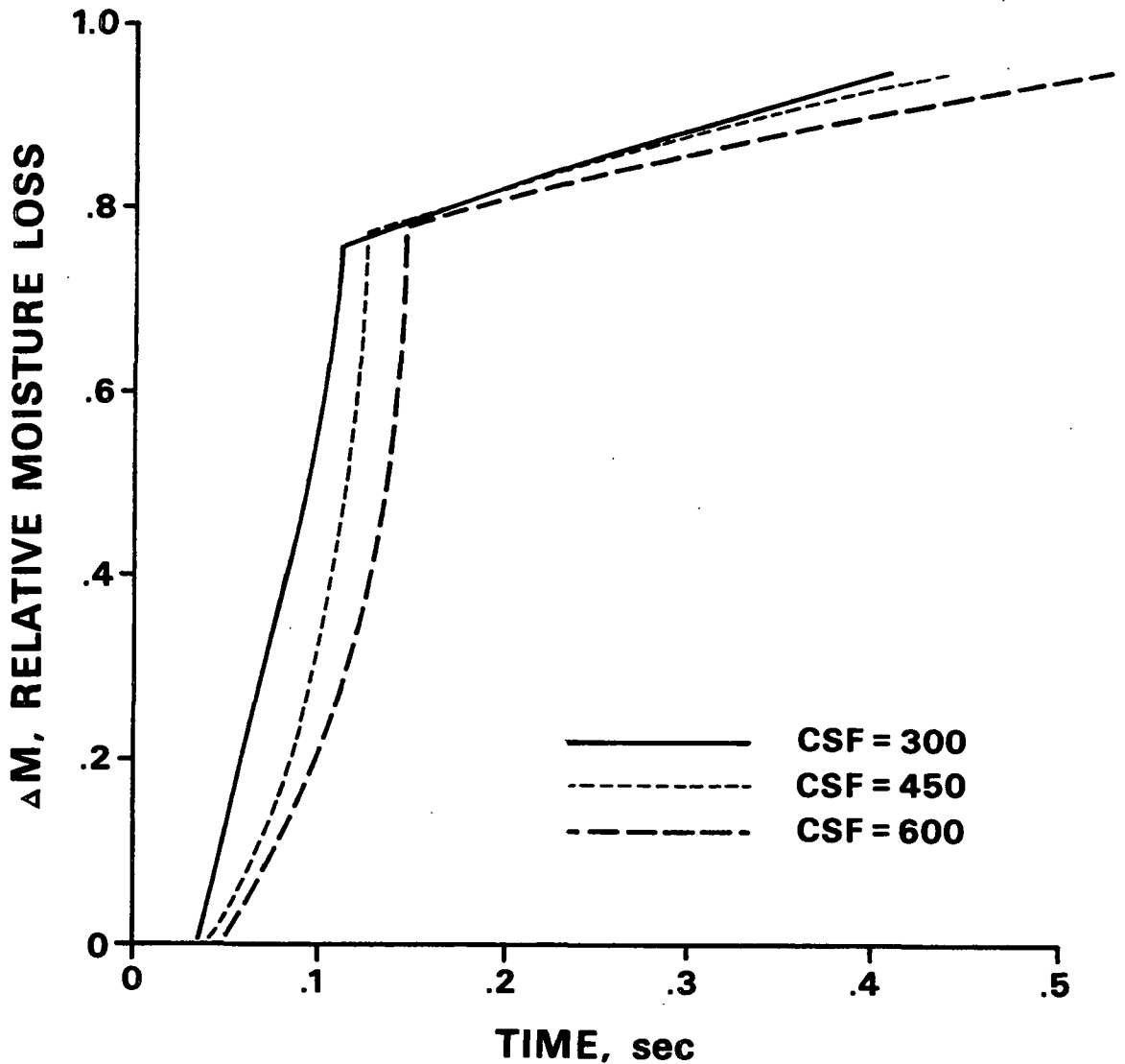


Figure 22. Effect of freeness on moisture removal for RAMP cases.

Figure 23 depicts the influence of peak pressure on drying. The curves are essentially parallel in slope but shifted in time. The results indicate that increasing pressure decreases drying time, but that the relative increase becomes smaller at higher pressures for the range of pressures examined here. This suggests that there may be some practical limit to the amount of pressure which is cost effective for a commercial implementation of high intensity drying technology.

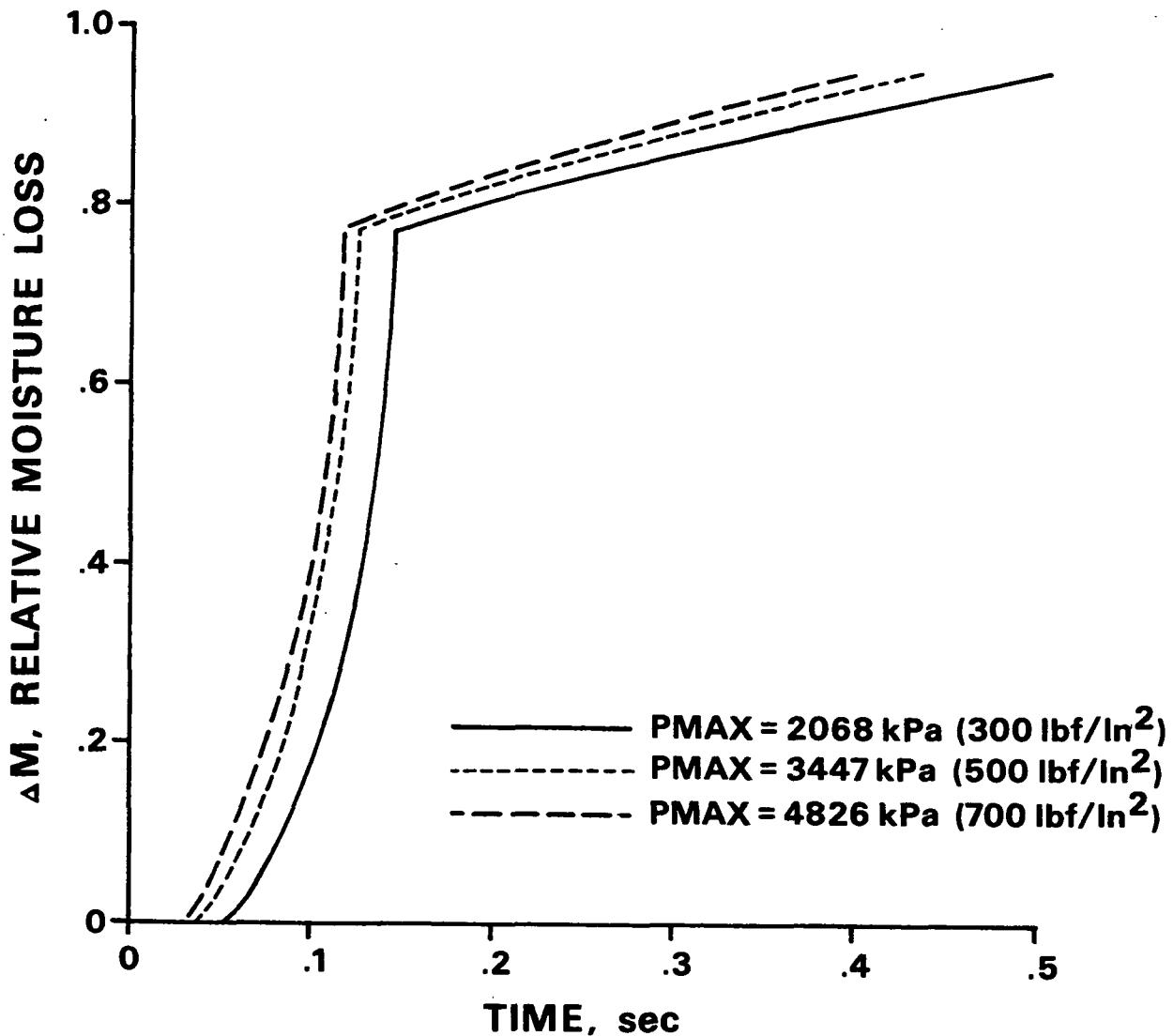


Figure 23. Effect of peak pressure on moisture removal for RAMP cases.

Figure 24 shows the effect of the pressure rise time, the time it takes to achieve the peak pressure. There is virtually no effect on drying time for the RAMP cases, since the rise time is such a small percentage of the total drying time needed. Comparing the SINE case to a RAMP case with the same rise time shows that they behave similarly until the SINE case pressure begins to drop rapidly. The SINE case continues to show a decreasing rate of dewatering as the

heat transfer to the sheet declines, and drying stops when the pressure reaches a point at which the heat transfer can no longer sustain liquid flow.

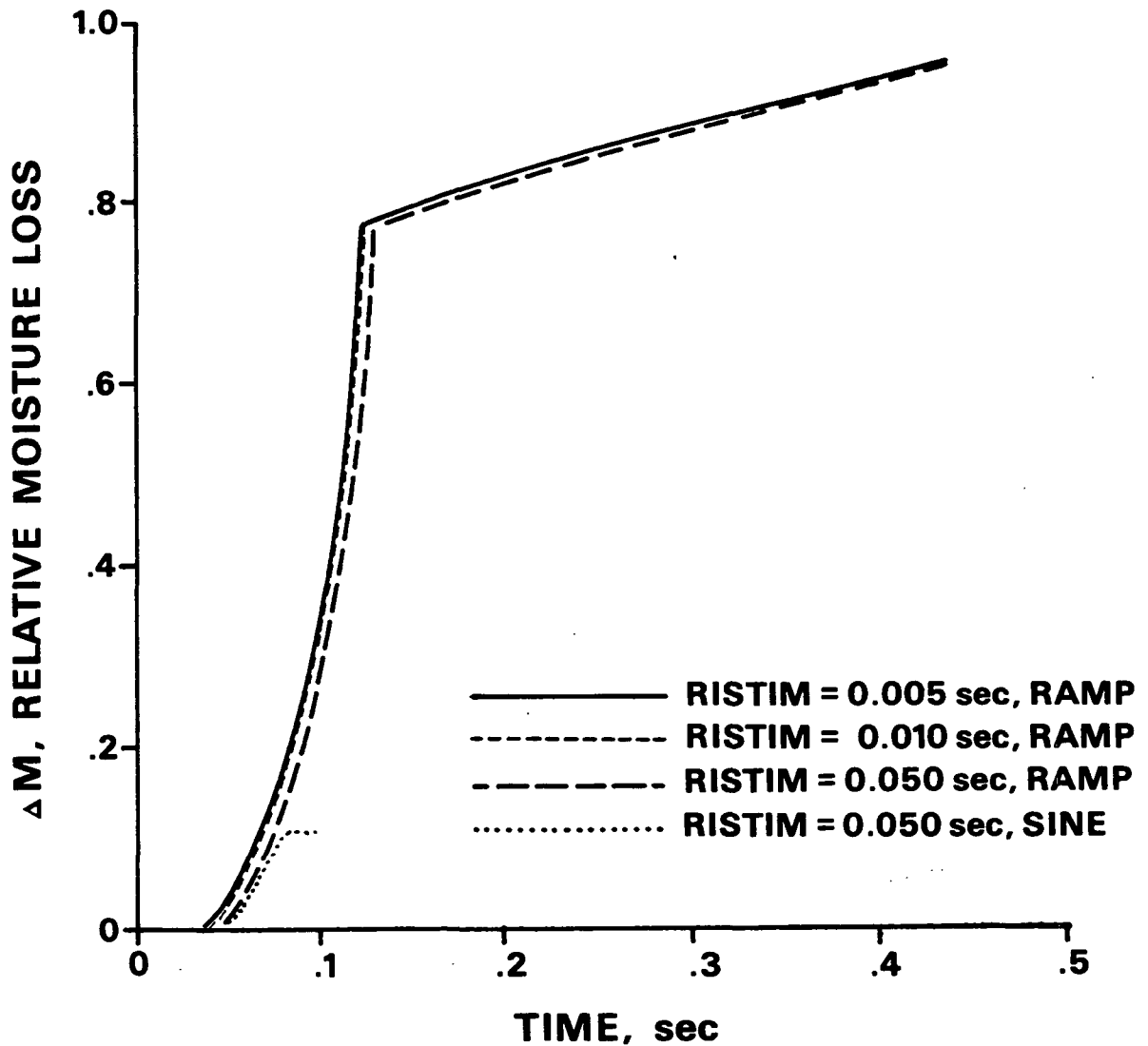


Figure 24. Effect of pressure rise time on moisture removal for RAMP cases and one SINE case.

The relative magnitudes of the changes are summarized in Table 2.

Table 2. Effect of changes in input parameters on drying time for RAMP cases.

<u>Parameter</u>	<u>Value Relative to Base Case Value</u>	<u>Change in Drying Time</u>
TH	- 25%	+123%
	+ 25%	- 39%
MRO	- 20%	- 2%
	+ 20%	+ 2%
BW	- 50%	- 60%
	+100%	+180%
CSF	- 33%	- 7%
	+ 33%	+ 18%
PMAx	- 40%	+ 16%
	+ 40%	- 9%
RISTIM	- 50%	<- 1%
	+400%	<+ 1%

SENSITIVITY ANALYSIS

The calculation method in HIDRYER1 requires that values be specified (in the program) for the number of grid points used in the finite difference equations (KMIN) and for the number of iterations used in determining the interface temperatures (IMAX). The default time increment (DTO) is an input parameter, and it too can influence the predicted drying output. There are no clear-cut methods of choosing appropriate values for these variables and so a sensitivity analysis is necessary to determine what numerical inputs give the best compromise between prediction accuracy and CPU ("computer") time.

Table 3 shows the results of variations in KMIN, IMAX, and DTO using the same inputs as for the RAMP base case (with the exception of DTO when sensitivity to DTO was tested, of course). The central line for each variable gives the value used in conducting the parametric study.

Table 3. Effect of grid spacing, iteration counter, and default time increment on drying time and CPU time.

<u>Variable and Value</u>	<u>Predicted Drying Time, s</u>	<u>CPU Time, hr:min:s</u>
KMIN 21	0.438	1:19:37
KMIN 101	0.432	0:28:20
KMIN 251	0.431	4:46:58
IMAX 5	0.432	0:22:26
IMAX 10	0.432	0:28:20
IMAX 15	0.432	0:35:34
DTO (hr) 10 ⁻⁵	0.456	0:27:54
10 ⁻⁷	0.432	0:28:20
10 ⁻¹⁰	0.430	9:38:27

Changing the value of KMIN results in minor changes in predicted drying time and more drastic changes in CPU time. When KMIN is increased from 101 to 251, the increase in CPU time is a direct consequence of the increased amount of calculations required. When KMIN is decreased from 101 to 21, one might anticipate a reduction in calculation time. However, because HIDRYER1 uses a forward time difference procedure, interface 2 may be advanced to a location such that its temperature is less than TB. When this occurs, no drying takes place until heat transfer to the transition zone raises its temperature in the vicinity of interface 2 to the point at which T2 is calculated to be above TB. Thus, several time increments may elapse in which there is no drying. Using fewer grid points reduces the effective heat transfer by predicting a lower temperature at any given point inside the outer zone and therefore there are more time increments early in the process when the sheet is still heating up and not drying.

A change in the number of iterations for the interface temperature calculations is reflected directly in the amount of CPU time required. Since there is essentially no change in the predicted drying time or behavior, it appears that

5 iterations are sufficient and the system is "well behaved" with regard to interface temperature calculations.

Decreasing the default time increment has a tremendous effect on CPU time. Typically, the interface motion time increment restriction and the finite difference time increment stability criterion are more restrictive than the default time increment. These are dominant in the transition regime. In the linear regime the finite difference criterion is not operative and the interfaces are sufficiently separated that the default time increment becomes the more restrictive time step. It is in just this regime, however, that a larger time increment can be most useful, since the rate of drying slows relative to the liquid dewatering part of drying. Limiting the default time increment chiefly limits the number of calculations in the linear regime only. Clearly, maintaining ΔT_0 on the order of 10^{-7} hour produces a vast improvement in accuracy with little sacrifice in CPU time.

SUMMARY

The parametric study shows that hot surface temperature and basis weight have the greatest influence on drying time to 6% moisture content. Peak pressure and freeness have a more moderate effect, and initial moisture ratio and rise time have almost no effect.

Using about 101 finite difference grid points, 5 iterations for interface temperature calculations, and a default time increment on the order of 10^{-7} hour appears to be an adequate compromise for balancing prediction accuracy and CPU time.

EXPERIMENTAL COMPARISONS

PURPOSE

Comparisons between experimental results and the model's predictions can suggest changes and improvements, can validate the mechanisms assumed in the model, and can identify areas requiring further experimental study.

EXPERIMENTAL CONDITIONS

Two kinds of experiments were selected for comparisons to HIDRYER1 output based on the manner and magnitude of mechanical pressure application: ramp-and-hold high intensity drying and short duration (impulse) high intensity drying. Examination of the assumptions used in developing the model suggests that it should best predict cases of high hot surface temperature and moderate mechanical pressure (so that good thermal contact is promoted but capillary flow is discouraged by maintaining larger pores) and a ramp-and-hold pressure pulse (since a static compression equation is used).

HIDRYER1 appears to be impractical for modeling cases of mechanical pressure at or below 350 kPa (50 psi). HIDRYER, the earlier version of the program, gives reasonable results in much shorter times. At a mechanical pressure of 321 kPa (46.6 psi) and hot surface temperature of 274°C (525°F), HIDRYER requires about 2 minutes of CPU time but HIDRYER1 needs about 5 hours. HIDRYER gives a better estimate of the experimentally determined⁹ drying time of 1.7 seconds: 1.4 seconds for HIDRYER and 0.68 second for HIDRYER1; and a better estimate of the peak vapor pressure of 120 kPa (17.4 psi): 125 kPa (18.1 psi) for HIDRYER and 24 kPa (3.5 psi) for HIDRYER1.

HIDRYER1 requires so much CPU time because it calculates all the properties and sheet behaviors, even when they change by only very small amounts. Conversely, HIDRYER has many built-in assumptions that eliminate the necessity for the

calculation of quantities that do not change much. For example, since HIDRYER takes values of thickness, absolute permeability, and the relative permeabilities as inputs and holds them fixed, it does not have to perform repetitive determinations of these quantities.

The chief drawback to using HIDRYER is that there are no simple guidelines for selecting valid "average" values representative of the quantities throughout the course of drying. Values for input parameters can be easily manipulated to produce good agreement with laboratory data, but the extent to which they reflect real sheet properties can always be questioned. HIDRYER1 attempts to provide an accurate picture at every instant of drying and was developed to address the chief drawback by removing the subjective aspect of running a simulation.

RAMP-AND-HOLD PRESSURE PULSE

Data are available⁹³ for a peak pressure of 4826 kPa (700 psi) at two hot surface temperatures: 149°C (300°F) and 274°C (525°F). Basis weight is 205 g/m² (0.042 lbm/ft²); moisture ratio is 1.3256; and freeness is 625 CSF. The hydraulic system for application of the pressure pulse causes a small overshoot of P_{MAX} before it settles to the designated value. RISTIM is selected as the time at which the mechanical pressure first reaches the target (about 0.12 second). It takes about an equal amount of time for the system to then settle and hold the target pressure value.

Figures 25 and 26 show predicted moisture removal curves with representative experimental points for the two cases. The experimental points are determined gravimetrically. The agreement appears to be better in the higher temperature case. This is probably due to the decrease in capillary effects at the higher temperature from lowered surface tension and viscosity and from the higher vapor pressure generated near the hot surface.

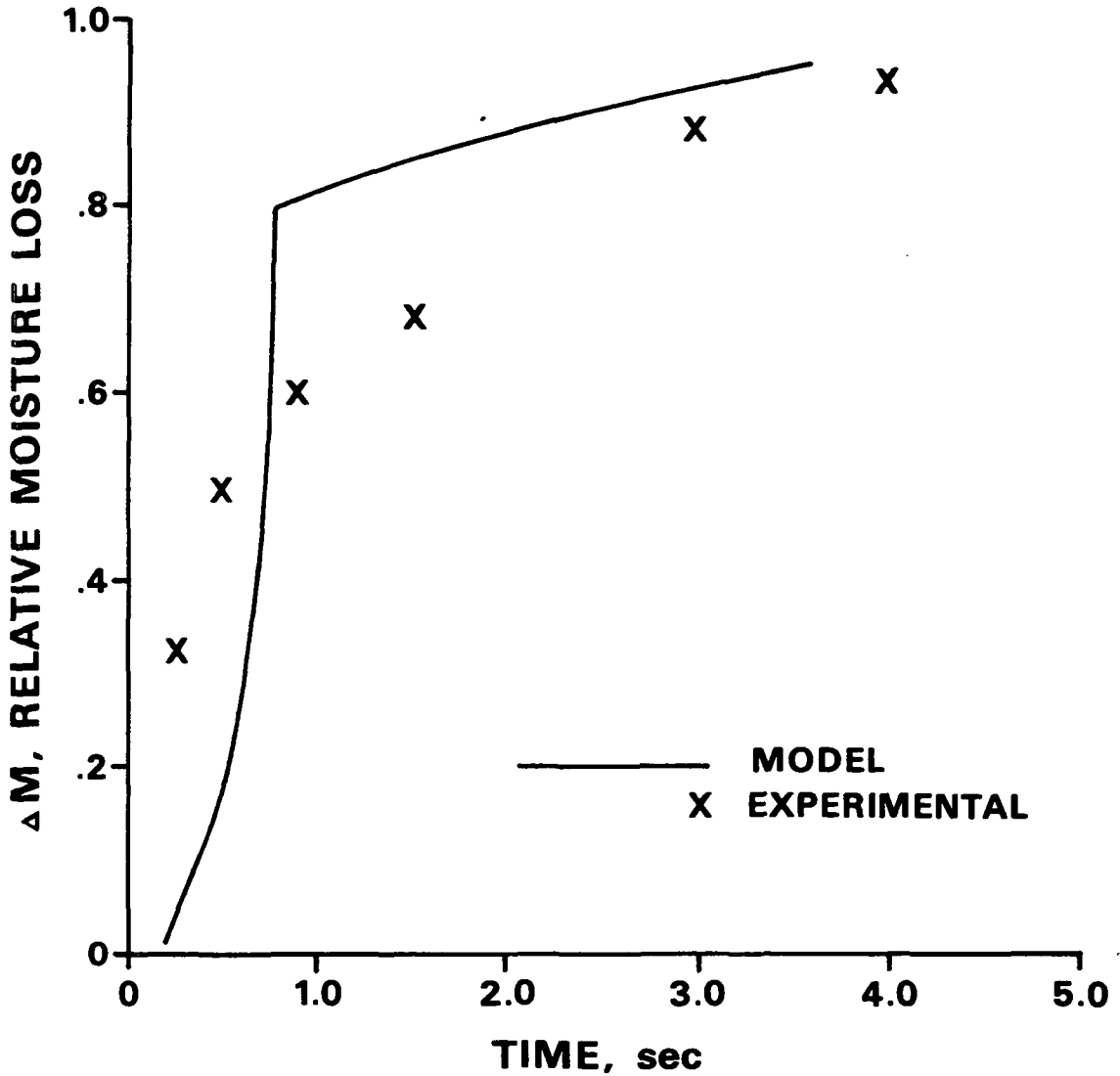


Figure 25. Predicted and measured moisture removal for 149°C (300°F) ramp-and-hold pressure pulse.

In both cases the model overpredicts the contribution of early liquid removal to overall moisture removal and underpredicts the rate of evaporative removal later in the process. Experimental results show liquid removal at about 30% of the total moisture removed,⁸ but the model predicts values in the range of 80%. Also, the predicted drying times are about half the experimental ones. This behavior is probably a function of the uniform fiber wall density assumption, which fixes the amount of liquid available for flow; the assumption of no vapor

flow through the outer zone during transition, which limits the rate of rise of internal sheet temperature; and the calculated permeability for the outer zone, which controls the flow resistance.

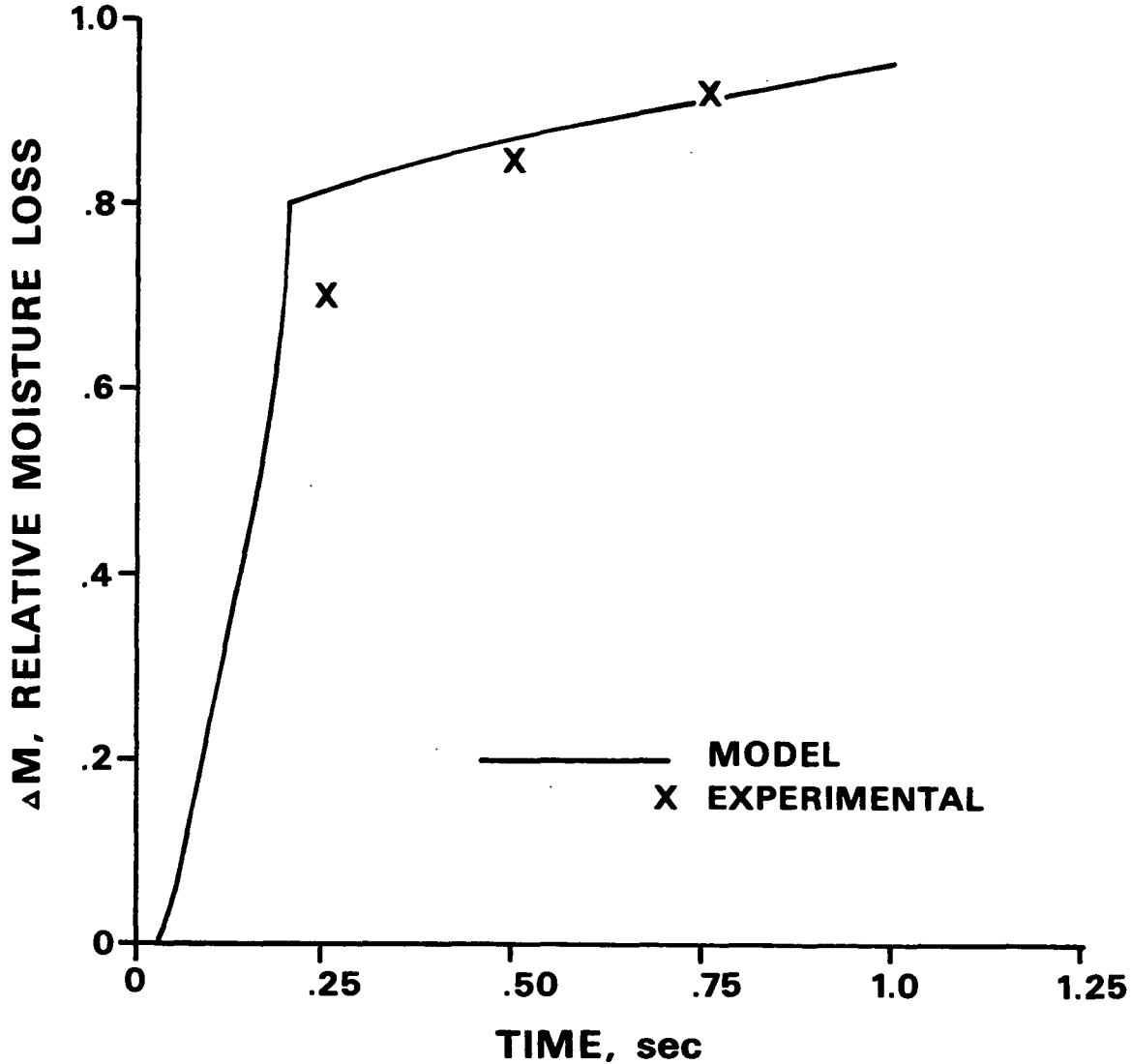


Figure 26. Predicted and measured moisture removal for 274°C (525°F) ramp-and-hold pressure pulse.

Figures 27 and 28 show heat flux comparisons for the two cases. The experimental heat flux is calculated from the measured hot surface temperature using Duhamel's Theorem. In both cases the model severely underpredicts the peak heat flux and less severely underpredicts the heat flux later in drying. The model curve also peaks before the experimental curve. This behavior is due to at

least two factors. First, the model assumes a constant hot surface temperature and determines heat flux by multiplying HC and the driving force (TH - TS). Experimentally, TH drops by about 4% of its initial value, therefore the value that the model predicts for HC must be low relative to the true value. Second, the experimental pressure actually exceeds the nominal target and this makes a contribution to the true value for HC but not for the calculated value for HC. Thus, the thermal and mechanical pressure lags of the physical system are not completely described by the model.

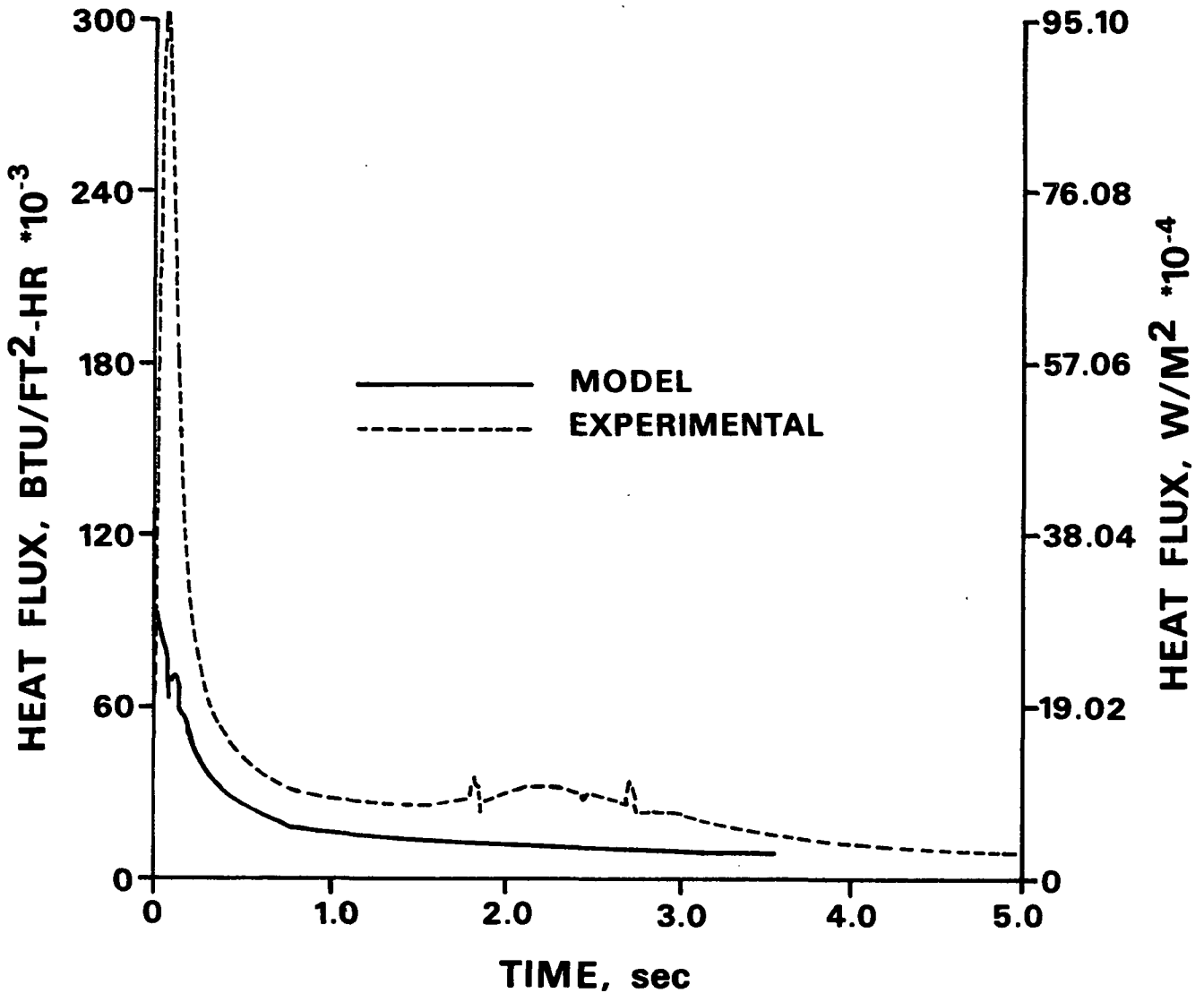


Figure 27. Predicted and measured heat flux for 149°C (300°F) ramp-and-hold pressure pulse.

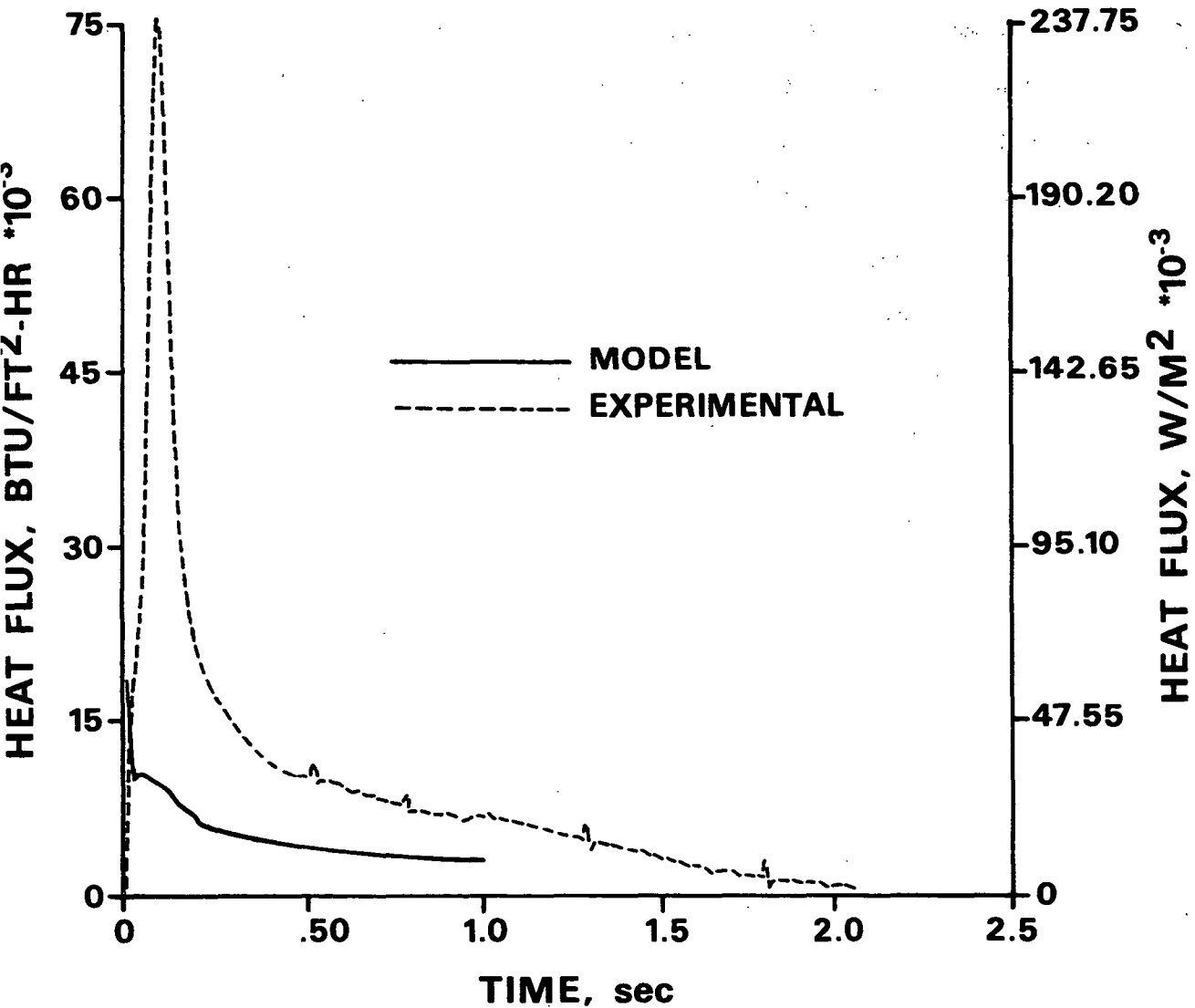


Figure 28. Predicted and measured heat flux for 274°C (525°F) ramp-and-hold pressure pulse.

Figures 29 and 30 show predicted and measured sheet thicknesses. The model curves qualitatively describe the compression pattern: a rapid compression ending in an abrupt change in compression rate followed by a moderate compression regime ending in an accelerating rate of compression followed by a quasi-equilibrium regime. The first regime results from the rapidly rising mechanical pressure. As the pressure attains the target value, heat transfer to the sheet begins to raise the hydraulic (vapor) pressure and the mechanical pressure plateaus, both of which slow the compression. Later, the heat flux drops, the interfaces move

into the sheet, moisture removal is dominated by liquid dewatering, and the vapor pressure decrease in the sheet increases the rate of compression. As the sheet enters the regime of drying by evaporation only the rate of moisture loss slows and the quasi-static compression regime starts. Quantitatively, the model underpredicts the initial sheet thickness and overpredicts the equilibrium thickness. This suggests a decrease in the M compression value and an increase in the N compression value would be appropriate so that the lower M value would dominate at lower pressures and the higher N value would dominate at higher pressures.

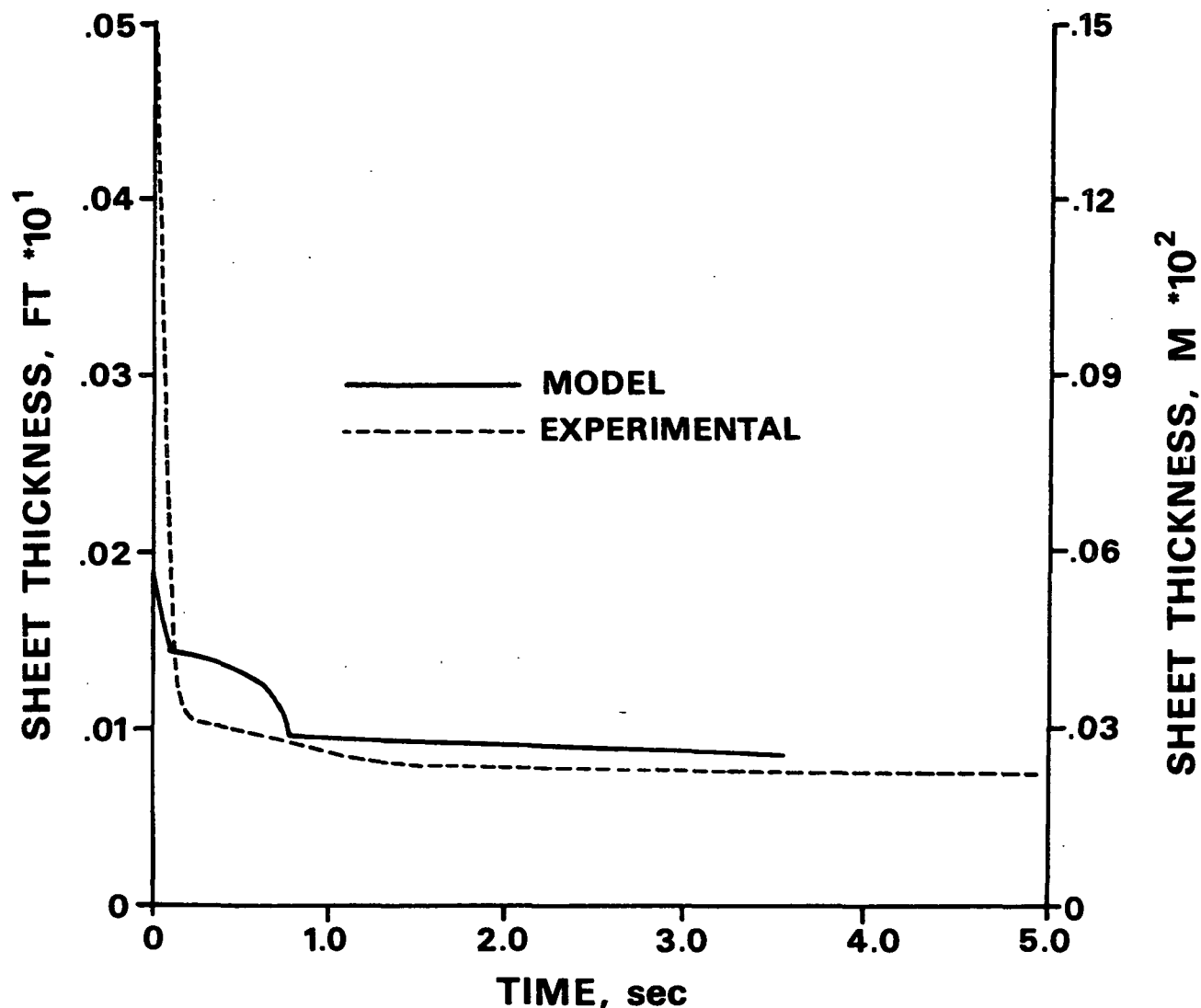


Figure 29. Predicted and measured sheet thickness for 149°C (300°F) ramp-and-hold pressure pulse.

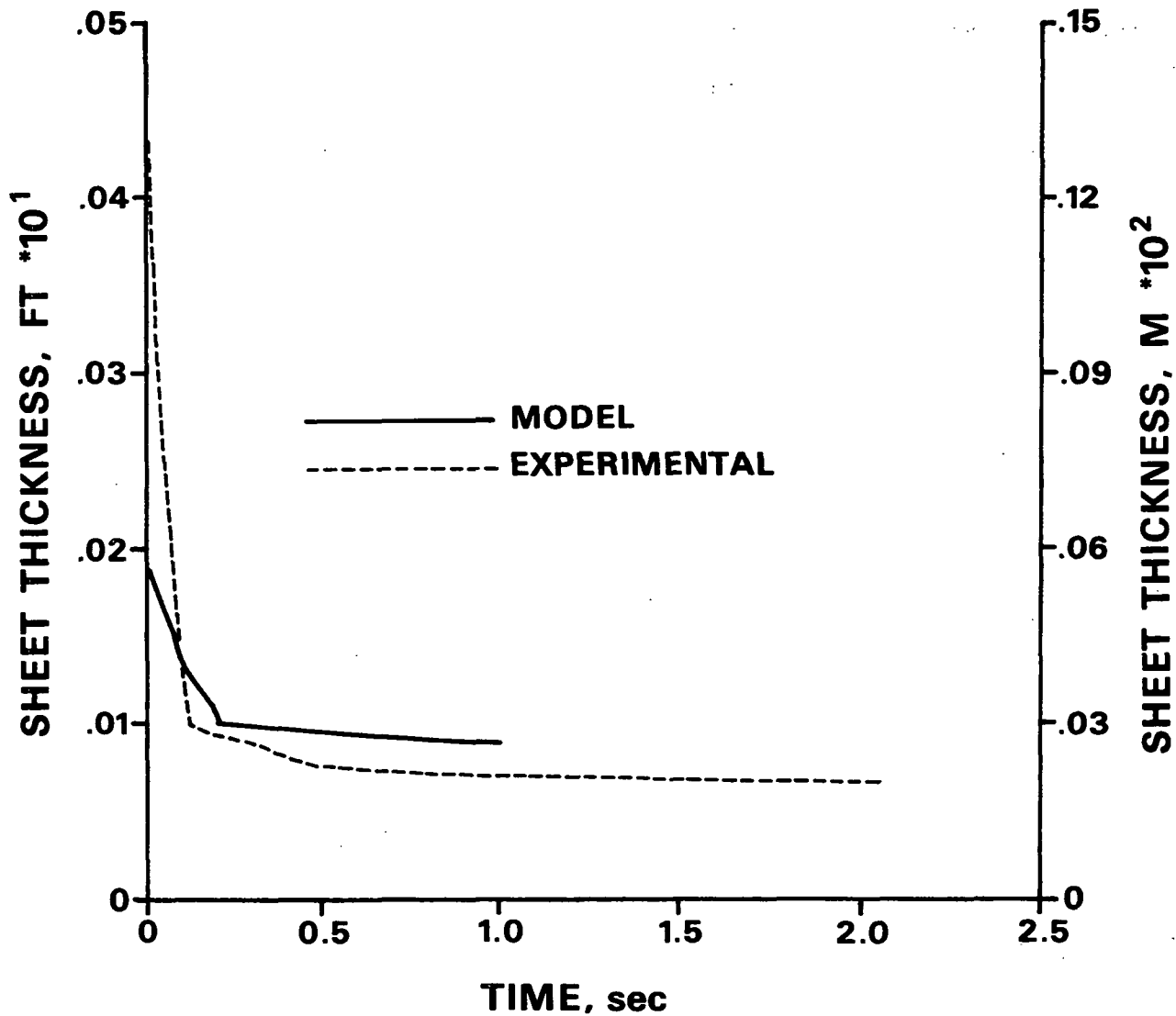


Figure 30. Predicted and measured sheet thickness for 274°C (525°F) ramp-and-hold pressure pulse.

Figures 31 and 32 again show that the model qualitatively describes these drying conditions. The temperature at a point midway through the basis weight of the sheet is plotted for both cases. The experimental curves indicate that the rate of heat transfer to the interior of the sheet is much higher than that predicted by the model. This is probably due to the model's assumption of no vapor flow through the outer zone during the transition regime. The large latent heat carried into the zone and released by vapor condensation raises the temperature there much faster than simple conduction would. Including this

effect would complicate the transition regime calculations by introducing a source term in the transient heat transfer equation and by requiring a more complicated mass balance (since the moisture ratio would be changing) but would be a reasonable next step in improving the model.

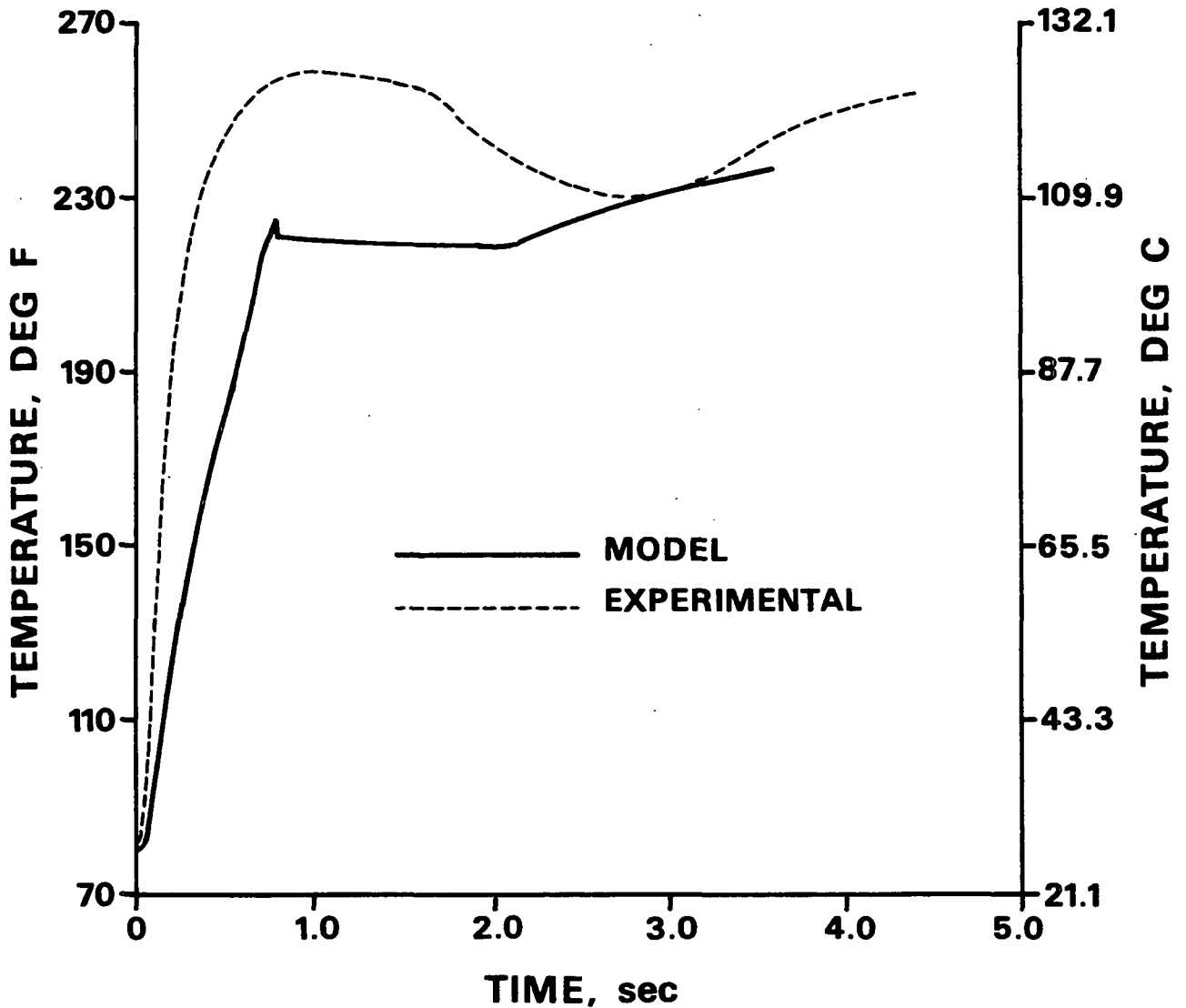


Figure 31. Predicted and measured midpoint temperature for 149°C (300°F) ramp-and-hold pressure pulse.

To demonstrate the effect of the proposed changes to the model, constants in the model were simultaneously modified by 10% of their original values. The reference values for contact coefficient and the N compression constant were increased. The apparent cell wall density, the absolute permeability, and the M

compression constant were decreased. To simulate the transport and condensation of vapor in the outer zone, the thermal conductivity was modified by the addition of a diffusion term for the heatup period⁹⁴ and a bulk vapor flow term for the transition period.⁹⁵ This combined "effective" conductivity can be orders of magnitude larger than the simple conductivity and should greatly increase heat transfer to the interior of the sheet. Note that no attempt was made to account for any changes in saturation from the condensing vapor. This approximation is reasonable because the large latent heat implies that only a small amount of condensation is necessary to produce a large change in temperature.

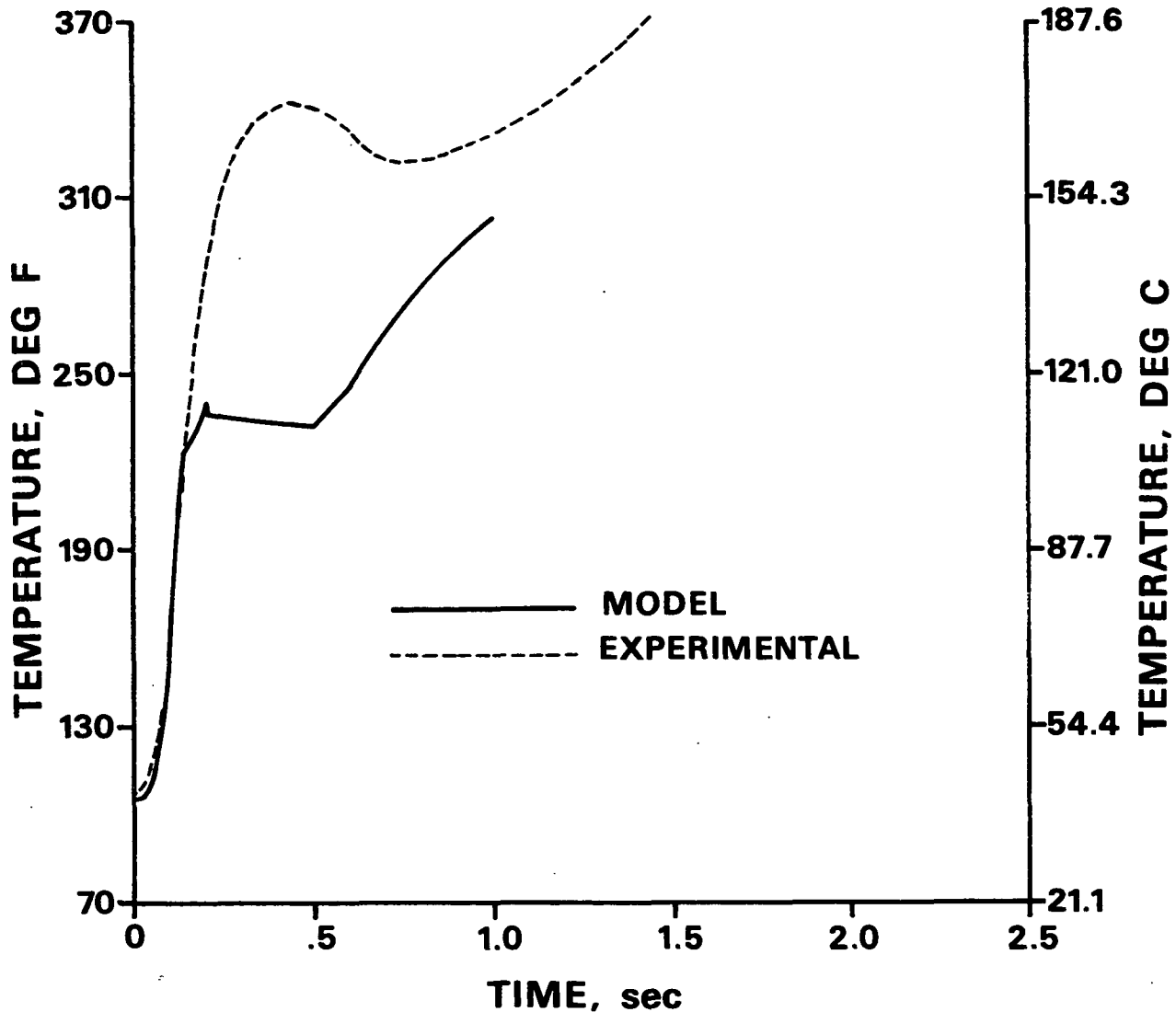


Figure 32. Predicted and measured midpoint temperature for 274°C (525°F) ramp-and-hold pressure pulse.

The results of this "optimization" are shown in Fig. 33 through 40 for the ramp-and-hold pressure cases. Figures 33 and 34 display the changes in drying behavior caused by the modifications. In both cases there is little effect on heatup time, since the diffusion term augmenting thermal conductivity is relatively small. The transition time is greatly reduced because the bulk flow term augmenting conductivity is very large. Trapping more water in the fibers causes a decrease in the amount of moisture removed in liquid form (from 80% down to 70%), and increases the drying time, since more moisture has to be removed by an evaporation mechanism.

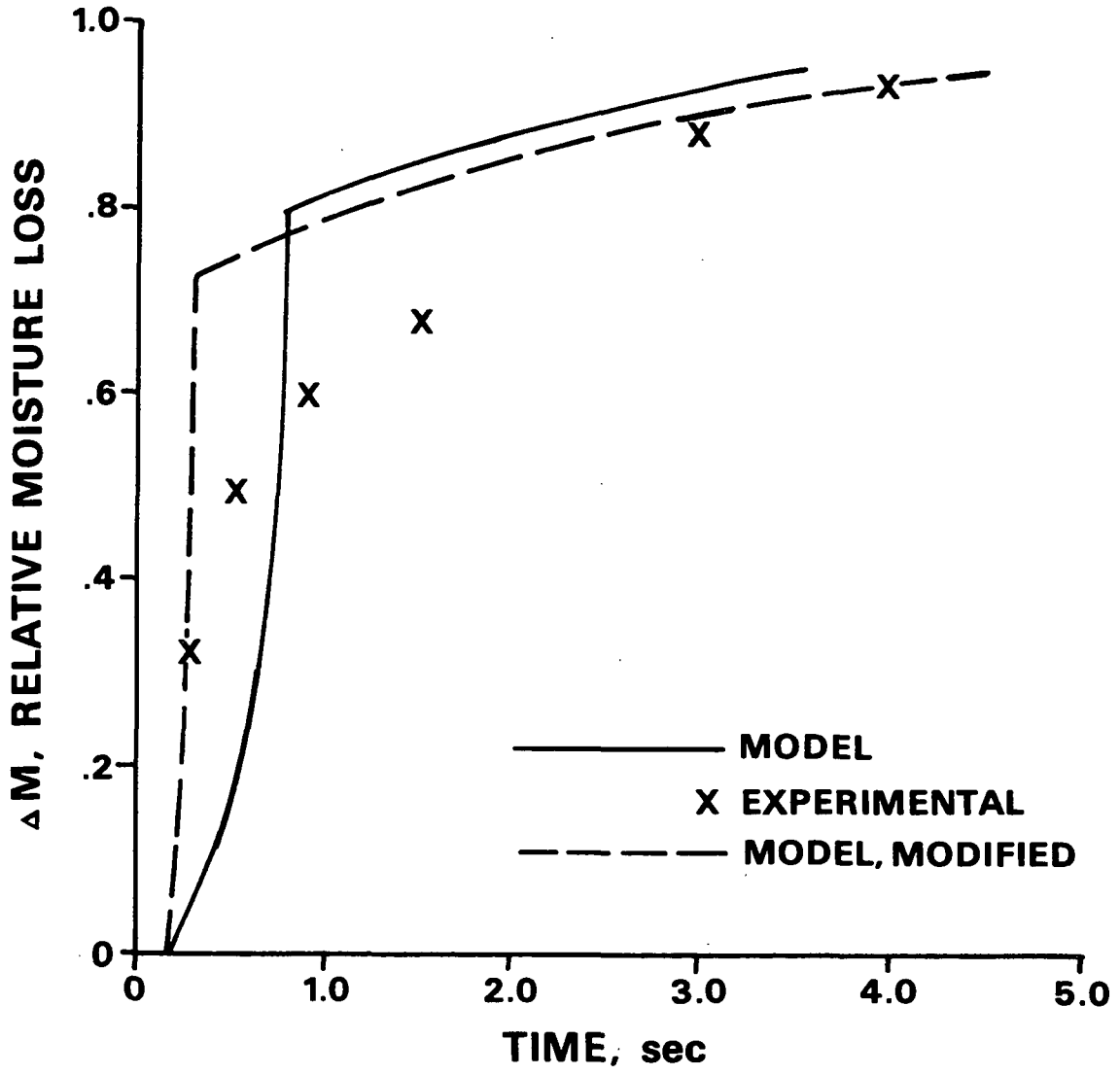


Figure 33. Predicted, measured, and modified model moisture removal for 149°C (300°F) ramp-and-hold pressure pulse.

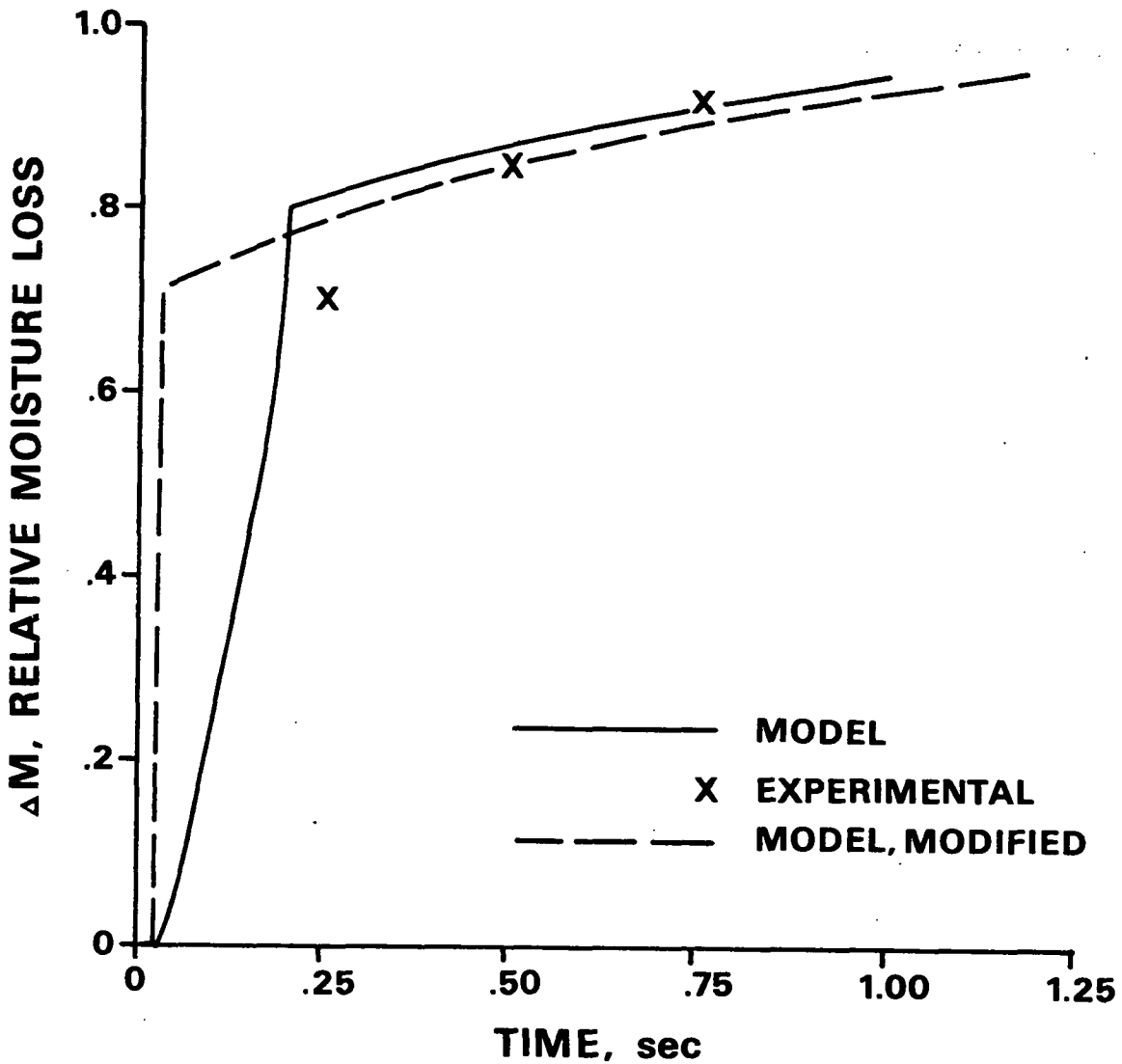


Figure 34. Predicted, measured, and modified model moisture removal for 274°C (525°F) ramp-and-hold pressure pulse.

Figures 35 and 36 show the influence on heat flux. In the 149°C (300°F) case the heat flux is decreased, which is the opposite of the anticipated trend. The change in compression constants causes a general increase in porosity and therefore an overall decrease in the contact coefficient even though the reference values for H_c were increased by 10%. In the 274°C (525°F) case, there is little effect because the higher driving force ($T_H - T_S$) tends to mask the influence of changes in the H_c reference values and compression constants.

Figures 37 and 38 depict the changes in predictions of sheet thickness. Changing the constants causes a slight increase in the initial thickness

prediction and significant changes in the slope and duration of the intermediate compression regime. The increase in N is not enough to offset the decrease in M and the modified model predicts an even higher thickness in the third compression regime. The slope is also changed in the third regime and shows a more rapid compression in the later stages of drying.

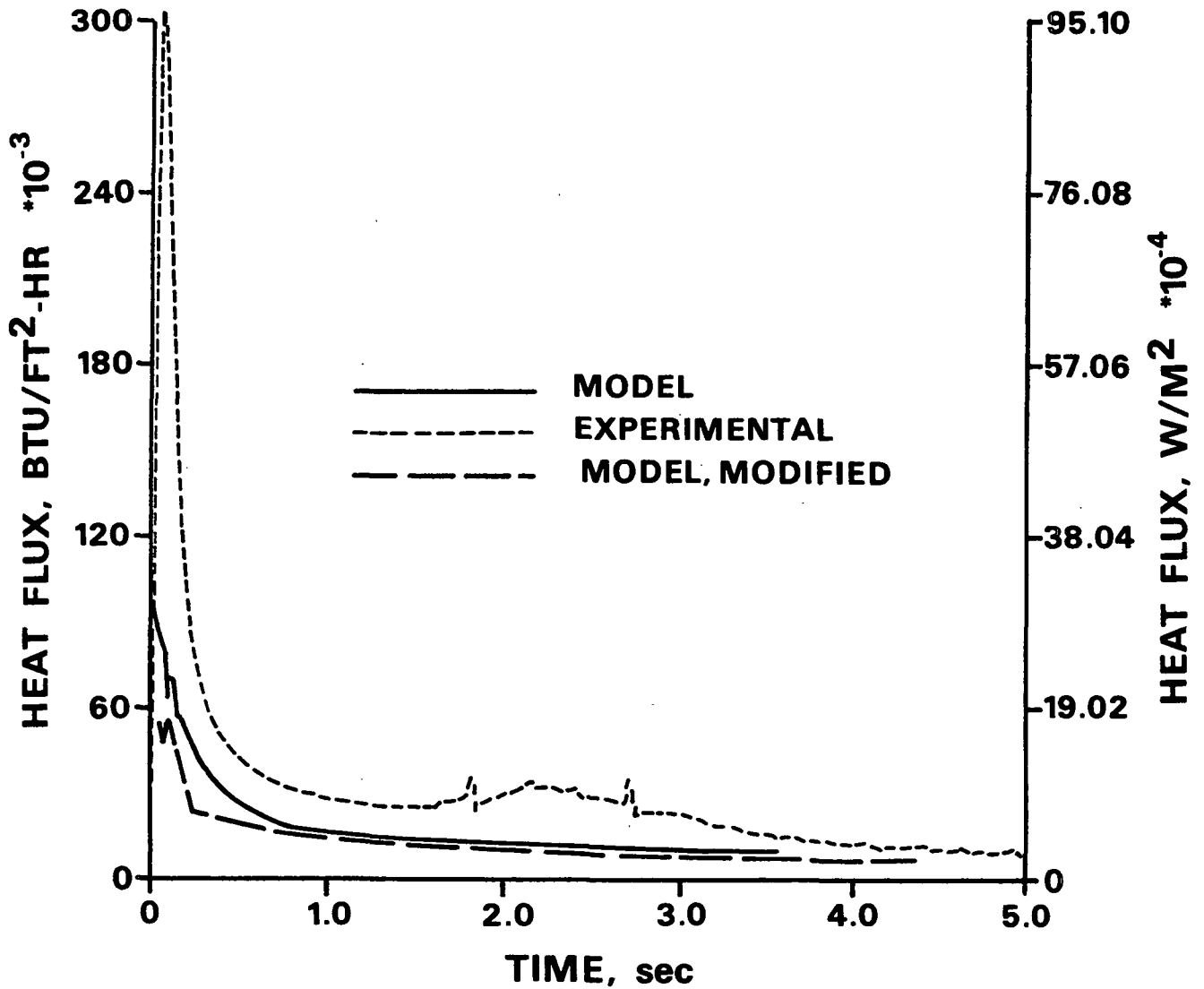


Figure 35. Predicted, measured, and modified model heat flux for 149°C (300°F) ramp-and-hold pressure pulse.

Figures 39 and 40 graph the effects of the modifications on the prediction of midpoint temperature. The first-peak midpoint temperature is significantly increased and the time required to achieve the peak is decreased. The duration of the predicted plateau period is increased. In a qualitative sense, the

changes benefit the lower temperature case more than the higher temperature case. This tends to indicate that the initial values for most constants were reasonable and that it is a change in mechanism going from lower temperature to higher temperature (such as the relative importance of capillary liquid flow) that causes the difference between measured and predicted behavior. Since the assumptions of HIDRYER1 are more appropriate to the higher temperature case, changing the constants should be expected to shift it away from its initially reasonable qualitative fit.

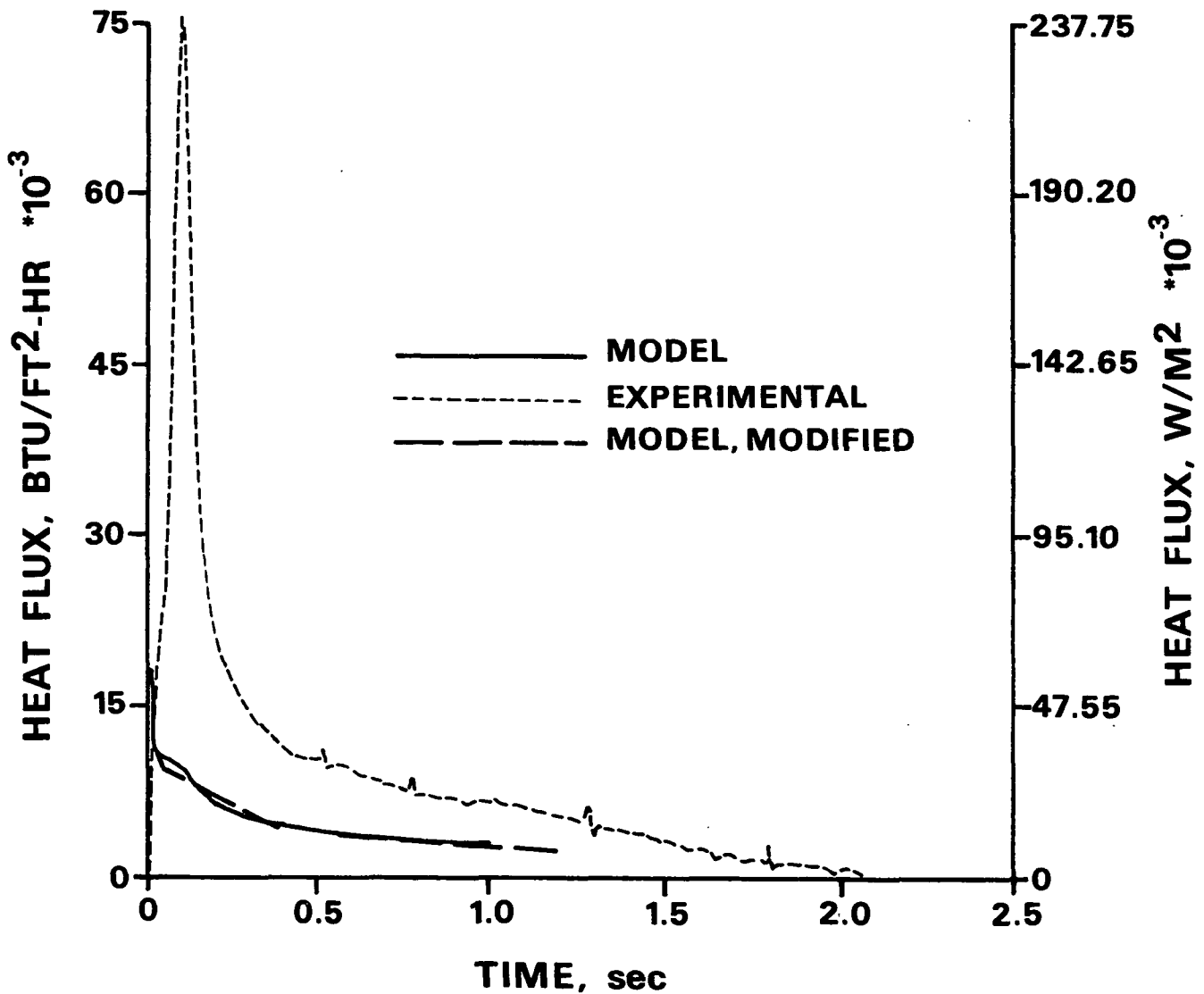


Figure 36. Predicted, measured, and modified model heat flux for 274°C (525°F) ramp-and-hold pressure pulse.

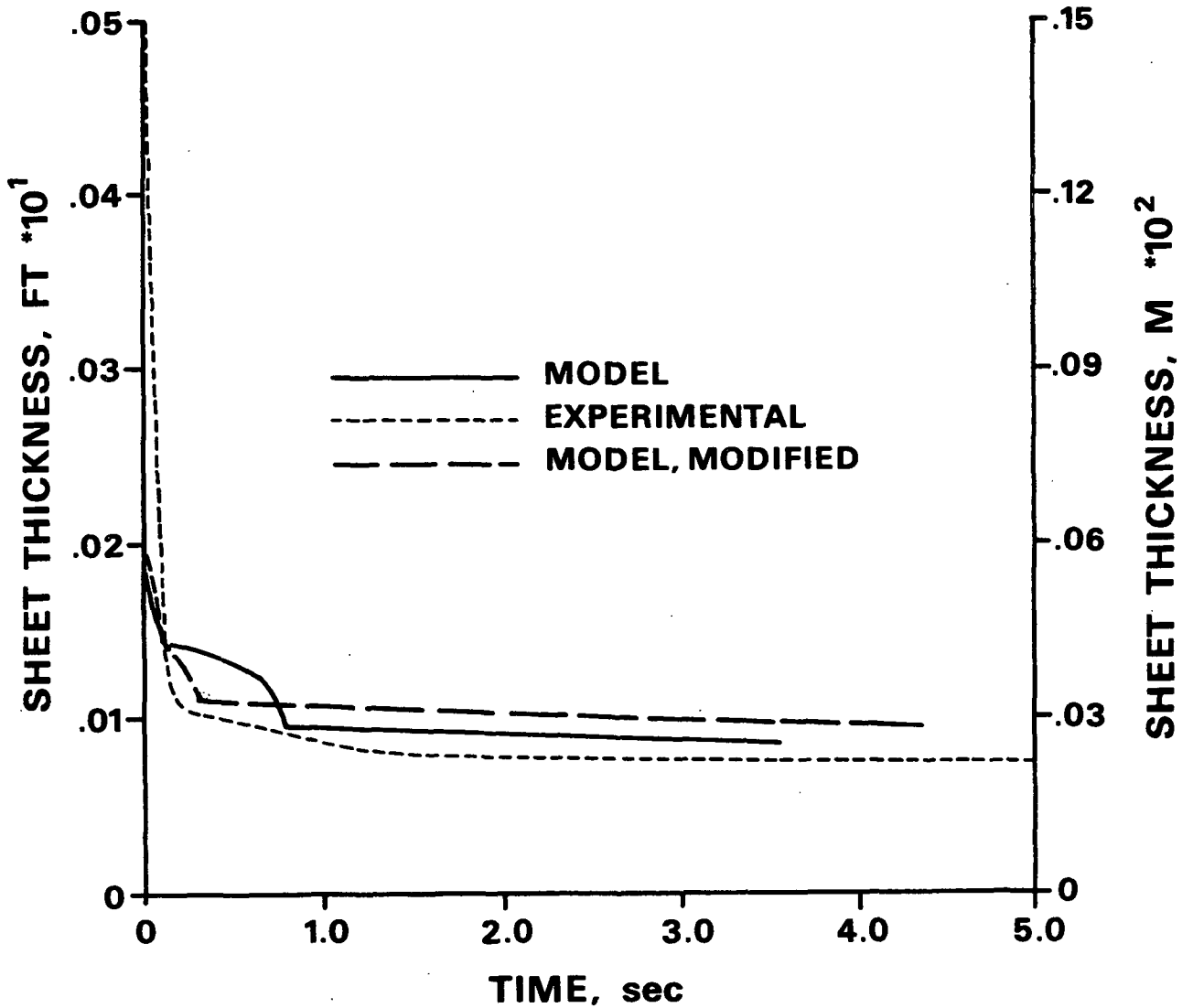


Figure 37. Predicted, measured, and modified model sheet thickness for 149°C (300°F) ramp-and-hold pressure pulse.

The previous figures clearly show that the model can be easily modified to alter its predictions by changing the constants in the model. An optimization of these constants in conjunction with further experimental information should be able to produce a highly accurate predictive tool.

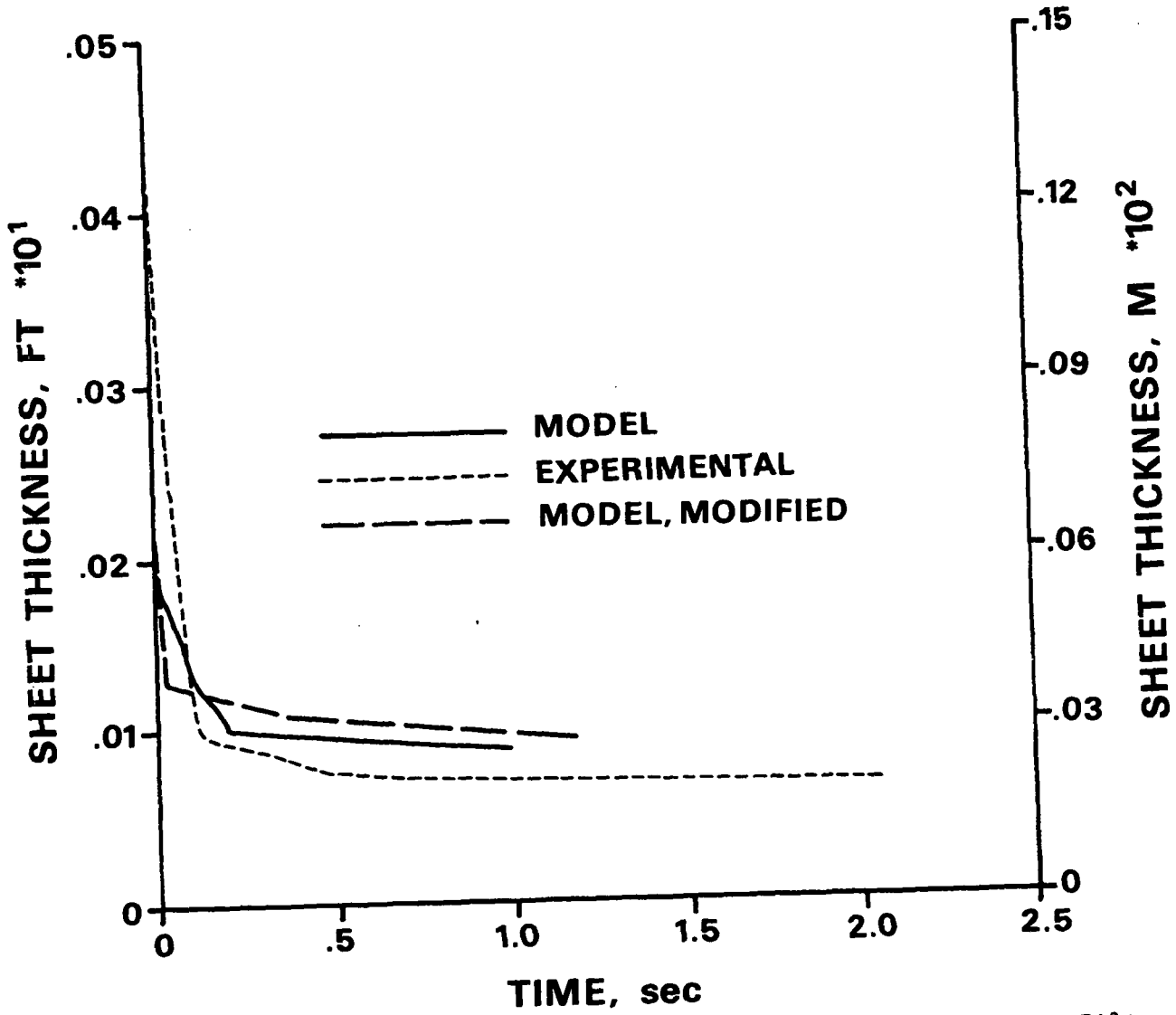


Figure 38. Predicted, measured, and modified model sheet thickness for 274°C (525°F) ramp-and-hold pressure pulse.

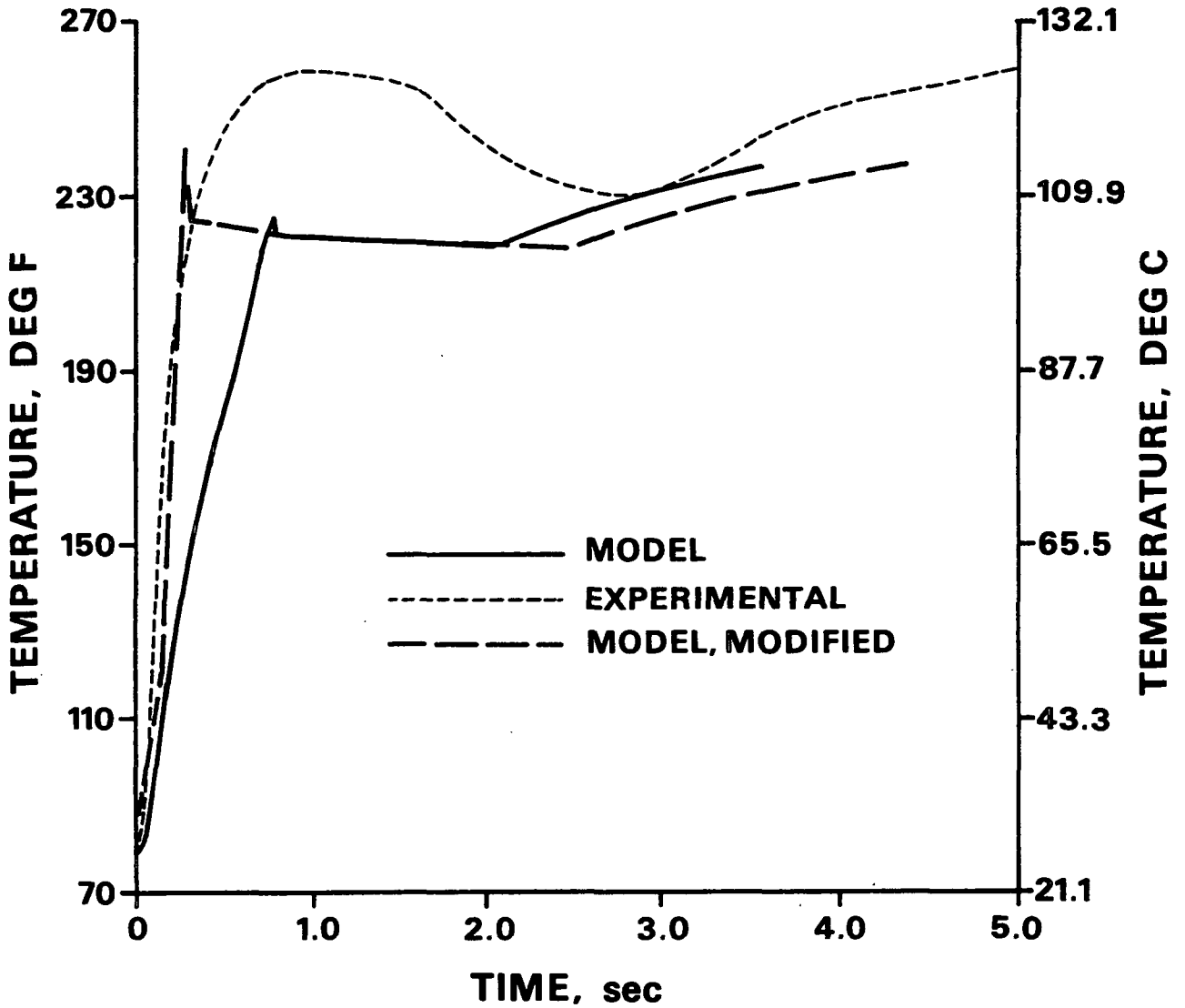


Figure 39. Predicted, measured, and modified model midpoint temperature for 149°C (300°F) ramp-and-hold pressure pulse.

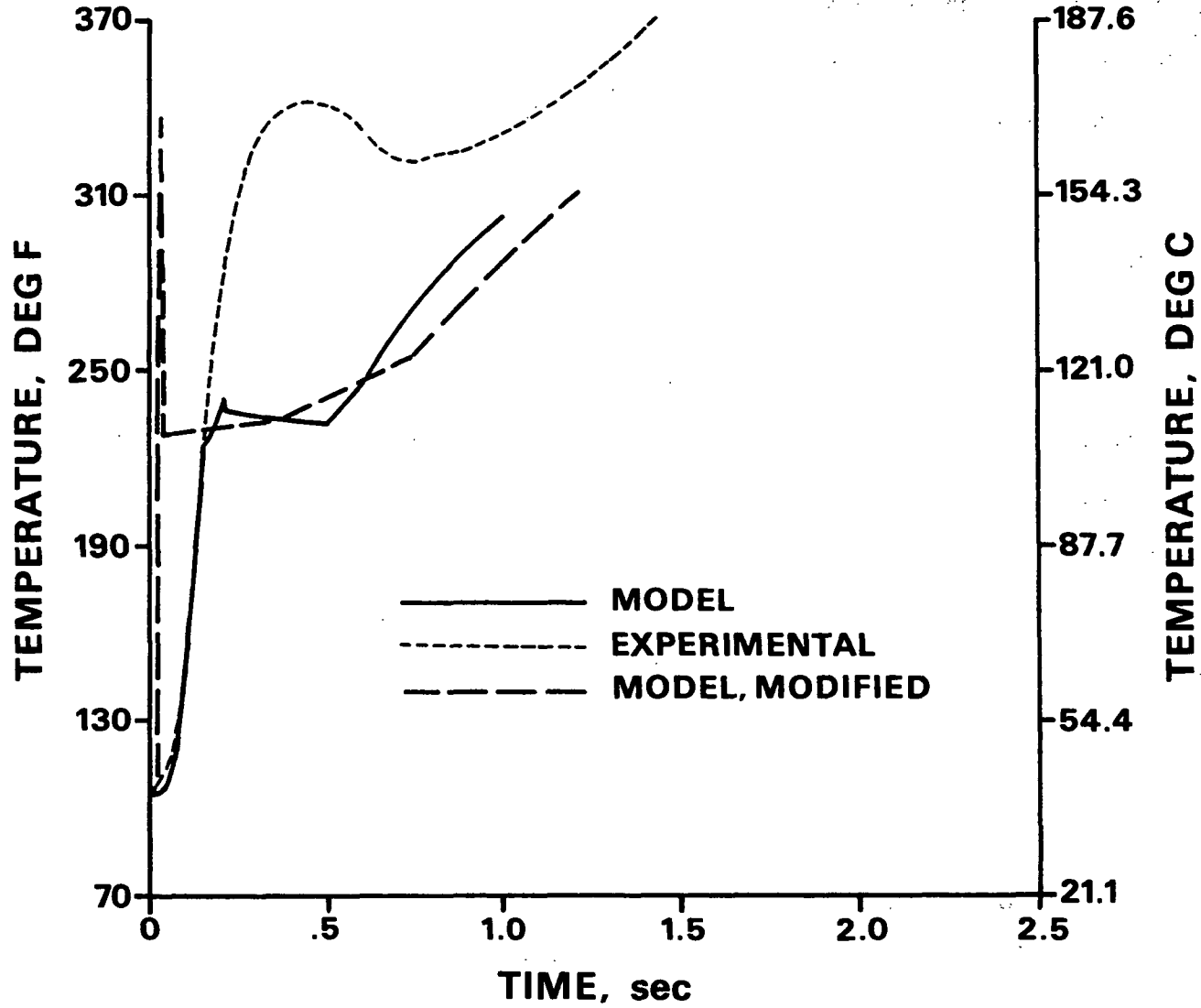


Figure 40. Predicted, measured, and modified model midpoint temperature for 274°C (525°F) ramp-and-hold pressure pulse.

SHORT DURATION (IMPULSE) PRESSURE PULSE

The time scale for the application of the mechanical pressure pulse in impulse drying is an order of magnitude shorter than the ramp-and-hold method. Rise times of a few milliseconds are possible. The heat and mass transfer phenomena that take place in both circumstances are fundamentally the same, but because of the dynamic nature of the impulse process the compression properties of the sheet assume great importance. The moisture loss by mechanical compression is

greater in the impulse case and the resulting sheet properties tend to be different. The impulse process is conceptually more identifiable with a (very high temperature) "heated wet pressing" operation than with a "drying" operation.

Figures 41 and 42 show comparisons of experimental and predicted sheet thicknesses for impulses delivered by a drop press simulator³ at two hot surface temperatures.⁹⁶ Figure 42 corresponds to a wet pressing case since the temperature is only 18°C (65°F). The difference in magnitudes for the predicted and experimental results comes from the values used for M and N in the model and because the model calculates the thickness at every point in time (i.e., there is no initial thickness input to the model). If the model curve is simply shifted vertically so that the initial predicted thickness matches the initial measured thickness, a better comparison can be made. This is also shown in Fig. 41 and 42. Note that this method could be built into the model by supplying the initial thickness and correcting the model's predictions by a constant value equal to the difference between initial measured and predicted thicknesses. (An alternative would be to supply the initial measured thickness and modify M and N so that the initial predicted thickness would match.) Apart from the difference in magnitudes, the model exhibits an elastic type of behavior consistent with its compression equation. The experimental result shows how the paper fails to recover after the peak pressure has been achieved. This is due in part to the viscous nature of the fiber matrix and in part from irreversible alterations in the matrix structure. The depression in the center of the predicted curve results from the combination of rapid rate of change in pressure and N (which is a function of pressure) as the peak pressure is reached.

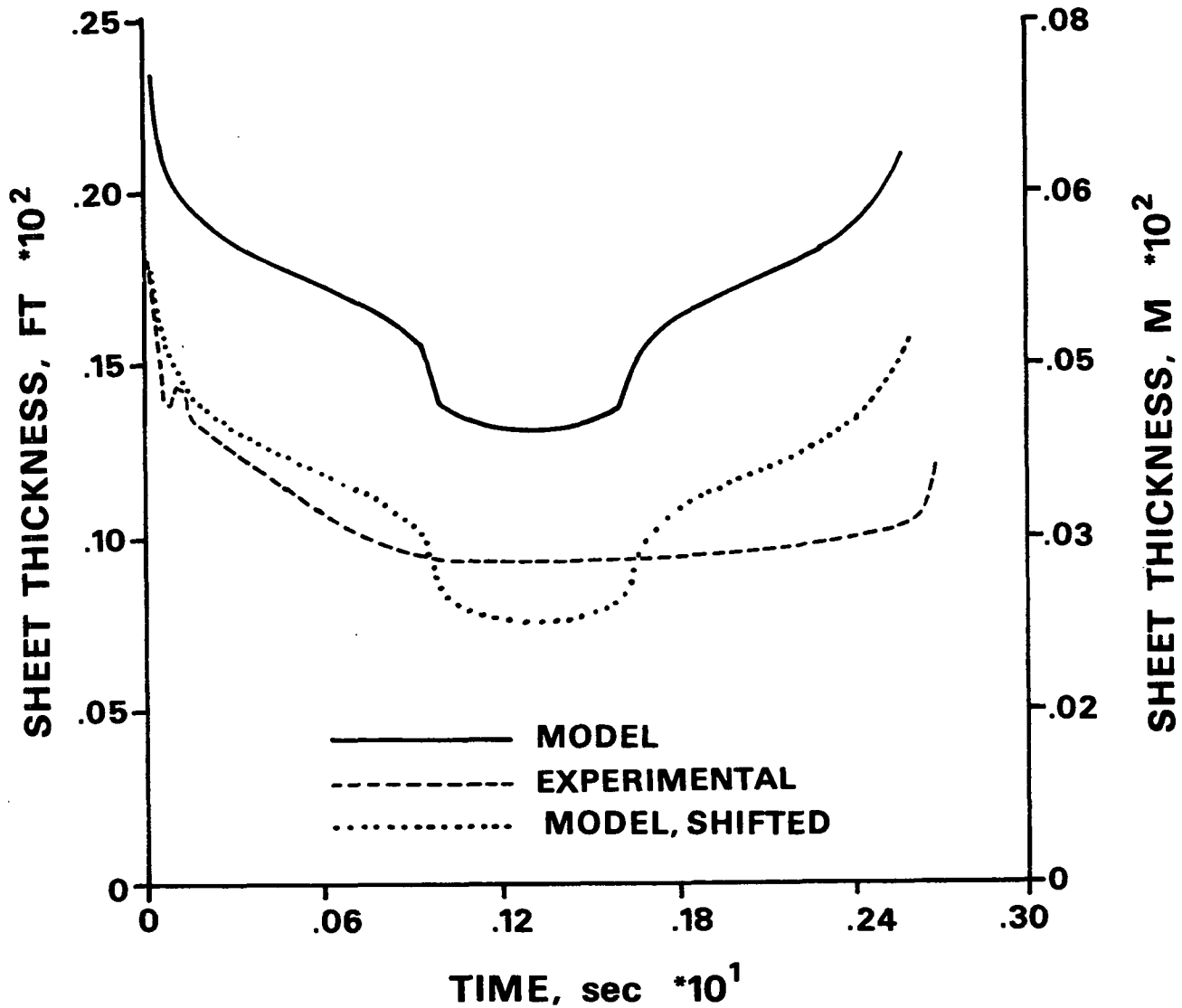


Figure 41. Predicted and measured sheet thickness for 18°C (65°F) impulse case.

In the 316°C (600°F) case, Fig. 42, the model more closely mimics the experimental result in a qualitative sense. Thermal softening at the elevated temperature moderates the rapid change in thickness as the peak pressure is attained. The model predicts a faster rate of compression in this case and a slower rate of thickness recovery relative to the lower temperature case. The experimental measurements show about the same rates in both cases. The model predicts a somewhat lower minimum thickness in the higher temperature case, which is the opposite of the experimental result. The model results are directly related to

the use of a compression equation in a drying model instead of using a heat transfer equation in a dynamic wet pressing model. A compression equation does not fully describe the internal sheet behavior to the extent necessary for direct application to impulse conditions.

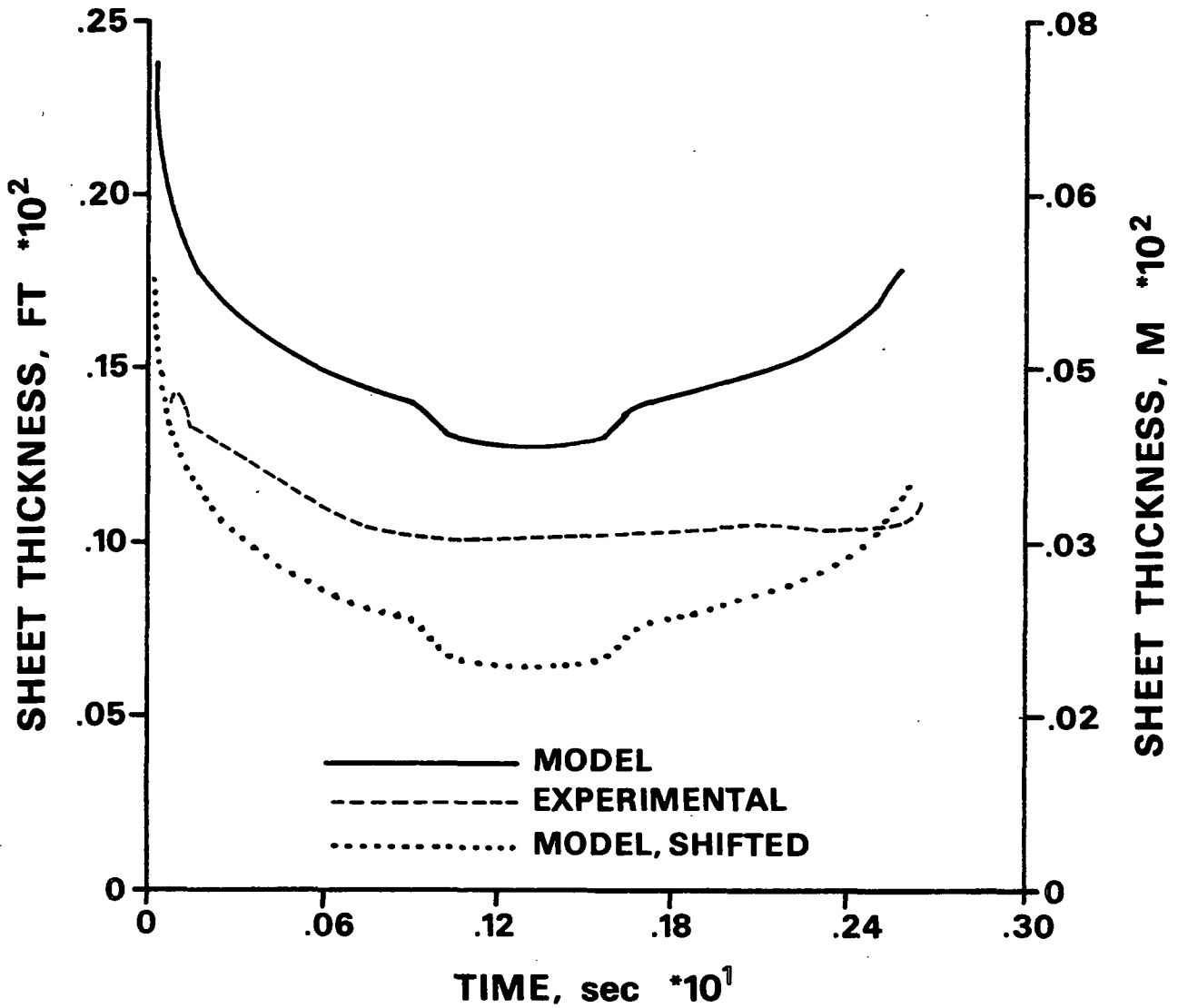


Figure 42. Predicted and measured sheet thickness for 316°C (600°F) impulse case.

Figure 43 shows the results from experiments in a heated, rotating roll press nip.⁹⁷ Equivalent dewatering can be achieved at many combinations of hot surface temperature and nip residence time.

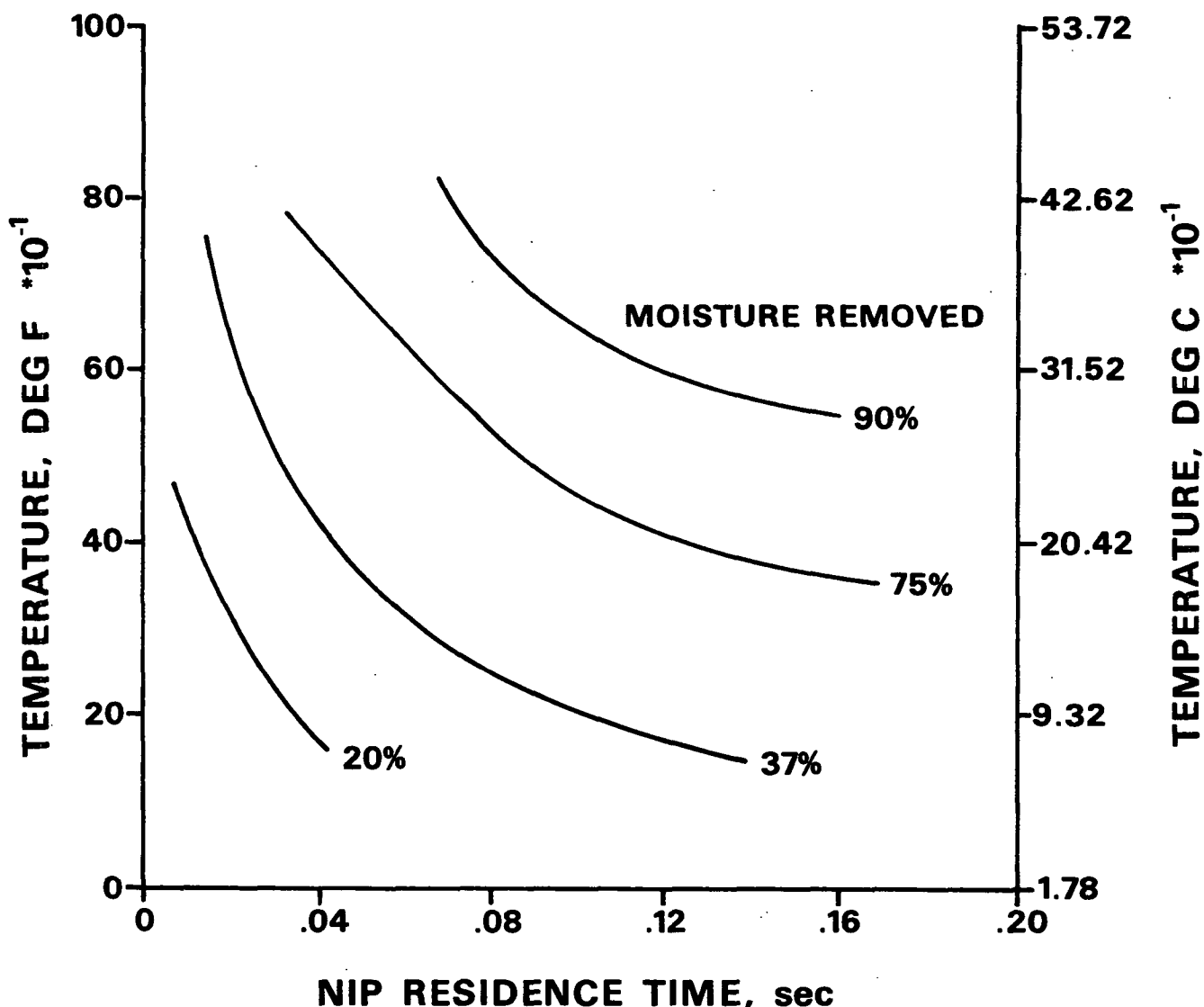


Figure 43. Impulse drying moisture removal for various combinations of hot surface temperature and nip residence time.

Table 4 summarizes the model's dewatering predictions for a variety of operating conditions selected from Fig. 43. The basis weight is 100 g/m^2 (0.0205 lbm/ft^2); moisture ratio is 1.381; freeness is 570 CSF; and P_{MAX} is 12144 kPa (1760 psi). There are certain combinations of time and temperature which cause the model to predict an apparent zone 3 density which is greater than the (assumed constant) effective fiber wall density of 1 g/cc. The higher temperature cases can complete the calculations at shorter nip residence times than the lower temperature cases. This is a consequence of the rate of dewatering (rates of heat transfer and vapor pressure generation) relative to the rate of compression.

Table 4. Comparison of predicted and measured moisture removal for impulse drying conditions.

<u>TH, °C (°F)</u>	<u>Nip Residence Time, s</u>	<u>Experimental Moisture Removal, %</u>	<u>Model Moisture Removal, %</u>
149 (300)	0.020	20	55 ^a
	0.060	37	33 ^a
204 (400)	0.011	20	30 ^a
	0.042	37	58 ^a
	0.130	75	75
260 (500)	0.030	37	64 ^a
	0.083	75	82
316 (600)	0.022	37	76
	0.063	75	83
	0.114	90	89
371 (700)	0.016	37	0 ^a
	0.044	75	83
	0.082	90	88

^a Computation terminated when zone 3 porosity becomes lower than the minimum allowable porosity.

Higher temperatures produce faster drying and higher hydraulic (vapor) pressures before the critical density is achieved by compression so that these cases can run to completion. At a basis weight of 50 g/m² (0.01025 lbm/ft²) the model runs to completion but predicts no dewatering, even at 316°C (600°F) and 4137 kPa (600 psi), when the nip residence time is 5.4 milliseconds. Experimental moisture removals of up to 80% have been demonstrated for these conditions.⁹⁸

In Table 4 all model cases overpredict the amount of moisture removed but the trend of increasing removal with increasing time is intact. The overprediction is a function of the assumed fiber wall density which determines the amount of (trapped) moisture unavailable for liquid flow. Decreasing the density would lower the amount available for flow but would raise the minimum porosity (lower

the effective critical density). The model therefore needs to be modified to treat both a compressible matrix, so that sheet thickness is a function of mechanical pressure; and compressible fibers, so that the liquid available for flow becomes a function of mechanical pressure and the limiting density is the density of cellulose (at a porosity of zero).

SUMMARY

HIDRYER1 gives good qualitative agreement with experimental results. The quantitative agreement could be improved by varying some of the constants used in the model and modifying the model to account for the phenomena of vapor flow and condensation during the transition regime and liquid expression from the fiber walls.

SUMMARY

This mathematical model is a significant first effort in the development of a convenient predictive tool for investigating high intensity drying options. The zone concept and simple solution method provide a methodology and framework for easy modification, expansion, and improvement.

The model requires few input parameters (hot surface temperature, boiling point temperature, basis weight, Canadian Standard Freeness, initial moisture ratio, mechanical pressure pulse) and qualitatively accounts for the observed macroscopic phenomena: internal sheet temperature, heat flux, sheet thickness, and moisture removal in liquid and vapor form. The degree of quantitative agreement varies with drying conditions. The agreement with all experimentally measured quantities could be improved by the specific suggestions in the thesis using a mathematical optimization procedure (with the empirical results as constraints on the output).

Capillary liquid flow appears to be significant at lower hot surface temperatures. Vapor flow with condensation appears to be significant during the transition regime under all conditions. A better model of dynamic sheet compression at high temperatures needs to be developed and tested.

RECOMMENDATIONS

The first extension of this work should be the modification of HIDRYER1 to run faster. This could be accomplished in several ways. The number of finite difference grid points could be reduced; the number of iterations for the calculation of the interface temperatures could be reduced; an alternative to the finite difference method could be used; or a reorganization of the computational algorithm could be performed. Any reduction in the CPU time would encourage more use of the model and allow a more comprehensive parametric investigation.

Second, a mathematical optimization of the model's constants would yield improvements in its quantitative predictions. There is already enough empirical evidence to make a reasonable effort in this area.

The third area for future research involves permeability. Transport models for paper have been limited in that a thorough investigation of the factors (freeness, moisture ratio, etc.) affecting permeability has not been performed. Isolated efforts are apparent, but are limited in scope and depth.

The fourth area is related to the compression properties of paper. The quantitative effects of moisture ratio, temperature, mechanical pressure, and freeness for a wide range of conditions are unknown. Each should be investigated individually and in combination to cover the complete range of process possibilities from wet pressing to high intensity drying.

ACKNOWLEDGMENTS

I would like to thank The Institute of Paper Chemistry for providing the facilities and financial support for this thesis.

The members of my advisory committee, Nai Chang, Peter Parker, and Douglas Wahren, offered many helpful insights and suggestions. My friend and principal adviser, Fred Ahrens, always found a way to keep me on the right track, whether by example, encouragement, or experience.

Finally, I would like to express my love and gratitude to my wife Deborah and my son Daniel for their endless supply of patience, support, love, and understanding.

NOMENCLATURE

The abbreviations for SI units in this section are: m (meter), s (second), kg (kilogram), K (kelvin), J (joule), N (newton), W (watt) , and Pa (pascal).

a	fraction of liquid water external to fibers
Al-4	equation constants
b	equation constant
Bl-5	equation constants
BI	heat transfer Biot number
BW	mass of dry fibers per unit sheet area, kg/m^2
BWl-4	BW of individual zones, kg/m^2
C	mass of dry fibers per unit sheet volume, kg/m^3
C1,C2	equation constants
COEFF	arbitrary equation coefficient
CONST	arbitrary equation constant
Cpf	specific heat of cellulose, $\text{J}/(\text{kg K})$
Cpv	specific heat of gas or vapor, $\text{J}/(\text{kg K})$
Cpw	specific heat of liquid water, $\text{J}/(\text{kg K})$
CSF	Canadian Standard Freeness
D	equation constant
Dl-7	equation constants and rates of change
DBWxDT	rate of change of zone x basis weight, $\text{kg}/\text{m}^2 \text{ s}$
Dc	equation constant
DIFF'	relative position increment
DIFF''	relative position increment
DT0	default time increment, s

E1,E2	equation constants
F1,F2	equation constants
G1-6	equation constants
H1-4	equation constants
Hc	hot surface to paper contact coefficient, $W/(m^2 K)$
Δh	latent heat of vaporization, J/kg
$\Delta h'$	incremental latent heat of desorption, J/kg
Δh^*	average latent heat of desorption, J/kg
I1	equation constant
i'	grid point designation
i''	grid point designation
IMAX	iteration counter
J1-5	equation constants
K	thermal conductivity, $W/(m K)$
K1-3	equation constants or zone thermal conductivities
KAKV	product of Ka_3 and K_v , m^2
KAKW	product of Ka_3 and K_w , m^2
K_a	absolute permeability, m^2
K_{a2-4}	zone absolute permeabilities, m^2
Kd	dry zone thermal conductivity, $W/(m K)$
KMIN	minimum number of grid points
K_v	relative gas or vapor permeability
K_w	relative liquid permeability
\bar{L}	distance in zone, m
L	zone thickness, m
L1-3	equation constants or zone thicknesses
M	compression equation constant, $(kg/m^3)/Pa^N$

M'	modified M value, $(\text{kg}/\text{m}^3)/\text{Pa}^N$
M1	equation constant
Mo	initial mass of water per unit area, kg/m^2
MR	mass of water per unit mass of dry fiber
MRi	starting MR
MRf	ending MR
MREL	mass of water removed divided by initial mass
MRO	initial MR
N	compression equation constant
N1,N2	equation constants
OHTC	overall heat transfer coefficient, $\text{W}/(\text{m}^2 \text{K})$
P	pressure, Pa
Patm	ambient pressure, Pa
Pcap	capillary pressure, Pa
PMAX	maximum gage mechanical pressure, Pa
Pmech	absolute mechanical pressure, Pa
Pmechg	gage mechanical pressure, Pa
PROP	arbitrary vapor or liquid property
Pv	vapor pressure, Pa
Pw	liquid pressure, Pa
\overline{Pw}	average hydraulic pressure, Pa
Q	conduction heat flux, W/m^2
r	pore radius, m
R	specific filtration resistance, m/kg
RATE1-3	rates of advance, m/s
RATIO1-3	interface position divided by DELTAT
RISTIM	time required to attain PMAX, s

S	saturation
S'	interfiber saturation
S2,S3	zone saturations
SEC	time, s
t	time, s
Δt	time increment, s
t'	time, s
T	temperature, K
T'	grid point temperature, K
T''	grid point temperature, K
T1-3	interface temperatures, K
TB	boiling point temperature, K
TBAR	average zone temperature, K
TH	hot surface temperature, K
TI	initial sheet temperature, K
TIME	time, s
TS	sheet surface temperature, K
U	same as OHTC, $W/(m^2 K)$
Vf	velocity of fibers, m/s
Vf'	interface velocity, m/s
Vgas	gas velocity, m/s
Vv	superficial vapor velocity relative to Vf, m/s
Vw	superficial liquid water velocity relative to Vf, m/s
Vwater	velocity of liquid water, m/s
x	relative position
Δx	relative position increment
z	position coordinate, m

γ	surface tension, N/m
δ	thickness, m
δ'	grid point coordinate, m
δ''	grid point coordinate, m
δ_{1-3}	interface positions, m
δ_T	total thickness, m
ϵ	porosity
ϵ'	interfiber porosity
$\epsilon_{2,3}$	zone porosities
θ	contact angle, radians
μ_v	vapor viscosity, N s/m ²
μ_w	liquid viscosity, N s/m ²
ρ_f	fiber density, kg/m ³
ρ_v	vapor density, kg/m ³
ρ_w	liquid density, kg/m ³
τ	time parameter
ϕ	equation coefficient
$\bar{\phi}$	averaged equation coefficient
ψ	equation coefficient

LITERATURE CITED

1. Byrd, V. Drying and heat transfer characteristics during bench-scale press drying of linerboard. *Drying 82*. A. Mujumdar, ed., Washington, Hemisphere Publishing, 1982:83-90.
2. Lehtinen, J. A new vacuum-drying method for paper, board, and other permeable mats. *Drying 80: Vol. 2 Proceedings of the 2nd International Drying Symposium*. A. Mujumdar, ed., Washington, Hemisphere Publishing, 1980:347-54.
3. Arenander, S.; Wahren, D. Impulse drying adds new dimension to water removal. *Tappi 66(9):123-6(Sept., 1983)*.
4. Ahrens, F.; Kartsounes, G.; Ruff, D. A laboratory study of hot surface drying at high temperature and mechanical loading. Preprints of the 68th annual CPPA Technical Section meeting, Montreal, Jan. 26-29, 1982, Vol. B, B93-B97 and *Pulp Paper Canada 85(3):T63-7(March, 1984)*.
5. Ahrens, F. Heat transfer aspects of hot surface drying at high temperature and mechanical loading. *J. Pulp Paper Sci. 9(3):TR79-82(July, 1983)*.
6. Fang, Y., The Institute of Paper Chemistry, Personal communication, April 4, 1983.
7. Burton, S. A dynamic simulation of impulse drying. A291 final report. Appleton, WI, The Institute of Paper Chemistry, 1983. 95 p.
8. Devlin, C., The Institute of Paper Chemistry, Personal communication, March 25, 1985.
9. Ahrens, F.; Astrom, A. High intensity drying of paper. Submitted to *Drying Technology: An International Journal*, December 31, 1984.
10. Udell, K. Heat transfer in porous media heated from above with evaporation, condensation, and capillary effects. *J. Heat Transfer 105(3):485-92 (Aug., 1983)*.
11. Chi, S. Heat pipe theory and practice. Washington, Hemisphere Publishing, 1976.
12. Holden, G., U.S. pat. 3,284,285(Nov. 8, 1966).
13. Kawka, W.; Rogut, R., *Przeglad Papier. 26(2):52-6(Feb., 1970)*.
14. Kawka, W.; Ingielewicz, H., *Przeglad Papier. 28(11):381-7(Nov., 1972)*.
15. Kawka, W., *Przeglad Papier. 30(1):10-18(Jan., 1974)*.
16. Kawka, W.; Ingielewicz, H., *Przeglad Papier. 34(2):53-8(Feb., 1978)*.

17. Kawka, W.; Ingielewicz, H.; Marek, I., *Przeglad Papier*. 34(3):82-7(March, 1978).
18. Kawka, W.; Stepien, K., *Przeglad Papier*. 35(11):402-4(Nov., 1979).
19. Kawka, W.; Szwarcztajn, E. EUCEPA-79 International Conference, London, May 21-24, 1979, Paper No. 31.
20. Kawka, W., *Przeglad Papier*. 39(11/12):403-7(Nov.-Dec., 1983).
21. Carr, W.; Holcombe, W.; Pearson, K.; Robertson, S.; Carter, W. Assessing the Machnozzle as a predrying device. *Textile Chemist Colorist* 15(8):21-6 (Aug., 1983).
22. Luikov, A.; Vasiliev, L. Heat and mass transfer in capillary porous bodies blown by a rarefied gas flow. *Low Temperature Heat Mass Transfer* 5(1970) as quoted in: Tolubinsky, V.; Antonenko, V.; Ostrovsky, Y.; Shevchuk, E. Drop carry-over phenomenon in liquid evaporation from capillary structures. *Letters Heat Mass Transfer* 5(6):339-47(Nov.-Dec., 1978).
23. Andersson, L.; Back, E. The effect of temperature up to 90°C on dewatering of wet webs, evaluated in a press simulator. *TAPPI 1981 Engineering Conference Proceedings*. Book 1:311-23(1981).
24. Andersson, L.; Back, E. Improvements in dewatering at increased pressing temperatures, a press simulator evaluation. *Tappi* 65(7):75-80(July, 1982).
25. Cutshall, K. Cross machine moisture control via hot pressing. *TAPPI 1984 Engineering Conference Proceedings*. Book 3:637-41(1984).
26. van Brakel, J.; Heertjes, P. *Proceedings of the 1st International Drying Symposium*. 70(1978) as quoted in: Brown, L.; Kashiwa, B.; Vanderborgh, N.; Corlett, R. The kinetic behavior of subbituminous coal drying; effects of confining pressure. *Drying 80: Vol. 2 Proceedings of the 2nd International Drying Symposium*. A. Mujumdar, ed., Washington, Hemisphere Publishing, 1980:425-433.
27. Ingersoll, L.; Zobel, O.; Ingersoll, A. *Heat conduction with engineering, geological, and other applications*. Madison, WI, University of Wisconsin Press, 1954:190-199.
28. Muehlbauer, J.; Sunderland, J. Heat conduction with melting or freezing. *Applied Mechanics Reviews* 18(12):951-9(Dec., 1965).
29. Tien, R.; Geiger, G. A heat transfer analysis of the solidification of a binary eutectic system. *J. Heat Transfer* 89(3):230-4(Aug., 1967).
30. Cho, S.; Sunderland, J. Heat conduction problems with melting or freezing. *J. Heat Transfer* 91(3):421-6(Aug., 1969).
31. Eckert, E.; Drake, R. *Analysis of heat and mass transfer*. New York, McGraw-Hill, 1972:224-8.

32. Cho, S.; Sunderland, J. Phase change problems with temperature dependent thermal conductivity. *J. Heat Transfer* 96(2):214-17(May, 1974).
33. White, R. A modified finite difference scheme for the Stefan problem. *Mathematics of Computation* 41(164):337-47(Oct., 1983).
34. Chawla, T.; Pedersen, D.; Leaf, G.; Minkowycz, W.; Shouman, A. Adaptive collocation method for simultaneous heat and mass diffusion with phase change. *J. Heat Transfer* 106(3):491-7(Aug., 1984).
35. Selim, M.; Seagrave, R. Solution of moving boundary transport problems in finite media by integral transforms, Parts I, II, III. *I&EC Fundam.* 12(1): 1-8, 9-13, 14-17(Feb., 1973).
36. Solomon, A. Some remarks on the Stefan problem. *Mathematics of Computation* 20:347-60(1966).
37. Bonacina, C.; Comini, G.; Fasano, A.; Primicerio, M. Numerical solution of phase change problems. *Int. J. Heat Mass Transfer* 16(10):1825-32(Oct., 1973).
38. Voller, V.; Cross, M. Accurate solutions of moving boundary problems using the enthalpy method. *Int. J. Heat Mass Transfer* 24(3):545-56(March, 1981).
39. Voller, V.; Shadabi, L. Enthalpy methods for tracking a phase change boundary in two dimensions. *Int. Comm. Heat Mass Transfer* 11(3):239-49(May-June, 1984).
40. Talmon, Y.; Davis, H.; Scriven, L. Progressive freezing of composites analyzed by isotherm migration methods. *AIChE J.* 27(6):928-37(Nov., 1981).
41. Talmon, Y.; Davis, H.; Scriven, L. Moving boundary problems in simple shapes solved by isotherm migration. *AIChE J.* 29(5):795-800(Sept., 1983).
42. Cho, S. An exact solution of the coupled phase change problem in a porous medium. *Int. J. Heat Mass Transfer* 18(10):1139-42(Oct., 1975).
43. Hilding, W.; Cheh, U. Transient temperature response during heating of an initially saturated plane porous wall. *Heat Transfer* 82: Vol. 6 Proceedings of the 7th International Heat Transfer Conference. U. Grigull; E. Hahne; K. Stephan; J. Straub, eds., Washington, Hemisphere Publishing, 1982:67-72.
44. Szentgyorgyi, S.; Molnar, K. Calculation of drying parameters for the penetrating evaporation front. *Drying* 84. A. Mujumdar, ed., Washington, Hemisphere Publishing, 1984:76-82.
45. Szentgyorgyi, S.; Molnar, K.; Orvos, M. Computer calculation method of the falling rate period of drying. *Drying* 84. A. Mujumdar, ed., Washington, Hemisphere Publishing, 1984:83-7.
46. Lin, S.; Chou, T. A parametric study of the freeze-dry process for preservation of activities of biological substances. *Drying* 84. A. Mujumdar, ed., Washington, Hemisphere Publishing, 1984:99-104.

47. Kisakurek, B.; Celiker, H. Modeling of simultaneous heat and mass transfer in freeze drying. *Drying* 84. A. Mujumdar, ed., Washington, Hemisphere Publishing, 1984:324-29.
48. Adesanya, B. Heat and mass transfer in a capillary porous body with particular reference to lumber. Doctoral Dissertation. Clemson, SC, Clemson University, 1982. 189 p.
49. Beard, J.; Rosen, H.; Adesanya, B. Temperature distributions and heat transfer during the drying of lumber. *Drying Technology: An International Journal* 1(1):117-40(Feb., 1983).
50. Dorri, B.; Emery, A.; Malte, P. Drying rate of wood particles with longitudinal mass transfer. *J. Heat Transfer* 107(1):12-18(Feb., 1985).
51. Hallstrom, A. Drying of porous hygroscopic materials: an extended shrinking core model. *Drying* 82. A. Mujumdar, ed., Washington, Hemisphere Publishing, 1982:19-24.
52. Sato, K.; Ishida, M.; Shirai, T. Prediction of pressure increase and evaporation temperature during the course of drying of porous solid soaked with water. *J. Chem. Eng. Japan* 9(1):35-9(1976).
53. Cross, M.; Gibson, R.; Young, R. Pressure generation during the drying of a porous half-space. *Int. J. Heat Mass Transfer* 22(1):47-50(Jan., 1979).
54. Gibson, R.; Cross, M.; Young, R. Pressure gradients generated during the drying of porous shapes. *Int. J. Heat Mass Transfer* 22(6):827-30(June, 1979).
55. Streck, F.; Nastaj, J. Mathematical modeling and simulation of vacuum contact drying of porous media in the falling rate period (boundary condition of the first kind). *Drying 80: Vol. 2 Proceedings of the 2nd International Drying Symposium*. A. Mujumdar, ed., Washington, Hemisphere Publishing, 1980:135-43.
56. Baines, W. Analysis of transient effects in drying of paper. *Pulp Paper Can.* 74(2):58-64(Feb., 1973).
57. Ahrens, F. Fundamentals of drying, project 3470. Status report to the Engineering and Colloid Science Research Advisory subcommittee. Appleton, WI, The Institute of Paper Chemistry, March 23-24, 1983:117-36.
58. Kreith, F. Principles of Heat Transfer. Scranton, Pa., International Textbook Company, 1958:430-6.
59. Yiannos, P. The apparent cell wall density of wood and pulp fibers. *Tappi* 47(8):468-71(Aug., 1964).
60. Devlin, C. An investigation of the drying mechanism of paper at high temperatures and mechanical pressures, A400 Revised Thesis Proposal. Appleton, WI, The Institute of Paper Chemistry, 1982:19.

61. Ahrens, F.; Journeaux, I. An experimental and analytical investigation of a thermally induced vacuum drying process for permeable mats. *Drying* 84. A. Mujumdar, ed., Washington, Hemisphere Publishing, 1984:281-91.
62. Han, S. Heat and mass transfer in hot-surface drying of fiber mats. *Pulp Paper Can.* 65(12):T537-49(Dec., 1964).
63. Carlsson, G.; Lindstrom, T.; Floren, T. Permeability to water of compressed pulp fiber mats. *Svensk Papperstid.* 86(12):R128-34(Sept., 1983).
64. Emmons, H. The continuum properties of fiber suspensions. *Tappi* 48(12): 679-87(Dec., 1965).
65. Leonard, B. A survey of finite differences of opinion in numerical muddling of the incomprehensible defective confusion equation. *Finite Element Methods for Convection Dominated Flows*, AMD Vol. 34. T. Hughes, ed., New York, ASME, 1979:1-17.
66. Patankar, S. *Numerical heat transfer and fluid flow*. Washington, Hemisphere Publishing, 1980:50-2.
67. Pounder, J. A400 Progress Report 5. Appleton, WI, The Institute of Paper Chemistry, Jan. 27, 1984. 26 p.
68. Prahl, J. *Thermodynamics of paper fiber and water mixtures*. Doctoral Dissertation. Cambridge, Harvard University, 1968. 159 p.
69. Pounder, J. A400 Progress Report 8. Appleton, WI, The Institute of Paper Chemistry, Oct. 19, 1984. 23 p.
70. Han, S. Drying of paper. *Tappi* 53(6):1034-46(June, 1970).
71. Fang, Y., The Institute of Paper Chemistry, Personal communication, March 20, 1983.
72. Pounder, J. A400 Progress Report 6. Appleton, WI, The Institute of Paper Chemistry, April 27, 1984. 24 p.
73. Campbell, W. The physics of water removal. *Pulp Paper Can.* 48:103-9, 122 ("Convention Issue", 1947).
74. Chang, N. Dynamic compression of handsheets. *TAPPI 1978 Engineering Conference Proceedings*. Book 1:93-106(1978).
75. Consolvo, W. Dynamic compression of a fiber mat. A291 final report. Appleton, WI, The Institute of Paper Chemistry, 1981. 33 p.
76. Caulfield, D.; Young, T.; Wegner, T. The role of web properties in water removal by wet pressing. *Tappi* 65(2):65-9(Feb., 1982).
77. Ceckler W.; Thompson, E. Final Report of the University of Maine at Orono Wet Pressing Project. Washington, U.S. Department of Energy, 1982. 335 p.

78. Gren, U.; Ljungkvist, K. Compressibility and permeability of chemical pulps. *Cellulose Chem. Tech.* 17(5):515-23(Sept.-Oct., 1983).
79. Hung, J.; Holm, R. A study of the drying of linerboard, Progress Report 2, Project 2693. Appleton, WI, The Institute of Paper Chemistry, 1969. 69 p.
80. Pounder, J. IPC Research Notebook 3711, March 2, 1985:60-3.
81. Pounder, J. IPC Research Notebook 3711, March 2, 1985:63-5.
82. Davies, C. The separation of airborne dust and particles. *Institution of Mechanical Engineers* 1B:185-98(1952).
83. Labrecque, R. The effects of fiber cross-sectional shape on the resistance to the flow of fluids through fiber mats. *Tappi* 51(1):8-15(Jan., 1968).
84. Ellis, E. Compressibility and permeability of never dried bleached softwood kraft pulp and its application to the prediction of wet press behavior. Doctoral Dissertation. Orono, ME, University of Maine at Orono, 1981. 287 p.
85. Guzy, C. Flow and retention in fibrous porous media. Doctoral Dissertation. Albuquerque, NM, University of New Mexico, 1983. 259 p.
86. El-Hosseiny, F.; Yan, J. Analysis of Canadian Standard Freeness Part 1: theoretical considerations. *Pulp Paper Can.* 81(6):T113-16(June, 1980).
87. Boyd, K. Canadian Standard Freeness. A347 term report. Appleton, WI, The Institute of Paper Chemistry, 1983. 26 p.
88. Ingmanson, W.; Whitney, R. The filtration resistance of pulp slurries. *Tappi* 37(11):523-41(Nov., 1954).
89. Wilder, J. Paper capillarity and rewetting during pressing. *Tappi* 51(2):104-9(Feb., 1968).
90. Robertson, A. The physical properties of wet webs, part 2, fiber properties and wet web behavior. *Svensk Papperstid.* 66(12):477-97(June 30, 1963).
91. Pounder, J. A400 Progress Report 4. Appleton, WI, The Institute of Paper Chemistry, Oct. 18, 1983. 29 p.
92. Pounder, J. A400 Progress Report 7. Appleton, WI, The Institute of Paper Chemistry, July 20, 1984. 28 p.
93. Devlin, C., Institute of Paper Chemistry, Personal communication, May 9, 1985.
94. Herminge, L. Heat transfer in porous bodies at various temperatures and moisture contents. *Tappi* 44(8):570-5(Aug., 1961).

95. Ahrens, F. An analysis of a thermally induced vacuum drying process for permeable mats. Heat Transfer 82: Vol. 6 Proceedings of the 7th International Heat Transfer Conference. U. Grigull; E. Hahne; K. Stephan; J. Straub, eds., Washington, Hemisphere Publishing, 1982:509-14.
96. Burton, S. Dynamics of densification in impulse drying. Engineering Project Advisory Committee Report. Appleton, WI, The Institute of Paper Chemistry, April 3-4, 1985:24-45.
97. Ahrens, F. Fundamentals of drying, Project 3470. Engineering Project Advisory Committee Report. Appleton, WI, The Institute of Paper Chemistry, March 21-22, 1984:53-64.
98. Belisle, S. A study of the characteristics of impulse drying. A291 final report. Appleton, WI, The Institute of Paper Chemistry, 1984. 46 p.

APPENDIX I

HIDRYER1 PROGRAM AND DOCUMENTATION

HIDRYER1/USE

To run HIDRYER1 the user needs to have or must be able to access three files on the Burroughs B6900 main frame:

HIDRYER1/JOB, the WFL job deck to run the object code;
OBJECT/HIDRYER1, the compiled and saved FORTRAN object code; and
HIDRYER1/PARAMS, the data file containing input parameters.

HIDRYER1/JOB is the following WFL job deck:

```
BEGIN JOB HIDRYER1(INTEGER Q,STRING NAME1,STRING NAME2);  
  QUEUE=Q;  
  RUN OBJECT/HIDRYER1;  
  FILE FILE1=#NAME1;  
  FILE FILE2=#NAME2;  
  STATION=MYSELF(SOURCESTATION);  
END JOB
```

To run the program the user enters

```
START HIDRYER1/JOB(Q,"NAME1","NAME2")
```

where Q is the queue number, NAME1 is HIDRYER1/PARAMS (or other data file conforming to the correct input syntax), and NAME2 is the name of the disk data file to which the output information is written and saved.

OBJECT/HIDRYER1 is obtained by compiling HIDRYER1 and saving the result. HIDRYER1 and its documentation are listed later in this appendix. About 20 seconds of processor time and 60 seconds of elapsed time are required for compilation of HIDRYER1.

HIDRYER1/PARAMS is a data file containing the following numerical information separated by commas:

TH,TB,BW,CSF,MRO,DTO,PMAX,RISTIM,IOPTP,IOPTU,METH,MITER

For example:

525.0,212.0,0.0420,650,1.500,1.37E-07,750.0,0.025,1,1,2,2

The input parameters are defined in the thesis and in the HIDRYER1/DOC section of this appendix. HIDRYER1 performs all calculations in English units, but the input and output may be given in either English or SI units.

HIDRYER1/DOC

HIDRYER1 is a FORTRAN implementation of the equations in this thesis. It mathematically performs a drying "experiment" based on the inputs from HIDRYER1/PARAMS and outputs the results to the printer and to a disk file named by the user.

The main part of the program is divided into four sections. The first section contains the file declarations, statements for inclusion of packaged subroutines, real variable declarations, values for constants, common statements, and preliminary input and output statements. The next three sections contain the equations for the heatup, transition, and linear drying regimes.

The main program is followed by a SUBROUTINE section containing 13 subroutines and a FUNCTION section containing 12 functions. The subroutine names and their purposes are:

CALLER: calls property subroutines
CNSTMN: determines constants for calculation of M and N
CNVRT1: converts from English to SI units
CNVRT2: converts from SI to English units
DLDTFN: calculates the compression of a saturated sheet
DUMFUN: calculates the Jacobian matrix for DLDTFN
PRESSR: calculates applied pressure and time derivative
PROP12: calculates and averages physical properties at T1 and T2
PROP23: calculates and averages physical properties at T2 and T3
PROP3B: calculates and averages physical properties at T3 and TB
PROPTB: calculates the physical properties at TB
WARNIN: corrects error conditions or prints warning messages
WRITER: writes output to printer and disk

Subroutine DLDTFN calls a set of subroutines from the International Mathematical and Statistical Library package for the solution of an initial value problem. More information on these subroutines may be found in the appropriate IMSL documentation.

The function names and their purposes are:

DELHD : calculates latent heat of vaporization increment
DPVDT : calculates derivative of vapor pressure with temperature
EVALM : calculates the M compression constant
EVALN : calculates the N compression constant
HFG : calculates the latent heat of vaporization
HYDRAL: calculates the hydraulic pressure
SPRES : calculates the specific filtration resistance

VF : calculates the liquid water specific volume
VG : calculates the water vapor specific volume
VISF : calculates the liquid water viscosity
VISG : calculates the water vapor viscosity
PV : calculates the vapor pressure

The main program variable names and definitions are:

A thermal diffusivity term
Ax interface rate-of-advance terms
ALF DELTA2 - DELTA1
ALFA DELTA3 - DELTA1
BET DELTA3 - DELTA2
BETA DELTAT - DELTA3
BIDX product of Biot number and DX
BW sheet basis weight
BWx basis weight of zone x
BWCORR basis weight correction factor
BWSUM sum of corrected zone basis weights
Cx dry fiber concentration of zone x
COEFF coefficient in mechanical pressure calculations
CONST C3/DFIBER
CPF specific heat of cellulose
CPW specific heat of water
CSF Canadian Standard Freeness
Dx rates of interface advance
DBWxDT rate of change of basis weight of zone x
DC product of density, specific heat and moisture ratio
DELTAx position of interface x
DELTAf position of grid point closest to outer interface
DELTAI position of grid point closest to inner interface
DELTAT sheet thickness
DELTSI DELTAT in SI units
DENOM denominator term used in various calculations
DF reciprocal of DFIBER
DFIBER density of cellulose
DHx constants in DELHD
DIFFF relative distance term
DIFFFX relative distance term
DIFFI relative distance term
DIFFIX relative distance term
DK product of MR, DFIBER, and KWATER
DLDT rate of change of saturated sheet thickness
DPDT rate of change of mechanical pressure
DPDTxy vapor pressure with temperature derivative over x and y
DPVDTB vapor pressure at TB
DSTAR interface rate of advance
DT time increment

DTx calculated time increments
DTDZxy temperature gradient over x and y
DTMAX maximum time increment
DTO default time increment (in hours)
DW density of liquid water
DX relative position increment
DXX relative position increment
Ex porosity of zone x
EMIN minimum allowable porosity
ESTAR interfiber porosity
ESx constants for calculation of ESTAR
Fx factors for temperature calculations
F3X product of F3 and DX
FACTOR factor for conversion of English units
FLAG signal for absence of zone 3
GAMM DELTAT - DELTA3
H time increment
HC contact coefficient
HCx constants for calculation of HC
HCDRY contact coefficient of dry cellulose
HCREF HCDRY at PREF2
HCWET contact coefficient of water
HFGx latent heat of vaporization at interface x
HFGTB latent heat of vaporization at TB
I loop iteration counter
IDUMMY subroutine work vector
IER subroutine error indicator
IFINI number of grid point closest to outer interface
IMAX maximum iteration counter
INDEX subroutine call parameter
INIT number of grid point closest to inner interface
IOPTx interface motion indicators
IOPTP pressure pulse option (1=ramp, 2=sine)
IOPTU units option (1=English, 2=SI)
IWK subroutine work vector
J print control variable
K loop iteration counter
Kx thermal conductivity of zone x
KABSx absolute permeability of zone x
KAKV product of KABS3 and KV
KAKW product of KABS3 and KW
KFIBER thermal conductivity of dry cellulose
KK grid point counter
KMIN initial number of grid points
KV vapor relative permeability
KW liquid relative permeability
KWATER thermal conductivity of water
L print control variable
LIQDEW mass of liquid water removed
LMAX print control variable
M number of points for internal temperature calculations
Mx compression constant for zone x
MC moisture content
METH subroutine parameter (1=Adams method, 2=Gear's method)

MFINAL target final moisture content
MITER subroutine parameter (0=iteration, 1=analytic, etc.)
MO initial mass of water present
MR moisture ratio
MREL relative amount of moisture removed
MREM amount of moisture remaining
MRO initial moisture ratio
MRSTAR intrafiber MR
N print control variable
Nx compression constant for zone x
NEXP exponent in calculation of Nx
OHTC overall heat transfer coefficient
OHTCSI OHTC in SI units
P structural pressure
Px structural pressure in zone x
PDENOM denominator in pressure calculation
PGAGSI PGAUGE in SI units
PGAUGE gage vapor pressure at T1
PHx hydraulic pressure in zone x
PHI thermal diffusivity term
PMAX maximum mechanical pressure
PMID pressure midway between PMAX and PREF1
PREFx reference mechanical pressures
PR3LOG natural log of PREF3
PSI velocity term
PS3 structural pressure of saturated sheet
PVTB vapor pressure at TB
PW liquid pressure
Q instantaneous heat flux
QINIT heat supplied during heatup regime
QSI Q in SI units
QTHEOR theoretical heat requirement
QOTHERx term in calculation of QTHEOR
QTOT total heat input during drying
QTOTAL heat supplied during transition and linear regimes
R resistance factor
RATEx rates of interface advance
RATIOx DELTAx/DELTAT
REM remainder in distance calculations
RISTIM time required to attain PMAX (in seconds)
Sx saturation of zone x
S3STAR interfiber saturation
SDUMMY subroutine work variable
SEC time in seconds
SIGN variable in LIQDEW calculation
STAR variable in MRSTAR calculation
SUM12 sum of BW1 and BW2
SUM123 sum of SUM12 and BW3
Tx temperature of interface x
TxSI Tx in SI units
TB boiling point temperature
TBARx average temperature of zone x
TC temperature at a fixed point in the sheet
TERMx terms used in various calculations

TH	hot surface temperature
THICKx	thickness of zone x
TI	initial sheet temperature
TIME	time
TIMEND	time endpoint for initial value problem
TIMER	factor used in temperature calculations
TMID	temperature midway through the sheet basis weight
TMIDSI	TMID in SI units
TNEW	new temperature at a given grid point
TOL	subroutine convergence tolerance
TOLD	old temperature at a given grid point
TOx	old temperature at interface x
TS	sheet surface temperature
TSSI	TS in SI units
U	fractional basis weight
V	velocity term
VFxy	specific volume of liquid water over x and y
VFTB	specific volume of liquid water at TB
VGxy	specific volume of water vapor over x and y
VGTB	specific volume of water vapor at TB
VISFxy	viscosity of liquid water over x and y
VISFTB	viscosity of liquid water at TB
VISGxy	viscosity of water vapor over x and y
VISGTB	viscosity of water vapor at TB
W	product of MRSTAR and C2
WK	subroutine work variable
X	product of MR and C3
XX	grid point variable
Y	product of (MR-MRSTAR) and C3
YL	thickness of saturated sheet
Z	Y/X
ZTC	location of fixed points within the sheet

In the subroutines, the variables not linked to the main program by COMMON statements are:

CALLER

all variables in common with main program

CNSTMN

Ax constants for calculation of CMx

Bx constants for calculation of CMx

Cx constants for calculation of CNx

CMx constants for calculation of M compression constant

CNx constants for calculation of N compression constant

Dx constants for calculation of CNx

Ex constants for calculation of TERM

TERM constant for calculation of CMx and CNx

CNVRT1

Ax constants in unit conversions

CNVRT2

Ax constants in unit conversions

DLDTFN

YPRIME rate of change of saturated sheet thickness

DUMFUN

PD partial derivative of YPRIME with respect to YL

PRESSR

Ax constants in sine pressure pulse calculation

PI numerical value 3.14159...

PROP12

all variables in common with main program

PROP23

all variables in common with main program

PROP3B

all variables in common with main program

PROPTB

all variables in common with main program

WARNIN

all variables in common with main program

WRITER

all variables in common with main program

In the functions, the variables not linked to the main program by COMMON statements are:

DELHD

all variables in common with main program

DPVDT

Ax constants used in property calculation

EVALM

A constant used in calculation of M compression constant

Ax constants used in calculation of A and B

B constant used in calculation of M compression constant

CMx constants in common with CNSTMN

CORRCT correction in calculation of M compression constant

EVALN

A constant used in calculation of N compression constant

Ax constants used in calculation of A and B

B constant used in calculation of N compression constant

C uncorrected value for N compression constant

CNx constants in common with CNSTMN

NDENOM denominator in correction of N compression constant

NMID value of N at PMID

NSAT value of N at PREF3

PTERM pressure term in correction of N compression constant

SIGN variable in correction of N compression constant

HFG

Ax constants used in property calculation

HYDRAL

all variables in common with main program

SPRES

Ax constants used in property calculation

RREF reference specific filtration resistance

X variable used in property calculation

VF

Ax constants used in property calculation

VG

Ax constants used in property calculation

VISF

Ax constants used in property calculation

VISG

Ax constants used in property calculation

PV

Ax constants used in property calculation

The following discussion of HIDRYER1 is divided into sections by program line numbers and headings. Refer to the program listing for the actual FORTRAN statements.

OPENING SECTION OF MAIN PROGRAM

1 : Format line.

Sets standard FORTRAN format.

5 - 23 : Headers

Program references and identification.

28 - 32 : File declarations.

File 1 is the parameter input file; file 2 is the disk output file; file 5 is the terminal; and file 6 is the line printer.

34 - 44 : Include statements.

Include the required subroutines from the IMSL package.

46 - 48 : Real variable declarations.

Sets variables ordinarily assumed to be integers to be real variables and dimensions some arrays.

50 : Dimension statement.

Sets dimension of an integer array.

52 : External statement.

Declares two subroutines external to the IMSL package.

55 - 64 : Fixed input assignment.

Assigns values to certain constants in the program.

67 - 85 : Subroutine common blocks.

Names common blocks for subroutines.

88 - 91 : Input statement.

Reads input parameters in free format from file 1.

94 - 101 : Write statements.

Write headings and repeat input parameters on line printer.

104 - 107 : Set print controls.

Set counters for frequency of printing output results.

110 - 114 : Set fixed internal points.

Set fixed fractions of basis weight at which temperatures are to be calculated. This is for direct comparison to experimental results.

117 - 120 : Compute properties at TB.

Convert to English units if necessary and compute vapor and liquid properties at TB for use later in the program.

HEATUP REGIME

129 - 168 : Initialize variables.

Set initial variable values for heatup regime and for use later in the main program.

171 - 223 : Calculate mechanical pressure and sheet properties.

Calculate mechanical pressure for nonsaturated or saturated sheets and determine sheet properties like thickness, porosity, etc.

226 - 232 : Calculate heat transfer parameters.

Determine contact coefficient, thermal conductivity and BIDX.

235 - 260 : Calculate interior temperatures.

Use finite difference methods to find internal temperatures for a non-saturated or saturated sheet undergoing compression.

263 - 275 : Calculate boundary temperatures.

Use finite difference methods to calculate boundary temperatures for nonsaturated or saturated sheets.

278 - 282 : Reset old temperature values.

Reset TOLD for next set of finite difference calculations.

285 - 291 : Compute temperatures at fixed locations.

Use linear interpolation to find temperatures at fixed basis weight fractions in the sheet.

294 - 314 : Increment quantities and write results.

Calculate quantities which must be calculated at every time increment and determine if the output should be printed on this iteration. If the output needs to be printed, then calculate additional output quantities that do not have to be determined at every time step.

317 - 320 : Increment print control variables.

Increase the values of the counters for print control.

323 - 327 : Determine exit criteria.

Check time and physical criteria for exit to transition regime or program termination.

330 - 345 : Write heatup regime final output.

Calculate final values for quantities and write output if it is not a duplication of the last printed output.

TRANSITION REGIME

354 - 356 : Write transition regime heading.

Write heading on printer to signal onset of transition regime.

359 - 404 : Initialize variables.

Set initial values for transition regime variables.

407 -417 : Compute required derivatives.

Calculate the rates of advance for the different interfaces which may be present in the sheet.

420 - 460 : Set maximum allowable time increment.

Examine rates of interface advance and determine the maximum allowable time increment which will not violate the interface position criteria.

Determine if new interface position permits the use of usual finite difference formulations or requires use of unequally spaced points.

Increment the time and include the factor TIMER to account for round-off or truncation errors in the determination of DT.

463 - 501 : Calculate new temperature distribution.

Use finite difference methods to determine internal and "boundary"

(INIT and IFINI) temperatures in the transition zone and in zone 4, if it exists.

504 -519 : Calculate rates of basis weight change.

Select the dominant rate at each interface and determine any liquid dewatering that takes place.

522 -535 : Calculate mechanical and hydraulic pressure.

Calculate applied mechanical pressure based on time and IOPTP and calculate the hydraulic (vapor) pressure for each zone. Obtain the effective structural pressure for each zone by subtraction.

538 - 585 : Calculate basis weight, concentration, and thickness.

Calculate rates of basis weight change and new basis weights. Correct basis weights for slight calculation errors. Evaluate the compression constants, dry fiber concentration, and thickness of each zone.

588 - 623 : Calculate porosity and saturation.

Calculate porosity based on dry fiber concentration, and saturation based on dry fiber concentration and moisture ratio. Correct zone 3 saturation if greater than unity.

626 - 645 : Increment interface positions.

Calculate new interface positions, locations of INIT and IFINI, and position increments for finite difference calculations.

648 - 658 : Compute thermal conductivity and contact coefficient.

Find thermal conductivity of each zone and contact coefficient.

661 - 669 : Calculate permeability factors.

Calculate specific filtration resistance, absolute permeability for the zones and KAKW.

672 - 680 : Set relative interface positions.

Compute the RATIOx values and calculate the remaining moisture and relative moisture loss.

683 - 735 : Compute new interface temperatures.

Calculate new interface temperatures based on equations appropriate for types and locations of interfaces present.

738 - 761 : Recompute variables for derivative calculations.

Calculate temperature gradient terms for zones and multipliers for rate expressions.

764 - 879 : Handle special case of intrafiber water only.

If FLAG = 1, then this section handles all calculations for the transition regime. The calculations are based on those of the previous sections and modified for this special case. If FLAG = 0, then this section is bypassed.

882 - 889 : Reset temperature distribution and time options.

Reset TOLD values for next finite difference calculations and reset IOPT1 and IOPT2 for the next time increment.

892 - 912 : Compute temperatures at fixed locations.

Same strategy as for lines 285 - 291.

915 - 934 : Increment quantities and write results.

Same strategy as for lines 294 - 314.

937 - 940 : Increment print control variables.

Same strategy as for lines 317 - 320.

943 - 949 : Determine exit criteria.

Same strategy as for lines 323 - 327.

952 - 968 : Write transition regime final output.

Same strategy as for lines 330 - 345.

LINEAR REGIME

977 - 979 : Write linear regime heading.

Same strategy as for lines 354 - 356.

982 - 989 : Set FLAG and go to first temperature calculation.

Set the value for FLAG and go directly to interface temperature calculation right from the transition regime.

992 - 1005 : Compute required derivatives.

Same strategy as for lines 407 - 417, with additional calculations for other types of interfaces that may be present.

1008 - 1032 : Set maximum allowable time increment.

Same strategy as for lines 420 - 460, but no restriction on interface position relative to grid points.

1035 - 1053 : Calculate rates of basis weight change.

Same strategy as for lines 504 - 519.

1056 - 1070 : Calculate mechanical and hydraulic pressure.

Same strategy as for lines 522 - 535.

1073 - 1121 : Calculate basis weight, concentration, thickness.

Same strategy as for lines 538 - 585.

1124 - 1159 : Calculate porosity and saturation.

Same strategy as for lines 588 - 623.

1162 - 1169 : Increment interface positions.

Same strategy as for lines 626 - 645, but no finite difference grid spacings need to be calculated.

1172 - 1182 : Compute thermal conductivity, contact coefficient.

Same strategy as for lines 648 - 658.

1185 - 1194 : Calculate permeability factors.

Same strategy as for lines 661 - 669, with KAKV also determined.

1197 - 1204 : Set relative interface positions.

Same strategy as for lines 672 - 680.

1207 - 1286 : Compute new interface temperatures.

Same strategy as for lines 683 - 735, but with equations appropriate for linear regime (including vapor flow in zone 3).

1289 - 1317 : Recompute variables for derivative calculations.

Same strategy as for lines 738 - 761.

1320 - 1338 : Compute temperatures at fixed locations.

Same strategy as for lines 892 - 912.

1341 - 1357 : Increment quantities and write results.

Same strategy as for lines 915 - 934.

1360 - 1363 : Increment print control variables.

Same strategy as for lines 937 - 940.

1366 - 1369 : Determine exit criteria.

Same strategy as for lines 943 - 949, but time and moisture content are the only criteria for the linear regime.

1372 - 1385 : Write final output.

Calculate and write total values for cumulative variables.

1388 - 1410 : Format statements.

Statements for printer headings and output variable format.

1413 - 1416 : End main program.

STOP and END statements for main program.

The remainder of HIDRYER1 is composed of the SUBROUTINE and FUNCTION sections, which have been previously described.

HIDRYE1 (CS/21/85)

RESET FREE

```

*****
**      HIGH INTENSITY DRYING PROGRAM      **
**                                          **
**              HIDRYE1                    **
**                                          **
**      INSTITUTE OF PAPER CHEMISTRY      **
**                                          **
**              JOSEPH H POUNDER          **
**                                          **
**              MARCH 25, 1985           **
*****

```

```

000001
000002
000003
000004
000005
000006
000007
000008
000009
000010
000011
000012
000013
000014
000015
000016
000017
000018
000019
000020
000021
000022
000023
000024
000025
000026
000027
000028
000029
000030
000031
000032
000033
000034
000035
000036
000037
000038
000039
000040
000041
000042
000043
000044
000045
000046
000047
000048
000049
000050

```

```

*****
*      PROGRAM DOCUMENTATION IS IN THE HIDRYE1/DCC FILE      *
*                                                                *
* INSTRUCTIONS FOR RUNNING THE PROGRAM ARE IN THE HIDRYE1/USE FILE *
*****

```

```

FILE 1(KIND=DISK,NEWFILE=FALSE,FILETYPE=7,MYUSE=IN)
FILE 2(KIND=DISK,NEWFILE=TRUE,MAXRECSIZE=21,PROTECTION=SAVE,
* MYUSE=CUT)
FILE 5(KIND=REMOTE,MYUSE=IO)
FILE 6(KIND=PRINTER)

```

```

INCLUDE "IMSL/DGRCS"
INCLUDE "IMSL/DGEAR"
INCLUDE "IMSL/DERIA"
INCLUDE "IMSL/DERPS"
INCLUDE "IMSL/DGRST"
INCLUDE "IMSL/LUCATF"
INCLUDE "IMSL/LUELMF"
INCLUDE "IMSL/LEGT18"
INCLUDE "IMSL/UEERTST"
INCLUDE "IMSL/UCETIO"
INCLUDE "IMSL/USPKC"

```

```

REAL KABS2,KABS3,KABS4,KAKV,KAKW,KFIBER,KV,KW,KWATER,K1,K2,K3,
*K4,LIGDEW,MC,MFINAL,MO,MR,MREL,MREM,MRO,MRSTAR,M1,M2,M3,M4,NEXP,
*N1,N2,N3,N4,TC(10),TREW(501),TOLD(501),WK(250),YL(2),ZTC(10)

```

DIMENSION IWK(1)

```

C
EXTERNAL DLDTFN,DUMFUN
C
C
C*****FIXED INPUTS ARE:
C
DATA
*DH1,DH2/33.2815,-14.9522/, ES1,ES2/1.55,0.55/, IMAX/10/,
*KMIN/101/, M/3/, DFIBER,KFIBER,CPF/96.76,0.14,0.346/,
*RWATER,CFW/0.394,1.00/, FACTOR/1.6679002E+07/, LMAX/25/,
*STAR/C.005624/, MFINAL/0.06/, TIMER/0.95/, TI/75.0/, J/ 25/,
*HCREP,HCRET/100.,1000./, PREF1,PREF2,PREF3/0.10,1.,1000./,
*HC1,HC2,HC3/1.45159,0.33333333,0.479354/, TOL/1.0E-05/,
*INDEX/1/, NEXP/3.0/
C
C
C*****SUBROUTINE COMMON BLOCKS ARE:
C
COMMON /GEAR/ DUMMY(48),SDUMMY(4),IDLHMY(38)
COMMON /LABEL1/ TB,PVTE,DFVCTB,VFTB,VGTB,MFGTB,VISGTB,VISFTB
COMMON /LABEL2/ TH,T1,T2,T3,TI,IMID
COMMON /LABEL3/ DPDT12,VF12,VG12,VISG12
COMMON /LABEL4/ DPDT23,VF23,VISF23,VG23,VISG23
COMMON /LABEL5/ DPDT38,VG38,VISG38
COMMON /LABEL6/ DXX,DIFFIX,CIFFFX,EMIN
COMMON /LABEL7/ PREF1,PMAX,RISTIM,P,IOPTP,DPDT
COMMON /LABEL8/ M1,M2,M3,M4,N1,N2,N3,N4
COMMON /LABEL9/ DLDT,FACTGR,BW,DW,DFIBER,COEFF,PS3
COMMON /LABL10/ CSF
COMMON /LABL11/ SEC,MREL,TS,RATIO1,RATIO2,RATIO3,DELTA1,0,OHTC,
* PGAGGE
COMMON /LABL12/ TSSI,T1SI,T2SI,T3SI,DELTSI,QSI,OHTCESI,PGAGSI,
* TMICSI
COMMON /LABL13/ DH1,DH2,MR,MRSTAR
COMMON /LABL14/ NEXP,PF3LOG,PREF3,PMID,PDENOM,DF
C
C
C*****READ INPUT FROM DATA FILE
C
READ(1,/) TH,TB,BW,CSF,MRO,DIO,PMAX,RISTIM,IOPTP,IOPTU,
* METH,MITER
C
C
C*****WRITE HEADINGS AND STARTING PARAMETERS
C
WRITE(6,900)
WRITE(6,905)
WRITE(6,910) TH,TB,BW,CSF,MRO,PMAX,RISTIM
WRITE(6,915)
WRITE(6,920) DIO,IOPTP,IOPTU,METH,MITER
WRITE(6,925)
C
C
C*****SET VARIABLES FOR PRINTING OF RESULTS

```

```

000051
000052
000053
000054
000055
000056
000057
000058
000059
000060
000061
000062
000063
000064
000065
000066
000067
000068
000069
000070
000071
000072
000073
000074
000075
000076
000077
000078
000079
000080
000081
000082
000083
000084
000085
000086
000087
000088
000089
000090
000091
000092
000093
000094
000095
000096
000097
000098
000099
000100
000101
000102
000103
000104

```

N=J
L=1

000105
000106
000107
000108
000109
000110
000111
000112
000113
000114
000115
000116
000117
000118
000119
000120
000121
000122
000123
000124
000125
000126
000127
000128
000129
000130
000131
000132
000133
000134
000135
000136
000137
000138
000139
000140
000141
000142
000143
000144
000145
000146
000147
000148
000149
000150
000151
000152
000153
000154
000155
000156
000157
000158
000159

*****SET POSITIONS FOR FIXED-POINT TEMPERATURE CALCULATIONS

CC 10 I=1,M
ZTC(I)=I/(M+1.)
10 CONTINUE

*****COMPUTE PROPERTIES AT SATURATION TEMPERATURE

IF(ICPTU.EQ.2) CALL CNVRT1
CALL PROPT6

***** THE HEATUP REGIME *****

*****INITIALIZE VARIABLES

CH=1./VF(TI)
VF23=1./CH
CF=1./DFIBER

FR3LOG=ALOG(PREF3)
FDENOM=(PREF3-PREF1)/2.
FMID=(PREF3+PREF1)/2.

MRSTAR=STAR*CH
IF(MRSTAR.GT.MRO) MRSTAR=MRO
IF(MRSTAR.EQ.MRO) FLAG=1
PG=MRO*Eh
EMIN=ES2/ES1
CALL CNSTMN(CSF)

N=KMIN
XX=(K-1)/(K+1)
CX=1./(K-1)

CC 20 I=1,K
TOLD(I)=TI
20 CONTINUE

IF(FLAG.EQ.1) RATIO2=1.
RATIO3=1.
PR=MRO

P1=EVALP(CO.,TB)
P2=EVALP(MRSTAR,TB)

```
C      M4=M1                                000160
C      N1=EVALN(1,C,0.)                    000161
      N2=EVALN(1,MRSTAR,0.)                000162
      N4=N1                                000164
C      CC=DFIBER*(CPF+MR*CPW)              000165
      CK=MR*DFIBER*KWATER                 000166
      A=(KFIBER+CK/DW)/DC                  000167
C      C                                     000168
C      C                                     000169
C      C                                     000170
C****CALCULATE MECHANICAL PRESSURE AND SHEET PROPERTIES 000171
C      3C IF(S3.EQ.1.) GO TO 40             000172
      CALL PRESSR(TIME)                     000173
      TBAR1=(TOLD(1)+TOLD(K))/2.           000174
      P3=EVALN(MR,TBAR1)                   000175
      N3=EVALN(2,P,F)                      000176
      DELTAT=BW/(P3*P**N3)                 000177
      PSI=A/DELTAT**2                      000178
      DT=TIMER*DX**2/(2.*PSI)              000179
      Fh=PVTB                               000180
      TIME=TIME+DT                          000181
      GO TO 50                              000182
C      4C YL(1)=DELTAT                     000183
      PR=CW*(YL(1)/BW-1./DFIBER)          000184
      TBAR1=(TOLD(1)+TOLD(K))/2.           000185
      P3=EVALN(MR,TBAR1)                   000186
      N3=EVALN(2,PR,F)                     000187
      CC=DFIBER*(CPF+MR*CPW)              000188
      CK=MR*DFIBER*KWATER                 000189
      A=(KFIBER+CK/DW)/DC                  000190
C      PHI=-CW*CPW*DLDT*DFIBER/(CC*BW)    000191
      PSI=A/(YL(1)**2)                     000192
C      DT=TIMER*DX/(2.*PSI/DX+ABS(PHI)/2.) 000193
      F2=PSI*DT/(DX**2)                   000194
      F3=PHI*DT/DX                         000195
      TERM1=PHI*DT/3.                      000196
      TERM2=2.*F2/9.                       000197
C      H=DT/100.                            000198
      TIMEND=TIME+DT                       000199
      CALL DGEAR(1,DLDTFN,DUMFUN,TIME,H,YL,TIMEND,TOL,METH,MITER, 000200
* INDEX,IHM,WN,IER)                      000201
      IF(IER.GT.128) WRITE(6,/) TOL,YL(1),TIMEND,H,TIME,METH,MITER, 000202
* INDEX                                    000203
      P=(BW/(YL(1)*N3))**(1./N3)          000204
      Fh=PVTB+1.5*DLDT/CGEFF              000205
      TIME=TIMEND                           000206
C      5C C3=M3*P**N3                       000207
      Y=(MR-MRSTAR)*C3                    000208
      C                                     000209
      C                                     000210
      C                                     000211
      C                                     000212
      C                                     000213
      C                                     000214
```

```

DELTA T=EW/C3
CONST=C3/DFIBER
E3=1.-CONST
IF(E3.LT.EMIN) CALL WARNIN(2,3,E3)
IF(E3.LT.EMIN) GO TO 9999
ESTAR=ES1*E3-ES2
S3=MR*C3/(E3*DW)
IF(S3.GT.1.) S3=1.
S3STAR=Y/(ESTAR*CW)

```

000215
000216
000217
000218
000219
000220
000221
000222
000223

*****CALCULATE HEAT TRANSFER PARAMETERS

```

HCDRY=HCREP*(HC1*(P/PREF2)**HC2-HC3)
HC=(HCDRY+MR*DFIBER*HCWET/DW)*CONST
M1=MFIBER*CONST
K3=K1+DK*CONST/DW
EIDX=HC*DELTA T*DX/M3

```

000224
000225
000226
000227
000228
000229
000230
000231
000232

.....CALCULATE INTERIOR TEMPERATURES

```

IF(S3.EQ.1.) GO TO 70
DO 6C I=2,K-1
TNEW(I)=TIMER*(TOLD(I+1)+TOLD(I-1))/2.+(1.-TIMER)*TOLD(I)
6C CONTINUE
GO TO 110

```

000233
000234
000235
000236
000237
000238
000239

```

70 IF(PHI.LT.0.) GO TO 90
DO 8C I=3,K-1
F3X=F3*(I-1)*DX
TNEW(I)=(F2-F3X/3)*TOLD(I+1)+(1.-2.*F2-F3X/2.)*TOLD(I)+
* (F2+F3X)*TOLD(I-1)-(F3X/6)*TOLD(I-2)
8C CONTINUE
TNEW(2)=(F2-F3*DX/2.)*TOLD(3)+(1.-2.*F2)*TOLD(2)+(F2+F3*DX/2.)*
* TOLD(1)
GO TO 120

```

000240
000241
000242
000243
000244
000245
000246
000247
000248
000249
000250
000251

```

90 DO 10C I=2,K-2
F3X=F3*(I-1)*DX
TNEW(I)=(F2-F3X)*TOLD(I+1)+(1.-2.*F2+F3X/2.)*TOLD(I)+
* (F2+F3X/3)*TOLD(I-1)+(F3X/6)*TOLD(I+2)
10C CONTINUE
TNEW(K-1)=(F2-F3*(K-2)*DX/2.)*TOLD(K)+(1.-2.*F2)*TOLD(K-1)+
* (F2+F3*(K-2)*DX/2.)*TOLD(K-2)
GO TO 120

```

000252
000253
000254
000255
000256
000257
000258
000259

.....CALCULATE BOUNDARY TEMPERATURES

```

110 TNEW(1)=TOLD(1)-(TNEW(2)-TOLD(2))/3.+(TIMER/9.)*(6.*BIDX*(TH-
* TOLD(1))-2.*TOLD(1)-3.*TOLD(2)+6.*TOLD(3)-TOLD(4))
TNEW(K)=TOLD(K)-(TNEW(K-1)-TOLD(K-1))/3.-(TIMER/9.)*(2.*TOLD(K)+
* 3.*TOLD(K-1)-6.*TOLD(K-2)+TOLD(K-3))
GO TO 130

```

000260
000261
000262
000263
000264
000265
000266
000267
000268
000269


```
C
12C TNEW(1)=TOLD(1)-(TNEW(2)-TOLD(2))/3.+TERM1*BIDX*(TH-TOLD(1))+
  * TERM2*(6.*BIDX*(TH-TOLD(1))-2.*TOLD(1)-3.*TOLD(2)+6.*TOLD(3)-
  * TOLD(4))
  TNEW(K)=TOLD(K)-(TNEW(K-1)-TOLD(K-1))/3.-TERM2*(2.*TOLD(K)+
  * 3.*TOLD(K-1)-6.*TOLD(K-2)+TOLD(K-3))
C
C
C.....RESET OLD TEMPERATURE VALUES
C
13C GO 140 I=1,N
  TOLD(I)=TNEW(I)
14C CONTINUE
C
C
C*****COMPUTE TEMPERATURES AT FIXED-POINT LOCATIONS
C
  GO 150 I=1,N
  KK=I*XX
  REM=I*XX-KK
  TC(I)=TNEW(1+KK)-REM*(TNEW(1+KK)-TNEW(2+KK))
150 CONTINUE
C
C
C*****INCREMENT QUANTITIES AND WRITE RESULTS
C
  T1=TNEW(1)
  CINIT=CINIT+(Q+HC*(TH-T1))*DT/2.
  C=HC*(TH-T1)
  IF(N.LT.J.AND.L.GT.LMAX.AND.TNEW(1).LT.TB) GO TO 160
C
  T1=T1
  T2=T1
  FGUAGE=Fh-PVTB
  IF(PGAUGE.LT.0.) PGAUGE=0.
  SEC=TIME*3600.
  T#IC=TC(1+N/2)
  CHTC=Q/(TH-T#IC)
  PREM=PR*BM
  PREL=1.-PRE)/MC
C
  T3=TNEW(K)
  CALL WRITER(IOPTU)
  A=1
  GO TO 170
C
C
C*****INCREMENT PRINT CONTROL VARIABLES
C
16C A=N+1
17C L=L+1
C
C
C*****DETERMINE EXIT CRITERIA
C
```

000270
000271
000272
000273
000274
000275
000276
000277
000278
000279
000280
000281
000282
000283
000284
000285
000286
000287
000288
000289
000290
000291
000292
000293
000294
000295
000296
000297
000298
000299
000300
000301
000302
000303
000304
000305
000306
000307
000308
000309
000310
000311
000312
000313
000314
000315
000316
000317
000318
000319
000320
000321
000322
000323
000324

IF(1800*TIME.GE.RISTIM.AND.IOPTP.EQ.2) GO TO 9999
IF((FLAG.EQ.1.AND.TNEW(K).LT.TB).OR.
* PV(TNEW(1)).LT.PW.OR.FV(TNEW(1)).LT.PVTB) GO TO 30

000325
000326
000327
000328
000329
000330
000331
000332
000333
000334
000335
000336
000337
000338
000339
000340
000341
000342
000343
000344
000345
000346
000347
000348
000349
000350
000351
000352
000353
000354
000355
000356
000357
000358
000359
000360
000361
000362
000363
000364
000365
000366
000367
000368
000369
000370
000371
000372
000373
000374
000375
000376
000377
000378

*****WRITE HEATUP REGIME FINAL OUTPUT

T1=TS
T2=T1
FGAUGE=PW-PVTB
IF(PGAUGE.LT.0.) PGAUGE=0.
SEC=TIME*3600.
TMID=TC(1+M/2)
CHIC=Q/(TH-TMID)
MREM=MR*BW
PREL=1.-MREM/MG

T3=TNEW(K)
IF(N.NE.1) CALL WRITER(IOPTU)
WRITE(6,930)
WRITE(6,935) (I,TNEW(I),I=1,K)

***** THE TRANSITION REGIME *****

*****WRITE TRANSITION REGIME HEADING

WRITE(6,940)

*****INITIALIZE VARIABLES

L=1
IF(FLAG.EQ.1) DELTA2=DELTA1
DELTA3=DELTA1
THICK2=DELTA2
THICK3=DELTA3
IF(FLAG.EQ.1.) THICK3=0.

RATIC2=DELTA2/DELTA1
RATIC3=DELTA3/DELTA1
LIQDEW=MG-E3*S3*DN*DELTA1

F=SPRES(F)/FACTOR
NAKW=S3STAR**4/(CR*C3)
EW3=BW
IF(FLAG.EQ.1) EW3=0.
IF(FLAG.EQ.1) EW2=BW
C1=M1*P**N1
C2=M2*P**N2

```
C4=M4*P**N4
W=MRSTAR*C2
X=MR*C3
C
T3=TB
Z=1.-MRSTAR/MR
CXX=DX
DIFFIX=DXX
DIFFI=DX
DIFFFX=DXX
DIFFF=DX
DELTA1=DIFFIX*THICK3
DELTA2=DELTA1-DIFFFX*THICK3
C
INIT=2
IFINI=K-1
C
IF(FLAG.EQ.1) GO TO 350
C
CTDZ23=(T2-T3)/DELTA1
C
CALL PROP23(1)
A2=KAKW*CPDT23/(VISF23*VF23*Y)
V=A2*Y*CPW*CTDZ23/((1.-E3)*DC)
FSI=A/DELTA1**2
PHI=V/DELTA1
C
C
C*****COMPUTE REQUIRED DERIVATIVES
C
180 C2=A2*CTDZ23
C4=A4*CTDZ12
C5=D2-A5*CTDZ12
C6=-A6*CTDZ38
IF(RATIO3.EQ.1..AND.TNEW(K).GE.TB) D6=K3*(TNEW(K)-TNEW(K-1))/
* ((HFG(T3)+DELHD(3))*CXX*THICK3*X)
C7=D2*Z
C
DENOM=D6+C7
C
C
C*****SET MAXIMUM ALLOWABLE TIME INCREMENT
C
CTMAX=TIMER*CX/(2.*PSI/DX+PHI/2.)
C
CT1=CTMAX
CT2=CTMAX
CT3=CTMAX
CT4=CTMAX
CT5=CTMAX
C
IF(DELTA1.NE.DELTA2) GO TO 190
IF(D2.NE.DENOM) DT1=(DELTA3-DELTA2)/(D2-DENOM)
```

000379
000380
000381
000382
000383
000384
000385
000386
000387
000388
000389
000390
000391
000392
000393
000394
000395
000396
000397
000398
000399
000400
000401
000402
000403
000404
000405
000406
000407
000408
000409
000410
000411
000412
000413
000414
000415
000416
000417
000418
000419
000420
000421
000422
000423
000424
000425
000426
000427
000428
000429
000430
000431

```

DT=AMIN1(DT1,DTMAX)                                000432
IF((C2*DT).GE.CIFFIX*THICK3) IOPT1=1                000433
GO TO 200                                             000434
190 IF(D4.NE.D5) DT1=(DELTA2-DELTA1)/(D4-D5)         000435
IF(DT1.LT.0.) DT1=DTMAX                              000436
IF(D5.NE.DENOM) DT2=(DELTA3-DELTA2)/(D5-DENOM)     000437
IF(DT2.LT.0.) DT2=DTMAX                              000438
DT=AMIN1(DT1,DT2,DTMAX)                             000439
IF((C5*DT).GE.CIFFIX*THICK3) IOPT1=1                000440
200 IF((-DENOM*DT).GE.DIFFFX*THICK3) IOPT2=1         000441
IF((CPT1.EQ.1.AND.IOPT2.EQ.1) GO TO 210              000442
IF(IOPT1.EQ.0) DT3=DIFFI*DX/(2.*PSI)                 000443
IF(DENOM.LE.0.) DT4=DIFFF*DX/(2.*PSI)               000444
IF(DENOM.GT.0..AND.RATIO3.NE.1.) DT5=(DXX-DIFFFX)*THICK3/DENOM 000445
IF(DT5.EQ.0.) DT5=DXX*THICK3/DENOM                  000446
DT=AMIN1(DT1,DT2,DT3,DT4,DT5,DTMAX)                 000447
IF(DELTA1.EQ.DELTA2.AND.D2*DT.GE.DIFFIX*THICK3) IOPT1=1 000448
IF(DELTA1.EQ.DELTA2.AND.D2*DT.LT.DIFFIX*THICK3) IOPT1=0 000449
IF(DELTA1.NE.DELTA2.AND.D5*DT.GE.CIFFIX*THICK3) IOPT1=1 000450
IF(DELTA1.NE.DELTA2.AND.D5*DT.LT.CIFFIX*THICK3) IOPT1=0 000451
IF((-DENOM*DT).GE.DIFFFX*THICK3) IOPT2=1           000452
IF((-DENOM*DT).LT.DIFFFX*THICK3) IOPT2=0           000453
DT=TIMER*DT                                           000454
210 TIME=TIME+DT                                       000455
*****CALCULATE NEW TEMPERATURE DISTRIBUTION          000456
LC=DFIBER*(CPF*MR*CPH)                                000457
DK=MR*DFIBER*KWATER                                  000458
A=(KFIBER+DK*VF23)/DC                                000459
V=D2*Y*CPH/((1.-E3)*DC)                              000460
FSI=A*(C3/8h)**2                                     000461
PHI=V*C3/8h                                          000462
F2=PSI*DT/DX**2                                     000463
F3=PHI*DT/DX                                         000464
TERM2=2.*F2/9.                                       000465
CC 220 I=INIT,INIT+1                                  000466
TNEW(I)=(F2-F3/2)*TOLD(I+1)+(1-2*F2)*TOLD(I)+(F2+F3/2)*TOLD(I-1) 000467
220 CONTINUE                                          000468
CC 230 I=INIT+2,IFINI                                  000469
TNEW(I)=(F2-F3/3)*TOLD(I+1)+(1.-2*F2-F3/2)*TOLD(I)+(F2+F3)* 000470
* TOLD(I-1)-(F3/6)*TOLD(I-2)                         000471
230 CONTINUE                                          000472
IF(IOPT1.EQ.0) TNEW(INIT)=TOLD(INIT)-PHI*DT+((TOLD(INIT+1)-T2)/ 000473
* (DX+DIFFI))+2.*PSI*DT*(TOLD(INIT+1)/(DX+(DIFFI+DX))-TOLD(INIT) 000474
000475
000476
000477
000478
000479
000480
000481
000482
000483
000484
000485

```



```
CBW1DT=C2*RATE1                                000540
CBW2DT=C3*RATE2-DBW1DT                          000541
DBW3DT=C3*(RATE3-RATE2)                        000542
IF(RATIO3.EQ.1..AND.RATE3.EQ.0.) DBW3DT=-C3*RATE2 000543
CBW4DT=-C3*RATE3                                000544

EW1=BW1+CBW1DT*DT                               000545
EW2=BW2+DBW2DT*DT                               000546
EW3=BW3+DBW3DT*DT                               000547
IF(FLAG.EQ.1) EW3=0.                             000548
EW4=BW4+DBW4DT*DT                               000549

IF(BW1.LT.0.) BW1=0.                             000550
IF(BW2.LT.0.) BW2=0.                             000551
IF(BW3.LT.0..OR.FLAG.EQ.1) BW3=0.               000552
IF(BW4.LT.0.) BW4=0.                             000553

250 EWSUM=BW1+BW2+EW3+BW4                        000554
EWCORR=EW/BSUM                                   000555

EW1=EW1*EWCORR                                  000556
EW2=EW2*EWCORR                                  000557
EW3=EW3*EWCORR                                  000558
EW4=EW4*EWCORR                                  000559

TBAR1=(T5+T1)/2.                                 000560
TBAR2=(T1+T2)/2.                                 000561
TBAR3=(T2+TNEW(IFINI))/2.                        000562
TBAR4=(TNEW(IFINI)+TNEW(K))/2.                   000563

P1=EVALP(0.,TBAR1)                               000564
P2=EVALP(MRSTAR,TBAR2)                           000565
P3=EVALP(MR,TBAR3)                                000566
P4=EVALP(0.,TBAR4)                               000567

M3=EVALN(2.,MR,P3)                               000568

C1=M1*P1**N1                                     000569
C2=M2*P2**N2                                     000570
C3=M3*P3**N3                                     000571
C4=M4*P4**N4                                     000572

THICK1=BW1/C1                                    000573
THICK2=BW2/C2                                    000574
THICK3=BW3/C3                                    000575
THICK4=BW4/C4                                    000576

*****CALCULATE POROSITY AND SATURATION          000577

E1=1.-C1/DFIBER                                  000578
E2=1.-C2/DFIBER                                  000579
E3=1.-C3/DFIBER                                  000580
ESTAR=E3-E2-E1                                    000581
000582
000583
000584
000585
000586
000587
000588
000589
000590
000591
000592
000593
```

```
E4=1.-C4/DFIBER
IF(C1.GT.DFIBER) CALL WARNIN(1,1,C1)
IF(E2.LT.EMIN) CALL WARNIN(2,2,E2)
IF(E3.LT.EMIN) CALL WARNIN(2,3,E3)
IF(C4.GT.DFIBER) CALL WARNIN(1,4,C4)
IF(C1.GT.DFIBER.OR.E2.LT.EMIN.OR.E3.LT.EMIN.OR.C4.GT.DFIBER)
* GO TO 9999
C
CALL CALLER(4)
W=MRSTAR*C2
X=MR*C3
Y=(MR-MRSTAR)*C3
Z=Y/X
C
S2=W*VF12/E2
S3=X*VF23/E3
S3STAR=Y*VF23/ESTAR
IF(S3.LE.1.) GO TO 270
IF(BW4.NE.0.) GO TO 260
S3=1.
S3STAR=1.
MR=E3/(VF23*C3)
X=E3/VF23
Y=(MR-MRSTAR)*C3
Z=Y/X
GO TO 270
260 BW4=BW4-(S3-1.)*BW3
IF(BW4.LT.0.) BW4=0.
BW3=BW-BW1-BW2-BW4
GO TO 250
C
C
C*****INCREMENT INTERFACE POSITIONS
C
270 DELTA1=THICK1
DELTA2=DELTA1+THICK2
DELTA3=DELTA2+THICK3
DELTA4=DELTA3+THICK4
IF(THICK3.EC.0.) DELTA3=DELTA4
C
IF(D5.GT.0.) INIT=((BW1+BW2)/BW)*(K-1)+2
IFINI=(K-1)-(K-1)*BW4/BW
IF(IFINI.LE.INIT) GO TO 450
CXX=DX*BW/BW3
CIFFFX=DX-BW4/BW
CIFFIX=1.-DIFFFX-(IFINI-INIT)*DX
IF(CIFFIX.GT.CXX) CALL WARNIN(3,1,C.)
IF(DIFFFX.GT.CXX) CALL WARNIN(4,1,C.)
DELTA1=DELTA2+CIFFIX*THICK3
DELTA4=DELTA3-CIFFFX*THICK3
CIFF1=DIFFIX*BW3/BW
CIFFF=DIFFFX*BW3/BW
C
C
C*****CALCULATE THERMAL CONDUCTIVITY AND CONTACT COEFFICIENT
```

K1=KFIBER*(1.-E1) 000649
K2=KFIBER*(1.-E2)+KWATER*E2*S2 000650
K3=KFIBER*(1.-E3)+KWATER*E3*S3 000651
K4=KFIBER*(1.-E4) 000652

HCDRY=HCREP*(HC1*(P1/PREF2)**HC2-HC3) 000653
PC=HCDRY*(1.-E1) 000654
IF(DELTA1.EQ.0.) HC=HCDRY*(1.-E2)*E2*S2*HCNET 000655
IF(DELTA2.EQ.0.) HC=HCDRY*(1.-E3)*E3*S3*HCNET 000656

*****CALCULATE PERMEABILITY FACTORS

R=SPRES(F)/FACTOR 000657
MABS2=1./(R*C2) 000658
MABS3=1./(R*C3) 000659
MABS4=1./(R*C4) 000660
KAK=KABS3*S3STAR**4 000661

*****SET RELATIVE INTERFACE POSITIONS AND REMAINING MOISTURE

RATIO1=DELTA1/DELTAT 000662
RATIO2=DELTA2/DELTAT 000663
RATIO3=DELTA3/DELTAT 000664
PREM=MR*Bb3+MRSTAR*Bb2 000665
PREL=1.-PREM/MC 000666
IF(RATIO2.EQ.1.) GO TO 390 000667

*****COMPUTE NEW VALUES FOR T1, T2 AND T3

IF(DELTA1.NE.DELTA2) GO TO 280 000668
ALFA=DELTA3-DELTA1 000669
TERM1=(1./MC*DELTA1/K1)*K3/(DELTA1-DELTA1) 000670
T1=(T1+TERM1*TNE*(INIT))/(1.+TERM1) 000671
T2=T1 000672
GO TO 290 000673

280 GO 290 I=1,IMAX

T01=T1 000674
T02=T2 000675
CALL PROP12 000676
HFG1=HFG(T1)+DELHD(1) 000677
HFG2=HFG(T2)+DELHD(2) 000678
ALF=DELTA2-DELTA1 000679
000680
000681
000682
000683
000684
000685
000686
000687
000688
000689
000690
000691
000692
000693
000694
000695
000696
000697
000698
000699
000700
000701


```

EET=DELTA3-DELTA2
C
TERM1=(1./HC*DELTA1/K1)*(1./ALF)*(HFG1*KABS2*DPDT12/
* (VG12*VISG12)*K2)
TERM2=(KABS2*DPDT12*HFG2/(K3*VG12*VISG12)+K2/K3)*
* (DELTA1-DELTA2)/ALF
DENOM=1.+TERM1+TERM2
C
T1=((1.+TERM2)*TH+TERM1*TNEW(INIT))/DENOM
T1=(T01+T1)/2.
T2=(TERM2*TH+(1.+TERM1)*TNEW(INIT))/DENOM
T2=(T02+T2)/2.
29C CONTINUE
C
IF(RATIO3.EQ.1.) GO TO 310
C
CALL PROF3E
HFG3=HFG(T3)+DELHD(3)
C
DO 300 I=1,IMAX
C
T03=T3
C
TERM1=(KABS4*HFG3*DPDT3B/(K3*VISG3B*VG3B))*(DELTA3-DELTA1)
* /(DELTA1-DELTA3)
C
T3=(TNEW(IFINI)+TERM1*TB)/(1.+TERM1)
T3=(T03+T3)/2.
300 CONTINUE
GO TO 320
C
310 T3=TB
C
320 IF((TNEW(IFINI)-T3)/DIFFFX.EQ.(T2-T3)) GO TO 450
C
C*****RECOMPUTE VARIABLES FOR DERIVATIVE CALCULATIONS
C
IF(DELTA1.NE.DELTA2) GO TO 330
CTDZ12=C.
CTDZ23=(T2-T3)/ALFA
IF(T2.LE.TB) DTDZ23=0.
GO TO 340
C
330 CTDZ12=(T1-T2)/ALF
IF(T2.LE.TB) CTDZ12=(T1-TB)/ALF
IF(T1.LE.TB) DTDZ12=0.
CTDZ23=(T2-T3)/BET
IF(T2.LE.TB) DTDZ23=0.
C
340 CTDZ3B=0.
IF(RATIO3.NE.1.) DTDZ3E=(T3-TB)/(DELTA1-DELTA3)
C
CALL CALLER(1)
000702
000703
000704
000705
000706
000707
000708
000709
000710
000711
000712
000713
000714
000715
000716
000717
000718
000719
000720
000721
000722
000723
000724
000725
000726
000727
000728
000729
000730
000731
000732
000733
000734
000735
000736
000737
000738
000739
000740
000741
000742
000743
000744
000745
000746
000747
000748
000749
000750
000751
000752
000753
000754
000755
```

```

A2=KAKH*DPDT23/(VISF23*VF23*Y)
A4=KABS2*DPCT12/(VISG12*VG12*W)
A5=A4*W/Y
A6=KABS4*DPCT3E/(VG3B*VISG3B*X)
GC TC 400

```

000756
000757
000758
000759
000760
000761
000762
000763
000764
000765
000766
000767
000768
000769
000770
000771
000772
000773
000774
000775
000776
000777
000778
000779
000780
000781
000782
000783
000784
000785
000786
000787
000788
000789
000790
000791
000792
000793
000794
000795
000796
000797
000798
000799
000800
000801
000802
000803
000804
000805
000806
000807
000808
000809

*****HANDLE SPECIAL CASE OF INTRA-FIBER WATER

```

35C DTMA)=TIMER*CX**2/(2.*PSI)
C1FFFF=CXX
I1=TNEW(1)
I2=TNEW(K)
HFG2=HFE(I2)+DELHD(1)
C7=0.
X=MR*C2

```

```

36C C6=K3*(I2-TNEW(IFINI))/(HFE2+DXX*THICK2*X)

```

```

CT1=DTMAX
CT2=DTMAX
DT1=(DELTA2-DELTA1)/(-D6)
CT=AMIN1(DT1,DTMAX)
IF((-D6*DT).GE.DIFFFX*THICK2) ICPT2=1
IF(ICPT2.EQ.1) GO TO 37C
CT2=DX*C1FFFF/(2.*PSI)
CT=AMIN1(CT1,DT2,DTMAX)
CT=TIMER*DT

```

```

37C TIME=TIME+DT

```

```

A=(KFIBER+DX*VF12)/DC
PSI=A*(C2/BH)**2
F2=PSI*DT/D)**2

```

```

CC 380 I=INI1,IFINI
TNEW(I)=F2*(TOLD(I+1)+TOLD(I-1))/2.+(1.-2.*F2)*TOLD(I)

```

```

38C CONTINUE

```

```

TNEW(1)=TOLD(1)-(TNEW(2)-TOLD(2))/3.+(2.*F2/9.)*(6.*BIDX*(TH-
* TOLD(1))-2.*TOLD(1)-3.*TOLD(2)+6.*TOLD(3)-TOLD(4))
I1=TNEW(1)
TOLD(1)=TNEW(1)

```

```

IF(ICPT2.EQ.0) TNEW(IFINI)=TOLD(IFINI)+2.*PSI*DT*(I2/(DIFFF*
* (DIFFF+DX))-TOLD(IFINI)/(C)*DIFFF)+TOLD(IFINI-1)/(DX*(DX+
* C1FFFF))

```

```

FATE2=D6
CALL PRESSR(TIME)
PH2=HYDRAL(I1,I2)
PH4=HYDRAL(I2,I1)
F2=F-PH2
F4=F-PH4

```

C		000810
	CEW2DT=C2*RATE2	000811
	CEW4DT=-DBW2CT	000812
C		000813
	EW2=BW2*DBW2DT*DT	000814
	EW4=BW4*DBW4DT*DT	000815
C		000816
	EWSUM=EW2+EW4	000817
	EWCORR=EW/EWSUM	000818
	EW2=EW2*EWCORR	000819
	EW4=EW4*EWCORR	000820
	TBAR2=(T1+T2)/2.	000821
	TBAR4=(T2+T3)/2.	000822
	P2=EVALP(MRSTAR,TBAR2)	000823
	P4=EVALP(O.,TBAR4)	000824
	C2=M2*P2**N2	000825
	C4=M4*P4**N4	000826
C		000827
	THICK2=EW2/C2	000828
	THICK4=EW4/C4	000829
C		000830
	E2=1.-C2/DFIBER	000831
	E4=1.-C4/DFIBER	000832
	IF(E2.LT.EMIN) CALL WARNIN(2,2,E2)	000833
	IF(C4.GT.DFIBER) CALL WARNIN(1,4,C4)	000834
	IF(E2.LT.EMIN.OR.C4.GT.DFIBER) GO TO 9999	000835
C		000836
	CALL PRCP12	000837
	X=MR*C2	000838
	Z=C.	000839
	S2=X*VF12/E2	000840
C		000841
	DELTA2=THICK2	000842
	DELTA4=DELTA2*THICK4	000843
	IFINI=(K-1)-(K-1)*BW4/BW	000844
	DXX=CX*EW/BW2	000845
	DIFFFX=DXX-BW4/BW	000846
	IF(DIFFFX.GT.O)X) CALL WARNIN(4,1,0.)	000847
	DELTA2=DELTA2-DIFFFX*THICK2	000848
	K2=KFIBER*(1.-E2)+KWATER*E2*S2	000849
	M4=MFIBER*(1.-E4)	000850
	HCDRY=HCREP*(HC1*(P2/PREF2)**HC2-HC3)	000851
	PC=HCDRY*(1.-E2)+E2*S2*HCDET	000852
	EIDX=HC*BW*DX/(K2*C2)	000853
C		000854
	F=SPRES(P)/FACTOR	000855
	MABS2=1./(R*C2)	000856
	MABS4=1./(R*C4)	000857
C		000858
	FATIG1=C.	000859
	FATIG2=DELTA2/DELTA4	000860
	FATIG3=1.	000861
C		000862
	MREY=MRSTAR*EW2	000863
	MREL=1.-MREY/PC	000864
C		000865

```

CALL PROP23(2)                                000866
HFG2=HFG(T2)*DELHD(1)                        000867

IF(RATIO2.EQ.1.) GO TO 390                    000868
DO 390 I=1,IMA)                               000869
TQ2=T2                                         000870
TERM1=(KAES4*HFG2*CPDT23/(K3*VIS623*VG23))*(DELTA2-DELTA1)/ 000871
* (DELTA1-DELTA2)                             000872
T2=(TNEW(IFINI)+TERM1*TB)/(1.+TERM1)         000873
T2=(TQ2+T2)/2.                               000874
390 CONTINUE                                  000875

IF(RATIO2.EQ.1.) T2=TB                       000876
IF((TNEW(IFINI)-T2)/DIFFF).EQ.(T1-T2)) GO TO 450 000877

*****RESET TEMPERATURE DISTRIBUTION AND TIME OPTIONS 000878

400 DO 410 I=INIT,K                          000879
TOLD(I)=TNEW(I)                              000880
410 CONTINUE                                  000881

ICPT1=0                                       000882
ICPT2=0                                       000883

*****COMPUTE TEMPERATURES AT FIXED-POINT LOCATIONS 000884

SLM12=BW1+B2                                  000885
SUM123=SUM12+B3                              000886
DO 420 I=1,M                                  000887
L=ZTC(I)*BW                                  000888
KK=I*XX                                       000889
REM=I*XX-KK                                  000890
IF(U.LT.BW1.AND.BW1.NE.0.) TC(I)=TS-(TS-T1)*(U/BW1) 000891
IF(U.GT.BW1.AND.U.LT.SUM12.AND.BW2.NE.0.) TC(I)=T1-(T1-T2)* 000892
* (L-BW1)/BW2                                000893
IF(U.GT.SUM12.AND.U.LT.SUM123.AND.BW3.NE.0.) TC(I)=TNEW(1+KK)- 000894
* REM*(TNEW(1+KK)-TNEW(2+KK))              000895
IF(U.GT.SUM123.AND.U.LT.B4.AND.BW4.NE.0.) TC(I)=T3-(T3-TB)* 000896
* (U-SUM123)/BW4                            000897

IF(U.EQ.BW1) TC(I)=T1                        000898
IF(U.EQ.SUM12) TC(I)=T2                     000899
IF(U.EQ.SUM123) TC(I)=T3                   000900
IF(U.EQ.BW) TC(I)=TB                       000901
420 CONTINUE                                  000902

*****INCREMENT QUANTITIES AND WRITE RESULTS 000903

PC=PREM/(MREM*BW)                            000904
TS=(TH*HC*DELTA1/K1+T1)/(1.+HC*DELTA1/K1) 000905
000906
000907
000908
000909
000910
000911
000912
000913
000914
000915
000916
000917
000918

```

```

C TOTAL=C TOTAL+(Q+MC*(TH-TS))*DT/2. 000919
C (=MC*(TH-TS) 000920
C IF(N.LT.J.AND.L.GT.LMAX.AND.MC.GT.MFINAL) GO TO 430 000921
C 000922
C PGAUGE=PV(T1)-FVTB 000923
C IF(PGAUGE.LT.0.) PGAUGE=0. 000924
C SEC=TIME*3600. 000925
C TMID=TC(1+M/2) 000926
C CHTC=G/(TH-TMID) 000927
C 000928
C IF(RATIO3.EQ.1.) T3=TNEW(K) 000929
C IF(FLAG.EQ.1) T3=TE 000930
C CALL WRITER(IOPTU) 000931
C T3=TB 000932
C A=1 000933
C GO TO 440 000934
C 000935
C 000936
C *****INCREMENT PRINT CONTROL VARIABLES 000937
C 000938
C 43C A=N+1 000939
C 44C L=L+1 000940
C 000941
C 000942
C *****DETERMINE EXIT CRITERIA 000943
C 000944
C IF(1800*TIME.GE.RISTIN.AND.IOPTP.EQ.2) GO TO 9999 000945
C IF(MC.LT.MFINAL) GO TO 9999 000946
C IF(RATIO2.EQ.1.) GO TO 450 000947
C IF(FLAG.NE.1.AND.MC.GT.MFINAL) GO TO 180 000948
C IF(FLAG.EQ.1.AND.MC.GT.MFINAL) GO TO 360 000949
C 000950
C 000951
C *****WRITE TRANSITION REGIME FINAL OUTPUT 000952
C 000953
C 45C PC=MREP/(MREM+EM) 000954
C TS=(TH+MC*DELTA1/K1+T1)/(1+MC*DELTA1/K1) 000955
C GTOTAL=C TOTAL+(Q+MC*(TH-TS))*DT/2. 000956
C (=MC*(TH-TS) 000957
C PGAUGE=PV(T1)-FVTB 000958
C IF(PGAUGE.LT.0.) PGAUGE=0. 000959
C SEC=TIME*3600. 000960
C TMID=TC(1+M/2) 000961
C CHTC=G/(TH-TMID) 000962
C 000963
C IF(RATIO3.EQ.1.) T3=TNEW(K) 000964
C IF(FLAG.EQ.1) T3=TE 000965
C IF(N.NE.1) CALL WRITER(IOPTU) 000966
C WRITE(6,930) 000967
C IF(IFINI.LE.K) WRITE(6,935) (I,TNEW(I),I=INIT,IFINI) 000968
C ***** 000969
C 000970
C 000971
C ***** 000972
C ***** THE LINEAR REGIME ***** 000973

```

000974

000975

000976

000977

000978

000979

000980

000981

000982

000983

000984

000985

000986

000987

000988

000989

000990

000991

000992

000993

000994

000995

000996

000997

000998

000999

001000

001001

001002

001003

001004

001005

001006

001007

001008

001009

001010

001011

001012

001013

001014

001015

001016

001017

001018

001019

001020

001021

001022

001023

001024

001025

001026

001027

001028

*****WRITE LINEAR REGIME HEADING

WRITE(6,945)

*****SET FLAG AND GO TO FIRST TEMPERATURE CALCULATION

L=1

T3=TE

NAKV=KABS3*(1.-S3STAR)**3*(1.+3.*S3STAR)

IF(RATIO2.EQ.1.) FLAG=1

DTMAX=DT0

GO TO 550

*****COMPUTE REQUIRED DERIVATIVES

460 C1=A1*DTDZ23

C2=A2*DTDZ23

C3=A3*DTDZ23

C4=A4*DTDZ12

C5=A5*DTDZ23

C6=-K3*DTDZ23/(HFG3*X)

C7=D2*2

C8=A8*DTDZ12

IF(DELTA1.EQ.DELTA2.AND.D1.GE.D2) D7=0.

IF(DELTA1.NE.DELTA2.AND.D5.GE.D2) D7=0.

DENOM=D6+C7

*****SET MAXIMUM ALLOWABLE TIME INCREMENT

DT1=DTMAX

DT2=DTMAX

IF(DELTA1.NE.DELTA2) GO TO 470

IF(C1.GE.C2.AND.D1.NE.C6) DT1=(DELTA3-DELTA1)/(C1-D6)

IF(C1.LT.C2.AND.C2.NE.DENOM) DT1=(DELTA3-DELTA2)/(C2-DENOM)

GO TO 490

470 IF(FLAG.EQ.1) GO TO 480

CSTAR=AMAX1(C2,D5)

IF(CSTAR.NE.DENOM) DT1=(DELTA3-DELTA2)/(CSTAR-DENOM)

IF(C4.GT.CSTAR) DT2=(DELTA2-DELTA1)/(C4-CSTAR)

GO TO 490

480 CSTAR=0.

IF(C4.NE.C8) DT1=(DELTA2-DELTA1)/(C4-C8)

490 IF(DT1.LE.0.) DT1=DTMAX

IF(DT2.LE.0.) DT2=DTMAX

```
C      CT=AMIN1(DT1,DT2,DTMAX)                                001029
C      CT=TIMER*CT                                           001030
C      TIME=TIME+DT                                          001031
C      TIME=TIME+DT                                          001032
C      TIME=TIME+DT                                          001033
C      TIME=TIME+DT                                          001034
C*****CALCULATE RATES OF BASIS WEIGHT CHANGE              001035
C      IF(Delta1.NE.Delta2) GO TO 500                        001036
C      IF(D1.GE.D2) RATE1=D1                                001037
C      RATE2=RATE1                                           001038
C      IF(D1.LT.D2) RATE2=D2                                001039
C      IF(D1.LT.D2.AND.D3.GE.D2) RATE1=RATE2                001040
C      IF(D1.LT.D2.AND.D3.LT.D2) RATE1=D3                  001041
C      GO TO 510                                             001042
C      GO TO 510                                             001043
C      GO TO 510                                             001044
C      500 RATE1=D4                                           001045
C      RATE2=DSTAR                                           001046
C      IF(FLAG.EQ.1) RATE2=D8                                001047
C      IF(FLAG.EQ.1) RATE2=D8                                001048
C      510 RATE3=DENGM                                        001049
C      IF(FLAG.EQ.1) EW3=0.                                  001050
C      IF(FLAG.EQ.1) RATE3=0.                                001051
C      IF(BW4.EQ.0.) LIQDEN=LIQDEN+RATE3*X*DT               001052
C      IF(BW4.EQ.0.) LIQDEN=LIQDEN+RATE3*X*DT               001053
C      IF(BW4.EQ.0.) LIQDEN=LIQDEN+RATE3*X*DT               001054
C      IF(BW4.EQ.0.) LIQDEN=LIQDEN+RATE3*X*DT               001055
C*****CALCULATE MECHANICAL AND HYDRAULIC PRESSURE        001056
C      CALL PRESSR(TIME)                                     001057
C      CALL PRESSR(TIME)                                     001058
C      CALL PRESSR(TIME)                                     001059
C      FM1=HYDRAL(T1,T1)                                     001060
C      FM2=HYDRAL(T1,T2)                                     001061
C      FM3=HYDRAL(T2,T3)                                     001062
C      FM4=HYDRAL(T3,TB)                                     001063
C      IF(FLAG.EQ.1) PH4=PH3                                 001064
C      IF(FLAG.EQ.1) PH4=PH3                                 001065
C      F1=F-PH1                                              001066
C      IF(P1.LE.0.) P1=PREF1                                  001067
C      F2=P-PH2                                              001068
C      F3=P-PH3                                              001069
C      F4=F-PH4                                              001070
C      F4=F-PH4                                              001071
C      F4=F-PH4                                              001072
C*****CALCULATE BASIS WEIGHT, CONCENTRATION AND THICKNESS 001073
C      CBW1DT=C2*RATE1                                       001074
C      CBW2DT=C3*RATE2-DBW1DT                                  001075
C      IF(FLAG.EQ.1) DBW2DT=C2*(RATE2-RATE1)                 001076
C      CBW3DT=C3*(RATE3-RATE2)                                001077
C      IF(RATIO3.EQ.1.AND.RATE3.GT.0.) DBW3DT=-C3*RATE2     001078
C      CBW4DT=-C3*RATE3                                       001079
C      IF(FLAG.EQ.1) DBW4DT=-C2*RATE2                         001080
C      IF(FLAG.EQ.1) DBW4DT=-C2*RATE2                         001081
C      IF(FLAG.EQ.1) DBW4DT=-C2*RATE2                         001082
```

EW1=BW1+DBW1DT*DT
 EW2=BW2+DBW2DT*DT
 EW3=BW3+DBW3DT*DT
 EW4=BW4+DBW4DT*DT

IF(BW1.LT.0.) BW1=0.
 IF(BW2.LT.0.) BW2=0.
 IF(BW3.LT.0..OR.FLAG.EQ.1) BW3=0.
 IF(BW4.LT.0.) BW4=0.

001083
 001084
 001085
 001086
 001087
 001088
 001089
 001090
 001091
 001092
 001093
 001094
 001095
 001096
 001097
 001098
 001099
 001100
 001101
 001102
 001103
 001104
 001105
 001106
 001107
 001108
 001109
 001110
 001111
 001112
 001113
 001114
 001115
 001116
 001117
 001118
 001119
 001120
 001121
 001122
 001123
 001124
 001125
 001126
 001127
 001128
 001129
 001130
 001131
 001132
 001133
 001134
 001135
 001136
 001137

520 EWSUM=BW1+BW2+BW3+BW4
 EWCCRR=EW/BSUM

EW1=EW1*EWCCRR
 EW2=EW2*EWCCRR
 EW3=EW3*EWCCRR
 EW4=EW4*EWCCRR

TBAR1=(T1+T2)/2.
 TBAR2=(T1+T2)/2.
 TBAR3=(T2+T3)/2.
 TBAR4=(T3+T4)/2.

P1=EVALM(0.,TBAR1)
 P2=EVALM(HRSTAR,TBAR2)
 P3=EVALM(HR,TBAR3)
 P4=EVALM(0.,TBAR4)
 IF(FLAG.EQ.1) P4=EVALM(0.,TBAR3)

C1=M1*P1**N1
 C2=M2*P2**N2
 C3=M3*P3**N3
 C4=M4*P4**N4

THICK1=EW1/C1
 THICK2=EW2/C2
 THICK3=EW3/C3
 THICK4=EW4/C4

*****CALCULATE POROSITY AND SATURATION

E1=1.-C1/DFIBER
 E2=1.-C2/DFIBER
 E3=1.-C3/DFIBER
 ESTAR=E3-E3-E32
 E4=1.-C4/DFIBER
 IF(C1.GT.DFIBER) CALL WARNIN(1,1,C1)
 IF(E2.LT.EMIN) CALL WARNIN(2,2,E2)
 IF(E3.LT.EMIN) CALL WARNIN(2,3,E3)
 IF(C4.GT.DFIBER) CALL WARNIN(1,4,C4)
 IF(C1.GT.DFIBER.OR.E2.LT.EMIN.OR.E3.LT.EMIN.OR.C4.GT.DFIBER)

* GO TO 9999


```
CALL CALLER(4)                                001138
D=MRSTAR*C2                                    001139
X=MR*C3                                         001140
Y=(MR-MRSTAR)*C3                              001141
Z=Y/X                                           001142
C                                                001143
S2=W*VF12/E2                                   001144
S3=X*VF23/E3                                   001145
S3STAR=Y*VF23/ESTAR                           001146
IF(S3.LE.1..OR.FLAG.EQ.1) GO TO 540           001147
IF(BW4.NE.0.) GO TO 530                       001148
S3=1.                                           001149
S3STAR=1.                                       001150
MR=E3/(VF23*C3)                               001151
X=E3/VF23                                       001152
Y=(MR-MRSTAR)*C3                              001153
Z=Y/X                                           001154
GO TO 540                                       001155
530 BW4=BW4-(S3-1.)*BW3                       001156
IF(BW4.LT.0.) BW4=0.                          001157
BW3=BW-BW1-BW2-BW4                             001158
GO TO 520                                       001159
C                                                001160
C                                                001161
C*****INCREMENT INTERFACE POSITIONS          001162
C                                                001163
540 DELTA1=THICK1                               001164
DELTA2=DELTA1+THICK2                           001165
DELTA3=DELTA2+THICK3                           001166
DELTA4=DELTA3+THICK4                           001167
IF(THICK3.EQ.0.) FLAG=1                       001168
IF(THICK3.EQ.C.) DELTA3=DELTA4                001169
C                                                001170
C                                                001171
C*****CALCULATE THERMAL CONDUCTIVITY AND CONTACT COEFFICIENT 001172
C                                                001173
M1=KFIBER*(1.-E1)                             001174
M2=KFIBER*(1.-E2)*KWATER*E2*S2               001175
M3=KFIBER*(1.-E3)*KWATER*E3*S3               001176
M4=KFIBER*(1.-E4)                             001177
C                                                001178
HCDRY=HCREP*(HC1*(P1/PREF2)**HC2-HC3)         001179
HC=HCDRY*(1.-E1)                              001180
IF(DELTA1.EQ.0.) HC=HCDRY*(1.-E2)+E2*S2*HCWET 001181
IF(DELTA2.EQ.0.) HC=HCDRY*(1.-E3)+E3*S3*HCWET 001182
C                                                001183
C                                                001184
C*****CALCULATE PERMEABILITY FACTORS        001185
C                                                001186
R=SPRES(P)/FACTOR                              001187
C                                                001188
KABS2=1./(R*C2)                                001189
KABS3=1./(R*C3)                                001190
KABS4=1./(R*C4)                                001191
```

KAKV=KABS3*(1.-S3STAR)**3*(1.+3.*S3STAR)
KAKH=KABS3*S3STAR**4

001192
001193
001194
001195
001196
001197
001198
001199
001200
001201
001202
001203
001204
001205
001206
001207
001208
001209
001210
001211
001212
001213
001214
001215
001216
001217
001218
001219
001220
001221
001222
001223
001224
001225
001226
001227
001228
001229
001230
001231
001232
001233
001234
001235
001236
001237
001238
001239
001240
001241
001242
001243
001244
001245
001246

*****SET RELATIVE INTERFACE POSITIONS AND REMAINING MOISTURE

RATIO1=DELTA1/DELTAT
RATIO2=DELTA2/DELTAT
RATIO3=DELTA3/DELTAT

MREM=MR*BM3+MRSTAR*BM2
MREL=1.-MREM/MC

*****COMPUTE NEW VALUES FOR T1, T2 AND T3

550 IF(DELTA1.NE.DELTA2) GO TO 570

DO 560 I=1,IMAX

T02=T2
T03=T3

CALL CALLER(2)

HFG2=HFG(T2)+DELHD(3)
HFG3=HFG(T3)+DELHD(3)

ALFA=DELTA3-DELTA2
BETA=DELTA1-DELTA3

TERM1=(1./HC+DELTA1/K1)*(1./ALFA)*(HFG2+KAKV*DPDT23/
* (VG23+VISG23)+K3)
TERM3=(BETA*(KAKV*DPDT23/(VG23+VISG23)+K3/HFG3))/
* (ALFA+KABS4*DPDT3B/(VG3B+VISG3B))
DENOM=1.+TERM1+TERM3

T2=(TH*(1.+TERM3)+TB*TERM1)/DENOM
T2=(T02+T2)/2.
T3=(TH*TERM3+TB*(1.+TERM1))/DENOM
T3=(T03+T3)/2.

560 CONTINUE

T1=T2
GO TO 590

570 DO 590 I=1,IMAX

T01=T1
T02=T2
T03=T3

CALL CALLER(3)

```
HFG1=HFG(T1)+DELHD(1) 001247
HFG2=HFG(T2)+DELHD(2) 001248
IF(FLAG.EQ.1) HFG2=HFG(T2)+DELHD(1) 001249
HFG3=HFG(T3)+DELHD(3) 001250
C 001251
ALF=DELTA2-DELTA1 001252
BET=DELTA3-DELTA2 001253
GAMM=DELTA1-DELTA3 001254
IF(BE1.EQ.0.) FLAG=1 001255
IF(FLAG.EQ.1) GO TO 580 001256
C 001257
TERM1=(1./HC+DELTA1/K1)*(1./ALF)*(HFG1*KABS2*DPDT12/ 001258
* (VG12*VISG12)+K2) 001259
TERM2=(BET*(KABS2*DPDT12/(VE12*VISG12)+K2/HFG2))/ 001260
* (ALF*(KAKV*DPDT23/(VG23*VISG23)+K3/HFG2)) 001261
TERM3=(GAMM*(KAKV*DPDT23/(VG23*VISG23)+K3/HFG3))/ 001262
* (BET*KABS4*DPDT38/(VG38*VISG38)) 001263
TERM4=TERM2*(1.+TERM3) 001264
DENOM=1.+TERM1+TERM4 001265
C 001266
T1=(TH*(1.+TERM4)+TB*TERM1)/DENOM 001267
T1=(T01+T1)/2. 001268
T2=(TH*TERM4+TB*(1.+TERM1))/DENOM 001269
T2=(T02+T2)/2. 001270
T3=(TH*TERM2+TERM3+TB*(1.+TERM1+TERM2))/DENOM 001271
T3=(T03+T3)/2. 001272
GO TO 590 001273
C 001274
580 TERM1=(1./HC+DELTA1/K1)*(1./ALF)*(HFG1*KABS2*DPDT12/ 001275
* (VG12*VISG12)+K2) 001276
TERM2=(BET*(KABS2*DPDT12/(VE12*VISG12)+K2/HFG2))/ 001277
* (ALF*KABS4*DPDT23/(VG23*VISG23)) 001278
DENOM=1.+TERM1+TERM2 001279
C 001280
T1=(TH*(1.+TERM2)+TB*TERM1)/DENOM 001281
T1=(T01+T1)/2. 001282
T2=(TH*TERM2+TB*(1.+TERM1))/DENOM 001283
T2=(T02+T2)/2. 001284
T3=TB 001285
590 CONTINUE 001286
C 001287
C 001288
C****RECCMPUTE VARIABLES FOR DERIVATIVE CALCULATIONS 001289
C 001290
IF(DELTA1.NE.DELTA2) GO TO 600 001291
CTD212=0. 001292
CTD223=(T2-T3)/ALFA 001293
GO TO 610 001294
C 001295
600 CTD212=(T1-T2)/ALF 001296
CTD223=0. 001297
IF(FLAG.EQ.0) CTD223=(T2-T3)/BET 001298
C 001299
```



```
IF(L.NE.1) CALL WRITER(IOPTU)
C WRITE(6,/) MREL,LIQDEW,S3,MR,RATE1,RATE2,RATE3,X,D7,DT
  N=1
  GO TO 660
C
C
C *****INCREMENT PRINT CONTROL VARIABLES
C
  650 N=N+1
  660 L=L+1
C
C
C *****DETERMINE EXIT CRITERIA
C
  IF(1800*TIME.GE.RISTIM.AND.IOPTP.EQ.2) GO TO 9999
  IF(MC.GT.MFINAL) GO TO 460
C
C
C *****WRITE FINAL OUTPUT
C
  IF(N.NE.1) CALL WRITER(IOPTU)
  WRITE(6,950) QINIT
  WRITE(6,955) QTOTAL
  CTOT=QINIT+QTOTAL
  WRITE(6,960) QTOT
  CTHER1=(BW*CPF+MC*CPW)*(TB-TI)
  CTHER2=MC*HFGTE
  CTHEOR=CTHER1+CTHER2
  IF(TB.LT.TI) CTHEOR=CTHER2
  WRITE(6,965) CTHEOR
  LIQDEW=LIQDEW*100./MC
  WRITE(6,970) LIQDEW
C
C
C *****FORMAT STATEMENTS
C
  500 FORMAT(" ***** HIDRYER1 PROGRAM OUTPUT *****")
  505 FORMAT(1H0," TH TS BW CSF MRG"
    *" PMAX RISTIM")
  510 FORMAT(2F9.2,F11.5,I8,F9.2,F10.2,F9.3)
  515 FORMAT(1H0," DTQ IOPTP IOPTU"
    *" METH MITER")
  520 FORMAT(E13.5,2I8,2I11)
  525 FORMAT(1H0," SEC MREL TS T1 T2"
    *" I3 RATIO1 RATIO2 RATIO3 DELTAT 0"
    *" QHTC PGALGE SEC")
  530 FORMAT(1H0)
  535 FORMAT(10C15,F8.3))
  540 FORMAT(1H0," START OF TRANSITION REGIME")
  545 FORMAT(1H0," START OF LINEAR REGIME")
  550 FORMAT(1H0,1X,F6.2," BTU/FT2 REQUIRED TO HEAT THE SHEET")
  555 FORMAT(1H0,1X,F6.2," BTU/FT2 REQUIRED FOR DOWATERING THE SHEET")
  560 FORMAT(1H0,1X,F6.2," BTU/FT2 TOTAL THERMAL ENERGY INPUT")
  565 FORMAT(1H0,1X,F6.2," BTU/FT2 THEORETICALLY REQUIRED FOR HEATUP")
```

*" AND EVAPORATION OF ALL LIQUID AT SATURATION TEMPERATURE")
57C FCRMAT(1HQ,1X,F6.2," PERCENT OF THE MOISTURE IS REMOVED IN"
*" LIQUID FORM")

001408
001409
001410

*****END MAIN PROGRAM

001411
001412
001413

9599 STOP
END

001414
001415
001416

001417
001418
001419

***** THE SUBROUTINES *****

001420
001421
001422

*****SUBROUTINE TO CONVERT FROM ENGLISH TO SI UNITS

001423
001424
001425
001426
001427

SUBROUTINE CNVRT1

DATA A1,A2,A3,A4,A5/9,5,32,4.8224,6.8948/

001428
001429
001430
001431

COMMON /LABEL1/ TB,PVTB,DFVDTB,VFTB,VGTB,HFGTB,VISGTB,VISFTB

001432
001433

COMMON /LABEL2/ TH,T1,T2,T3,TI,TMID

001434

COMMON /LABEL7/ FREF1,FMAX,FISTIM,P,IOPTP,DPDT

001435

COMMON /LABEL9/ DLOT,FACTCR,BW,CN,DFIBER,COEFF,PS3

001436

TH=A1*TH/A2+A3

001437
001438

TB=A1*TB/A2+A3

001439

BW=BW/A4

001440

FMAX=FMAX/A5

001441

RETURN

001442
001443

END

001444

001445

*****SUBROUTINE TO DETERMINE THE CONSTANTS FOR CALCULATION OF M AND N

001446
001447
001448

SUBROUTINE CNSTMN(X)

DATA

*A1,A2,A3,A4,A5,A6/2.9613453E+00,-2.8919415E-01,5.7420518E+01,

001449
001450
001451
001452

* -3.3796161E+01,4.411387E+00,1.2974508E+00/,

001453

*E1,B2,B3,B4,B5,B6/2.005747E-01,2.2200153E-02,-8.3841418E+01,

001454

* -3.5825139E+01,7.6054413E+01,-1.0786651E+01/,

001455

*C1,C2,C3,C4,C5,C6/-1.992423E-02,-2.1085106E-03,-1.1519896E-01,

001456

* -3.1081894E-01,3.5352481E-01,-4.1291326E-02/,

001457

*C1,C2,D3,D4,D5,D6/1.405545E-02,9.497606E-04,-6.4943036E-02,

001458

* 3.5853945E-02,-2.7498142E-03,-1.305774E-03/,

001459

*E1,E2/100.,540./

001460

001461

001462

```
COMMON /LABEL15/ CM1,CM2,CM3,CM4,CM5,CM6      001463
COMMON /LABEL16/ CN1,CN2,CN3,CN4,CN5,CN6      001464
C                                               001465
TERM=((X-E1)/E2)**2                            001466
IF(X.LT.0.) TERM=0.                            001467
CM1=A1+B1*TERM                                 001468
CM2=A2+E2*TERM                                 001469
CM3=A3+B3*TERM                                 001470
CM4=A4+B4*TERM                                 001471
CM5=A5+E5*TERM                                 001472
CM6=A6+B6*TERM                                 001473
C                                               001474
CN1=C1+D1*TERM                                 001475
CN2=C2+D2*TERM                                 001476
CN3=C3+D3*TERM                                 001477
CN4=C4+D4*TERM                                 001478
CN5=C5+D5*TERM                                 001479
CN6=C6+D6*TERM                                 001480
C                                               001481
RETURN                                          001482
END                                             001483
C*****                                         001484
C                                               001485
C                                               001486
C*****SUBROUTINE TO CALCULATE PROPERTIES AT TB 001487
C                                               001488
SUBROUTINE PROPTB                               001489
C                                               001490
COMMON /LABEL1/ TB,PVTB,DFVDTB,VFTB,VGTB,HFGTB,VISGTB,VISFTB 001491
C                                               001492
FVTB=PV(TB)                                    001493
CPVDTB=DFVDT(TB)                              001494
VFTE=VF(TB)                                    001495
VGTB=VG(TB)                                    001496
HFGTE=HFG(TB)                                  001497
VISGTB=VISG(TB)                                001498
VISFTB=VISF(TB)                                001499
C                                               001500
RETURN                                          001501
END                                             001502
C*****                                         001503
C                                               001504
C                                               001505
C*****SUBROUTINE TO CALL PROPERTY SUBROUTINES 001506
C                                               001507
SUBROUTINE CALLER(I)                            001508
C                                               001509
COMMON /LABEL2/ TH,T1,T2,T3,TI,THID           001510
C                                               001511
IF(I.EQ.4) GO TO 10                             001512
C                                               001513
CALL PROP3B                                     001514
IF(I.EQ.2) GO TO 20                             001515
C                                               001516
10 CALL PROP12                                  001517
```

1F(I.EQ.3) GO TO 2C

CALL PROP23(1)
GC TO 30

2C CALL PROP23(2)

3C RETURN
END

001518
001519
001520
001521
001522
001523
001524
001525
001526
001527

*****SUBROUTINE TO CALCULATE T1-T2 AVERAGE PROPERTIES

SUBROUTINE PROP12

COMMON /LABEL2/ TH,T1,T2,T3,TI,TMID
COMMON /LABEL3/ DPDT12,VF12,VG12,VISG12

CPDT12=(DPVD1(T1)+DPVD1(T2))/2.
VF12=(VF(T1)+VF(T2))/2.
VG12=(VG(T1)+VG(T2))/2.
VISG12=(VISE(T1)+VISG(T2))/2.

RETURN
END

001528
001529
001530
001531
001532
001533
001534
001535
001536
001537
001538
001539
001540
001541
001542
001543
001544

*****SUBROUTINE TO CALCULATE T2-T3 AVERAGE PROPERTIES

SUBROUTINE PROP23(1)

COMMON /LABEL2/ TH,T1,T2,T3,TI,TMID
COMMON /LABEL4/ DPDT23,VF23,VISF23,VG23,VISG23

GC TO (10,20) 1

1C VF23=(VF(T2)+VF(T3))/2.
VISF23=(VISF(T2)+VISF(T3))/2.
GC TO 30

2C VG23=(VG(T2)+VG(T3))/2.
VISG23=(VISE(T2)+VISG(T3))/2.

3C CPDT23=(DPVD1(T2)+DPVD1(T3))/2.

RETURN
END

001545
001546
001547
001548
001549
001550
001551
001552
001553
001554
001555
001556
001557
001558
001559
001560
001561
001562
001563
001564
001565
001566
001567

*****SUBROUTINE TO CALCULATE T3-T8 AVERAGE PROPERTIES

001568
001569
001570
001571


```

SUBROUTINE PROP3B
C
COMMON /LABEL1/ TB,PVTB,DPVDTB,VFTB,VGTB,HFGTB,VISGTB,VISFTB
COMMON /LABEL2/ TH,T1,T2,T3,TI,THID
COMMON /LABEL5/ DPDT3B,VG3B,VISG3B
C
CPDT3B=(DPVDT(T3)+DPVDTB)/2.
VG3B=(VG(T3)+VGTB)/2.
VISG3B=(VISE(T3)+VISGTB)/2.
C
RETURN
END
C*****
C
C*****SUBROUTINE TO CALCULATE APPLIED PRESSURE AND ITS DERIVATIVE
C
SUBROUTINE PRESSR(A)
C
DATA PI,A2/3.1415927,4.712389/
C
COMMON /LABEL7/ PREF1,PMAX,RISTIM,P,IOFTP,DPDT
C
EO TO (10,20) IOFTP
C
10 CPDT=PMAX*3600./RISTIM
F=PREF1+A*DPDT
IF(P.GT.PMAX) F=PMAX
IF(F.GE.PMAX) CPDT=0.
EO TO 30
C
20 A1=PI*3600./RISTIM
P=PREF1+PMAX*(1.+SIN(A1*A+A2))/2.
DPDT=A1*PMAX*COS(A1*A+A2)/2.
IF(1800.*A.GE.RISTIM) P=PREF1
IF(1800.*A.GE.RISTIM) CLDT=C.
C
30 RETURN
END
C*****
C
C*****SUBROUTINE TO CALCULATE THE THICKNESS OF A SATURATED MEDIUM
C
SUBROUTINE CLDTFN(N,TIME,YL,YPRIME)
C
REAL YL(N),YPRIME(N),TIME
C
COMMON /LABEL1/ TB,PVTB,DPVDTB,VFTB,VGTB,HFGTB,VISGTB,VISFTB
COMMON /LABEL7/ PREF1,PMAX,RISTIM,F,IOFTP,DPDT
COMMON /LABEL8/ M1,M2,M3,M4,N1,N2,N3,N4
COMMON /LABEL9/ CLDT,FACTCR,BW,DW,DFIBER,COEFF,PS3
C
CALL PRESSR(TIME)
FS3=(BW/(YL(1)*M3))**(1./N3)

```

001572
001573
001574
001575
001576
001577
001578
001579
001580
001581
001582
001583
001584
001585
001586
001587
001588
001589
001590
001591
001592
001593
001594
001595
001596
001597
001598
001599
001600
001601
001602
001603
001604
001605
001606
001607
001608
001609
001610
001611
001612
001613
001614
001615
001616
001617
001618
001619
001620
001621
001622
001623
001624
001625
001626

```

R=SPRES(P)/FACTOR                                001627
COEFF=3./(VISF18*BW*R)                            001628
YPRIME(1)=(FS3-P)*COEFF                           001629
CLOT=YPRIME(1)                                     001630

```

```

RETURN                                             001631
END                                                 001632

```

```

*****
*****SUBROUTINE TO CALCULATE THE JACOBIAN FOR A SATURATED MEDIUM

```

```

SUBROUTINE DUMFUN(N,TIME,YL,PD)                   001633

```

```

REAL TIME,YL(N),FD(1,1)                           001634

```

```

COMMON /LABEL8/ M1,M2,M3,M4,N1,N2,N3,N4          001635

```

```

COMMON /LABEL9/ DLOT,FACTOR,BW,Dh,DFIBER,COEFF,PS3 001636

```

```

FD(1,1)=-COEFF*PS3/(N3*YL(1))                    001637

```

```

RETURN                                             001638

```

```

END                                                 001639

```

```

*****
*****SUBROUTINE TO WRITE OUTPUT

```

```

SUBROUTINE WRITER(I)                               001640

```

```

COMMON /LABEL2/ TH,T1,T2,T3,TI,TMID              001641

```

```

COMMON /LABL11/ SEC,MREL,TS,RATIO1,RATIO2,RATIO3,DELTA,T,Q,QHTC, 001642

```

```

* PGALGE                                           001643

```

```

COMMON /LABL12/ TSSI,T1SI,T2SI,T3SI,DELTSI,QSI,CHTCSI,PGAGSI, 001644

```

```

* TMIDSI                                           001645

```

```

IF(I.EQ.2) GO TO 10                                001646

```

```

WRITE(6,20) SEC,MREL,TS,T1,T2,T3,RATIO1,RATIO2,RATIO3,DELTA,T,Q, 001647

```

```

* QHTC,PGAUCE,SEC                                  001648

```

```

WRITE(2,20) SEC,MREL,TS,T1,T2,T3,RATIO1,RATIO2,RATIO3,DELTA,T,Q, 001649

```

```

* QHTC,PGAUCE,TMID                                 001650

```

```

GO TO 30                                           001651

```

```

10 CALL CNVRT2                                     001652

```

```

WRITE(6,20) SEC,MREL,TSSI,T1SI,T2SI,T3SI,RATIO1,RATIO2,RATIO3, 001653

```

```

* DELTSI,QSI,CHTCSI,PGAGSI,SEC                    001654

```

```

WRITE(2,20) SEC,MREL,TSSI,T1SI,T2SI,T3SI,RATIO1,RATIO2,RATIO3, 001655

```

```

* DELTSI,QSI,CHTCSI,PGAGSI,TMIDSI                 001656

```

```

20 FORMAT(1X,F8.5,F8.4,4F9.3,3F8.4,F10.6,F11.1,F8.2,F8.3,F10.5) 001657

```

```

30 RETURN                                          001658

```

```

001627
001628
001629
001630
001631
001632
001633
001634
001635
001636
001637
001638
001639
001640
001641
001642
001643
001644
001645
001646
001647
001648
001649
001650
001651
001652
001653
001654
001655
001656
001657
001658
001659
001660
001661
001662
001663
001664
001665
001666
001667
001668
001669
001670
001671
001672
001673
001674
001675
001676
001677
001678
001679
001680

```

```

      END
C*****
C
C
C*****SUBROUTINE TO CONVERT FROM ENGLISH TO SI UNITS
C
C      SUBROUTINE CNVRT2
C
C      DATA A1,A2,A3,A4,A5,A6,A7/5,32,9,0.3048,3.1546,5.6783,6.8948/
C
C      COMMON /LABEL2/ TH,T1,T2,T3,TI,TMID
C      COMMON /LABEL11/ SEC,MREL,TS,RATIO1,RATIO2,RATIO3,DELTA1,Q,QHTC,
C      * PGAUGE
C      COMMON /LABEL12/ TSSI,T1SI,T2SI,T3SI,DELTSI,QSI,QHTCSI,PGAQSI,
C      * TMIDSI
C
C      TSSI=A1*(TS-A2)/A3
C      T1SI=A1*(T1-A2)/A3
C      T2SI=A1*(T2-A2)/A3
C      T3SI=A1*(T3-A2)/A3
C      TMIDSI=A1*(TMID-A2)/A3
C      DELTSI=DELTA1*A4
C      QSI=Q*A5
C      QHTCSI=QHTC*A6
C      PGAQSI=PGAUGE*A7
C
C      RETURN
C      END
C*****
C
C
C*****SUBROUTINE TO CORRECT ERROR CONDITION OR PRINT WARNING MESSAGE
C
C      SUBROUTINE WARNIN(I,J,X)
C
C      COMMON /LABEL6/ DXX,DIFFIX,DIFFFX,EMIN
C      COMMON /LABEL9/ CLDT,FACTCR,BM,CW,DFIBER,COEFF,PS3
C
C      GO TO (10,20,30,40) I
C
C      10 WRITE(6,50) J,X,DFIBER
C      GO TO 70
C
C      20 WRITE(6,60) J,X,EMIN
C      GO TO 70
C
C      30 DIFFIX=DXX
C      GO TO 70
C
C      40 DIFFFX=DXX
C
C      50 FORMAT('*** ZONE ',I2,' DENSITY ',E16.10,' IS GREATER THAN THE'
C      * ' MAXIMUM ALLOABLE DENSITY ',E16.10,' *** COMPUTATION')

```

```

001681
001682
001683
001684
001685
001686
001687
001688
001689
001690
001691
001692
001693
001694
001695
001696
001697
001698
001699
001700
001701
001702
001703
001704
001705
001706
001707
001708
001709
001710
001711
001712
001713
001714
001715
001716
001717
001718
001719
001720
001721
001722
001723
001724
001725
001726
001727
001728
001729
001730
001731
001732
001733

```

*" TERMINATED")

001734

60 FORMAT("*** ZONE ",I2," POROSITY ",E16.10," IS LESS THAN THE"
*" MINIMUM ALLOWABLE POROSITY ",E16.10," *** COMPUTATION"
*" TERMINATED")

001735

001736

001737

001738

001739

70 RETURN
END

001740

001741

001742

001743

001744

***** THE FUNCTIONS *****

001745

001746

001747

001748

001749

*****VAPOR PRESSURE FUNCTION

001750

FUNCTION PV(T)

001751

001752

DATA

001753

001754

*A1,A2,A3,A4,A5/1.5284E+00,-6.42281E-02,9.7657E-04,-5.85595E-06,
* 1.91309E-08/

001755

001756

001757

PV=A1+T*(A2+T*(A3+T*(A4+T*A5)))

001758

001759

RETURN
END

001760

001761

001762

001763

001764

*****VAPOR PRESSURE DERIVATIVE FUNCTION

001765

FUNCTION DPVDT(T)

001766

001767

DATA

001768

001769

*A1,A2,A3,A4/-6.42281E-02,9.7657E-04,-5.85595E-06,1.91309E-08/

001770

001771

DPVDT=A1+T*(2.*A2+T*(3.*A3+4.*A4*T))

001772

001773

RETURN
END

001774

001775

001776

001777

001778

*****LIQUID SPECIFIC VOLUME FUNCTION

001779

FUNCTION VF(T)

001780

001781

DATA

001782

001783

*A1,A2,A3,A4,A5/1.60571E-02,-2.35188E-06,3.69301E-08,-6.94068E-11,
* 8.04005E-14/

001784

001785

001786

VF=A1+T*(A2+T*(A3+T*(A4+T*A5)))

001787

```
C                                001788
      RETURN                                001789
      END                                  001790
C*****                                001791
C                                001792
C                                001793
C*****VAPOR SPECIFIC VOLUME FUNCTION  001794
C                                001795
      FUNCTION VG(T)                       001796
C                                001797
      DATA                                001798
      *A1,A2,A3,A4,A5/9.40601E+00,-4.37418E-02,9.59205E-05,-1.41015E-07, 001799
      * 9.35084E-11/                       001800
C                                001801
      VG=EXP(A1+T*(A2+T*(A3+T*(A4+T*A5)))) 001802
C                                001803
      RETURN                                001804
      END                                  001805
C*****                                001806
C                                001807
C                                001808
C*****LATENT HEAT FUNCTION           001809
C                                001810
      FUNCTION HFG(T)                      001811
C                                001812
      DATA                                001813
      *A1,A2,A3,A4,A5/1.09351E+03,-5.6626E-01,8.20598E-05,-5.70484E-07, 001814
      * -6.91038E-10/                     001815
C                                001816
      HFG=A1+T*(A2+T*(A3+T*(A4+T*A5)))    001817
C                                001818
      RETURN                                001819
      END                                  001820
C*****                                001821
C                                001822
C                                001823
C*****LIQUID VISCOSITY FUNCTION     001824
C                                001825
      FUNCTION VISF(T)                    001826
C                                001827
      DATA                                001828
      *A1,A2,A3,A4/-1.3917E-04,1.85E-07,6.4841E-02,-7.0869E-01/ 001829
C                                001830
      VISF=A1+T*A2+A3/T+A4/T**2          001831
C                                001832
      RETURN                                001833
      END                                  001834
C*****                                001835
C                                001836
C                                001837
C*****VAPOR VISCOSITY FUNCTION      001838
C                                001839
      FUNCTION VISG(T)                    001840
C                                001841
```

```

DATA
*A1,A2/5.499E-06,1.3908E-08/
VISG=A1+T*A2
RETURN
END

```

```

001842
001843
001844
001845
001846
001847
001848

```

***** EVALUATION FUNCTION

```

FUNCTION EVALM(X,T)
DATA A1,A2,A3/1.5,1.,0.25/
COMMON /LABEL2/ TH,T1,T2,T3,TI,TIME
COMMON /LABEL15/ CM1,CM2,CM3,CM4,CM5,CM6
A=X+A1
E=X+A2
CORRCT=(T/TI)**A3
EVALM=(CM1+CM2*X+CM3/A+CM4/A**2+CM5/B+CM6/B**2)*CORRCT

```

```

001849
001850
001851
001852
001853
001854
001855
001856
001857
001858
001859
001860
001861
001862
001863
001864
001865

```

```

RETURN
END

```

```

001866
001867

```

***** EVALUATION FUNCTION

```

FUNCTION EVALN(CI,X,Y)
REAL NDENOM,NMID,NSAT
DATA A1,A2/1.5,1./
COMMON /LABEL4/ DPDT23,VF23,VISF23,VG23,VISG23
COMMON /LABEL7/ PREF1,PMAX,RISTIM,P,IOPTP,DPDT
COMMON /LABEL16/ CN1,CN2,CN3,CN4,CN5,CN6
COMMON /LABEL8/ M1,M2,M3,M4,N1,N2,N3,N4
COMMON /LABEL13/ CH1,DH2,MR,MRSTAR
COMMON /LABEL14/ NEXP,PR3LOG,PREF3,PMID,PDENOM,DF

```

```

001868
001869
001870
001871
001872
001873
001874
001875
001876
001877
001878
001879
001880
001881
001882
001883
001884

```

```

A=X+A1
E=X+A2
C=CN1+CN2*X+CN3/A+CN4/A**2+CN5/B+CN6/B**2
EVALN=C
IF(CI.EQ.1) GO TO 10
IF(X.LE.MRSTAR) GO TO 10

```

```

001885
001886
001887
001888
001889
001890
001891

```

```

NSAT=ALOG(1./(M3*(X*VF23+DF)))/PR3LOG
NMID=(NSAT+C)/2.
NDENOM=NSAT-NMID
FTERM=ABS(Y-PMID)/PDENOM

```

```

001892
001893
001894
001895
001896

```

```

C
SIGN=1.
IF(Y.LT.PMID) SIGN=-1.
IF(Y.EQ.PMID) SIGN=0.
EVALN=NMID+SIGN*NDENOM*PTERM**2*(1./NEXP)
IF(Y.LT.PREF1) EVALN=C
IF(Y.GT.PREF3) EVALN=NSAT
C
WRITE(5,/) I,X,Y,C,NSAT,NMIC,NDENOM,PTERM,PMID,PDENOM,EVALN
C
10 RETURN
END
C*****
C
C*****SPECIFIC FILTRATION RESISTANCE FUNCTION
C
FUNCTION SPRES(P)
C
DATA A1,A2,A3,A4,A5,A6/7.027,2.013E-05,0.142,0.464,0.187,0.344/
C
COMMON /LABL10/ CSF
C
RREF=((A1-ALOG(CSF))/A2)**2
R=P/A3
SPRES=RREF*(A4+A5*X+A6*SQRT(X))
C
RETURN
END
C*****
C
C*****HYDRAULIC PRESSURE FUNCTION
C
FUNCTION HYDRAL(A,B)
C
COMMON /LABEL1/ TB,PVTB,DFVCTB,VFTB,VGTB,HFGTB,VISGTB,VISFTB
C
HYDRAL=(FV(A)+PV(B))/2.-PVTB
C
RETURN
END
C*****
C
C*****LATENT HEAT INCREMENT FUNCTION
C
FUNCTION DELHD(I)
C
COMMON /LABL13/ DH1,DH2,MR,MRSTAR
C
EQ TO (10,20,30) I
C
10 DELHD=DH1*(1.-EXP(DH2*MRSTAR))/MRSTAR
EC TO 40

```

```

001897
001898
001899
001900
001901
001902
001903
001904
001905
001906
001907
001908
001909
001910
001911
001912
001913
001914
001915
001916
001917
001918
001920
001921
001922
001923
001924
001925
001926
001927
001928
001929
001930
001931
001932
001933
001934
001935
001936
001937
001938
001939
001940
001941
001942
001943
001944
001945
001946
001947
001948
001949
001950

```

20 DELHD=DF1*(EXP(DH2*MRSTAR)-EXP(DH2*MR))/(MR-MRSTAR)
GC TC 40

30 DELHD=DF1*(1.-EXP(DH2*MR))/MR

40 RETURN
END

001951
001952
001953
001954
001955
001956
001957
001958
001959

.....

The programs for the various stages of model development and the data files used to generate the graphs for this thesis are stored on magnetic tape in the Institute computer center.

The model equations, supplementary relationships, and data file information and names are in Institute research notebooks 3578 and 3711.